# APPLICATION OF AN OPTIMAL TUNING TECHNIQUE OF ON-LOAD TAP-CHANGING TRANSFORMER FOR POWER QUALITY IMPROVEMENT IN TRANSMISSION LINE NETWORK

**BY**

**LAWAL RABE**

**DEPARTMENT OF ELECTRICAL ENGINEERING,**
**FACULTY OF ENGINEERING,**
**AHMADU BELLO UNIVERSITY,**
**ZARIA, NIGERIA**

**DECEMBER, 2021**

# APPLICATION OF AN OPTIMAL TUNING TECHNIQUE OF ON-LOAD TAP-CHANGING TRANSFORMER FOR POWER QUALITY IMPROVEMENT IN TRANSMISSION LINE NETWORK

**By**

**LAWAL, Rabe**

**P18EGEE8076**

**Rabelawal426@gmail.com**

**A DISSERTATION SUBMITTED TO THE SCHOOL OF POSTGRADUATE STUDIES, AHMADU BELLO UNIVERSITY, IN PARTIAL FULFILLMENT OF THE REQUIREMENTS FOR THE AWARD OF MASTER OF SCIENCE (MSc) DEGREE IN ELECTRICAL ENGINEERING**

**DEPARTMENT OF ELECTRICAL ENGINEERING,**
**FACULTY OF ENGINEERING,**
**AHMADU BELLO UNIVERSITY,**
**ZARIA, NIGERIA**

**DECEMBER, 2021**

## DECLARATION

I, Lawal Rabe hereby declare that the work in this dissertation entitled “Application of an Optimal Tuning Technique of on-load tap changing transformers for the improvement of power quality improvement in transmission line network” has been carried out by me in the department of Electrical Engineering Ahmadu Bello University Zaria, the information derived from literature has been duly acknowledged in the text and a list of reference provided. No part of this dissertation was previously presented for another degree or diploma at this or any other institution.

LAWAL Rabe ___---------- ---------- _____

Signature Date

## CERTIFICATION

This Dissertation entitled "DEVELOPMENT OF OPTIMAL TUNING TECHNIQUE OF ON-LOAD TAP CHANGING TRANSFORMER FOR IMPROVEMENT OF POWER QUALITY IN THE TRANSMISSION LINE NETWORK" by Lawal RABE meets the regulations governing the award of Degree of Masters of Science (MSc) in Power systems Engineering of the Ahmadu Bello University Zaria and is approved for its contribution to knowledge and literary presentation

**Dr. G.A Olarinoye**

(Chairman Supervisory Committee)

_____ _____

Signature Date

**Dr. P. U Okorie**

(Member Supervisory Committee) _____ _____

Signature Date

**Prof. Y Jubril**

(Head of Department) _____ _____

Signature Date

**Prof. Sani A. Abdullahi**

(Dean School of Postgraduate Studies) _____ _____

Signature Date

## DEDICATION

This dissertation is dedicated to Almighty Allah the Gracious, merciful and most beneficent who grant me the life, health and ability to get to this level. Also, to the memory of my late father Malam mamman, my late grandparents, Alh. Malam Haruna Mai Gwanjo and Hajiya Khadija (Ada) and my late uncles Alhaji Rabe Reza and Alhaji Garba Mai Doya.

## ACKNOWLEDGEMENTS

My profound gratitude goes to Almighty Allah for his infinite blessing and guidance upon me throughout the process of achieving the completion of this research work.

I wish to express my sincere gratitude to my caring and kind Chairman Supervisory Committee, Dr. G.A Olarinoye for his flexible, consistent and professional guidance from the beginning of this work to the end, your humility, tolerance and sense of direction sir gave the comfort and concentration to discover and learned so much about the fundamental concept of this work and beyond, I thank you so much sir for all of these and I pray God Almighty will also answer and grant your needs in life.

My appreciation also goes to the member supervisory committee, Dr. P.U Okorie for his continuous encouragement, concern and tutelage throughout the period of this work. The success recorded in this work wouldn't have been complete without your contributions.

I must also express my gratitude to the HOD, Prof. Y Jibril for his keen and valuable advices at all times, and not forgetting his huge administrative assistance and contribution that help in fast-tracking the completion of this work.

I wish to express my appreciation to my power system lecturer, Dr. A.B Kunya whom I consulted so many times on specific and unclear sections of the work. Much thanks go to all the lecturers of the department of electrical engineering to mentioned a few; Prof. B. Jimoh, Dr. A. Abdulkarim an amiable PG coordinator, Dr. A.S Abubakar, Dr. S.M Sani, Dr. Gaddafi, Dr. Abdulrahman, Engr. Umar Musa, Engr. Ibrahim and several others space could not allow me to mentioned, I thank you all for your contributions in one way or the other.

I am grateful to my hard-working class rep, Abdulaziz Nurudeen and the entire class of M.Sc. P18EE, the non-academic staffs and students of the Department of Electrical Engineering, thank you all I pray that Almighty will reward all of you abundantly.

Finally, I say I am highly indebted to my beloved wife Zainab A. Abdullahi, my children Abdulgafar Rabe Lawal, Nabil Rabe Lawal, Abubakar Rabe Lawal and Khadijat Rabe Lawal and not forgetting my boss Engr. Ahmed I. Shuaibu for your love, support, understanding and patience that enables me successfully complete this research work.

Rabe Lawal

December, 2021

## ABSTRACT

For reliable and efficient operation of power system, voltage level and reactive power flow along transmission lines has to be adequately regulated. To control reactive power flow over transmission lines and compensate for varying voltage drops, tap changing transformers are required. By altering the voltage magnitudes at the windings of the transformers through winding tap adjustment, reactive power flow can be controlled. The transformers can be off-loaded or on-line tap changer. In the latter, the transformers are disconnected from the system when the tap setting is to be adjusted, while in the former, the tap adjustment is carried out with the transformers connected. In this research work, Grey Wolf Optimization (GWO) algorithm is applied to determine the optimal On-Line Tap Changer (OLTC) of the available transformers in the system in order to improve the voltage profile and regulate reactive power. The constraints considered in the formulation of the problem are demand-generation balance, bus voltage limits, line thermal overloading limits and tap-changer adjustment limits according to IEEE C57.131 2012 requirement. To verify the effectiveness of the developed technique, it is implemented on IEEE 14-bus, IEEE 30-bus and 57-bus Nigerian Transmission systems. The performances of the proposed technique is compared with those obtained using Particle Swarm Optimization (PSO). From the simulation carried out in MATLAB environment, it is observed there is significant reductions in the overall voltage deviation (VD) as well as the reactive power loss (RPL) when the OLTCs are optimized. For instance, in the IEEE 14-bus system, the VD was reduced from 2.0892*pu* (base case) to 1.0153*pu* due to the optimal tuning of the OLCTs using GWO and 1.4783*pu* when PSO was applied. This represents 51.40% improvement in the case of the developed GWO over that of the base case and 31.32% improvement over the case of the PSO. Similarly, the RPL was reduced from 277.298*MVar* of the base case value to 156.542*MVar* due to the optimal tuning of the OLCTs using GWO and 206.591*MVar* when PSO was applied representing 43.54% and 25.49% improvements respectively. These have demonstrated the applicability of the GWO and its superiority over PSO in optimizing the OLTCs in the IEEE 14-bus and 30-bus systems. In the Nigerian 57-bus system, by applying the GWO, the total VD was reduced from 6.7808*pu* (base case) to 4.4519*pu* representing 34.35% improvement. Finally, the value of RPL was reduced by 36.56% from its original value of 185.4685*Mvar*.


**TABLE OF CONTENT**

**COVER PAGE**.....1
**FLY LEAF**.....ii
**TITLE PAGE**.....iii
**DECLARATION**.....2
**CERTIFICATION**.....3
**DEDICATION**.....4i
**ACKNOWLEDGEMENTS**.....5ii
**ABSTRACT**.....6ii
**LIST OF FIGURES**.....9
**LISTS OF TABLES**.....10
**LIST OF APPENDICES**.....11
**LISTS OF SYMBOLS AND ABBREVIATION**.....12
**CHAPTER ONE**.....15
1.1 **GENERAL INTRODUCTION**.....15
**1.2 Problem Statement**.....17
**1.3 Significance of the research**.....17
**1.4 Aim and Objectives of the Study**.....18
**1.5 Scope and Limitation**.....43
**CHAPTER TWO**.....5
**LITERATURE REVIEW**.....5
**2.1 Introduction**.....5
**2.2 Review of Fundamental Concepts**.....5
2.2.1 Transformer On-Load Tap-changer.....5
2.2.1 Power Quality.....6
2.2.1.1 Classification of Power Quality Problem.....6
2.2.1.2 Power Quality Improvement Techniques and Solutions.....6
2.2.2 Transmission Line Model with Tap-changing Transformer.....6
2.2.3 Power Flow Analysis of Power System Network.....8
2.2.4 Optimization Algorithm.....33
2.2.4.2 Bus Classification.....11
2.2.4.3 Power Flow Equation.....12
2.2.4.4 Power Flow Solution.....13
2.2.5 Optimization Algorithm.....17
2.2.5.1Grey Wolf Optimizer.....19

**2.3 Review of Similar Works**.....36

**CHAPTER THREE**.....43
**METHODOLOGY**.....43
**3.1 Research Methodology**.....**Error! Bookmark not defined.**
**3.2 Test Systems Description**.....**Error! Bookmark not defined.**
3.2.1 IEEE 14-Bus Test System.....44
3.2.2 IEEE 30-Bus Test System.....30

3.2.3 Nigeria 330kV Transmission System.....31

**3.3 Methodology**.....48
3.3.2 Objective Function.....48
3.3.2.1 Minimization of Reactive Power Loss.....33

3.3.3 Constraints.....49

3.3.4 GWO Parameters Selection.....50
**CHAPTER FOUR**.....51
**RESULTS AND DISCUSSION**.....51
**4.1 Introduction**.....51
**4.2 Optimizing OLTCs of the IEEE 14-Bus System**.....51
4.2.1 Base Case of the IEEE 14-Bus System.....51
4.2.2 IEEE 14-Bus System with Optimized OLTCs.....51
**4.3 Optimizing OLTCs of the IEEE 30-Bus System**.....54
4.3.1 Base Case of the IEEE 30-Bus System.....40
4.3.2 IEEE 30-Bus System with Optimized OLTCs.....40
**4.4 Optimizing OLTCs of the Nigerian 57-Bus Transmission System**.....57
4.4.1 Base Case of the Nigerian 57-Bus System.....57
4.4.2 Nigerian 57-Bus System with Optimized OLTCs.....58
**CHAPTER FIVE**.....61
**CONCLUSION AND RECOMMENDATION**.....61
**5.1 Conclusions**.....61
**5.2 Significant Contributions**.....62
**5.3 Recommendation for Further Work**.....47

**REFERENCES**.....63

**LIST OF FIGURES**

Figure 2.1 Power Quality Sinik et al., (2019)
Figure 2.2 On-Load Tap Changer Circuit (Viawan, 2008).....21
Figure 2.3 Transmission Line with tap changing transformers at both ends (Saadat, 1999)...23
Figure 2.4 Voltage phasor diagram (Saadat, 1999). .....23
Figure 2.5 Typical bus in power system (Saadat, 1999).....27
Figure 2.6 shows the flowchart of the Newton-Raphson power flow technique (Efkarpidis, et al., 2016) ..... **Error! Bookmark not defined.**
Figure 2.7 Flowchart of Optimal Design Procedure.....33
Figure 2.8 Classification of optimization algorithms (Das, et al., 2009).....34
Figure 2.9 Flowchart of GWO (Agarwal, et al., 2018).....36
Figure 3.1 Single Line Diagram of IEEE 14 Bus (Tiwari, et al., 2018 ) .....45
Figure 3.2 Single Line Diagram of IEEE 30 Bus (Saadat, 1999) .....46
Figure 4.1: Voltage profile of IEEE 14-bus Optimized with GWO .....52
Figure 4.2: Improvement of GWO over the PSO on the Voltage Profile of IEEE 14-bus.....53
Figure 4.3: Improvement of GWO over the PSO on the Reactive Power of IEEE 14-bus.....37
Figure 4.4: Improvement of GWO over the PSO on the Active Power of IEEE 14-bus.....54
Figure 4.5: Improvement of GWO over the PSO on the Voltage Profile of IEEE 30-bus.....55
Figure 4.6: Improvement of GWO over the PSO on the Reactive Power of IEEE 30-bus .....57
Figure 4.7: Improvement of GWO over the PSO on the Active Power of IEEE 30-bus.....57
Figure 4.8: Voltage profiles of Nigerian 57-bus system.....59
Figure 4.8 Reactive Power Profiles of the Nigerian 57-bus system .....60
Figure 4.10: Active Power Profiles of Nigerian 57-bus system .....60

## LISTS OF TABLES

Table 2.1: Bus classification (Tiwari, et al., 2018 ).....26
Table 3.1 Initialization parameters of the gwo .....50
Table 4.1: Oltcs of the transformers in ieee 14-bus system.....51
Table 4.2: Summary of the voltage deviation in ieee 14-bus system .....53
Table 4.3: Summary of the reactive power in ieee 14-bus system .....54
Table 4.4: Oltcs of the transformers in ieee 30-bus system.....55
Table 4.5: Summary of the voltage deviation in ieee 30-bus system .....56
Table 4.6: Summary of the Reactive Power in IEEE 30-Bus System.....41
Table 4.7: Oltcs of the transformers in nigerian 57-bus system .....58
Table 4.8: Summary of the voltage deviation in ieee 30-bus system .....59

## LIST OF APPENDICES

APPENDIX A ..... 67
Appendix A1: Line Data for IEEE 14-Bus Network ..... 67
Appendix A2: Line Data for IEEE 14-Bus Network ..... 68
APPENDIX B ..... 69
Appendix B1: Line Data for IEEE 30-Bus Network ..... 69
Appendix B2: Bus Data for IEEE 30-Bus Network ..... 70
APPENDIX C ..... 72
Appendix C1: Line Data for Nigerian 57-Bus Network ..... 72
Appendix B2: Bus Data for Nigerian 57-Bus Network ..... 74
Appendix D1: Base Case Load flow Analysis of IEEE 14-Bus Network ..... 76
Appendix D2: Load flow Analysis of IEEE 14-Bus Network with Optimized OLTCs ..... 77
Appendix E1: Base Case Load flow Analysis of IEEE 30-Bus Network ..... 80
Appendix E2: Load flow Analysis of IEEE 30-Bus Network with Optimized OLTCs ..... 82
Appendix F1: Base Case Load flow Analysis of Nigerian 57-bus Network ..... 85
Appendix F2: Load flow Analysis of Nigerian 57-bus Network with Optimized OLTCs ..... 89

## LISTS OF SYMBOLS AND ABBREVIATION

| | |
|---|---|
| $P_{ij}$ | Active power in $i^{th}$ $j^{th}$ buses |
| $P_{ij}$ | Reactive power in $i^{th}$ $j^{th}$ buses |
| $V_j$ | Voltage of the $j^{th}$ bus |
| $i^{th}$ | $i^{th}$ bus |
| $j^{th}$ | $j^{th}$ bus |
| $t_R$ | Tap setting at the receiving end |
| $t_s$ | Tap setting at the sending eng |
| ∅ | Phase angle |
| ΔP | Change in active power |
| ΔQ | Change in reactive power |
| $\Delta\delta$ | Change in phase angle |
| ∑ | Summation |
| a | Acceleration factor |
| D | Distance between position vectors of both prey X (E) and |
| jX | Reactance in the line |
| P | Active power |
| Q | Reactive power |
| β | Weighing coefficient of reactive power |
| $\partial$ | Phase shift between two ends of the line |
| t | Current iteration number |

| | |
|---|---|
| G | Generator |
| C | Synchronous condenser |
| $\varphi$ | Weighing coefficient of voltage deviation |
| ACO | Ant Colony Optimization |
| ATC | Autonomous Tap Control |
| BNB | Branch and Bound |
| DOCR | Directional Over Current Relays |
| DVR | Dynamic Voltage Regulator |
| FACTs | Flexible Alternating Current Transmission System |
| GWO | Grey Wolf Optimization |
| HV | High Voltage |
| IEEE | Institute of Electrical and Electronic Engineering |
| KCL | Kirchoff Current Law |
| LF | Load Flow |
| LFA | Load Flow Analysis |
| LV | Low voltage |
| MATLAB | Math Laboratory |
| MINLP | Mixed Integer Nonlinear Programing |
| MPC | Model Predictance Control |
| NR | Newton Raphson |
| OLTC | On Load Tap Changer |

| | |
|---|---|
| OTC | Optimal Tap Control |
| PAO | Power Allocation Optimization |
| PS | Power System |
| PSO | Particle Swarm Optimization |
| PV | Photovoltaic |
| RPCE | Reactive Power Compensation Equipment |
| RPL | Reactive Power Loss |
| SC | Shunt Capacitor |
| SCADA | Supervisory Control and Data Acquisition |
| SMO | Spider Monkey Optimization |
| STATCOM | Static Synchronous Compensator |
| SVC | Static VAR Compensator |
| TC | Tap Changer |
| TOs | Tap Operations |
| UPFC | Unified Power Flow Controller |
| VAR | Volt AMP Reactive |
| VD | Voltage Deviation |
| VLC | Voltage Level Control |
| VSM | Voltage Stability Margin |
| VVC | Volt VAR Control |

# CHAPTER ONE

# INTRODUCTION

## 1.1 Background

Voltage stability has been identified as one of the most important operational needs for efficient and reliable operation of power system. This is due to the fact that both the utility and customer equipment are designed to operate at certain voltage ranges. Operating the equipment at voltage levels outside the allowable range could degrade the performance and may eventually lead to its damage Nasar, (1998). Unlike the case of changes in active power which affect mainly the system frequency, reactive power is majorly dependent on changing in voltage magnitude. As such, reactive power and voltage magnitude are controlled simultaneously as in the case of active power and frequency.

There are numerous techniques put in place to improve voltage stability and of course reactive power regulation in power system. These techniques are broadly classified into two categories;

*i*- Reactive power injection or absorption from the system using Flexible Alternating Current Transmission System (FACTS) devices

*ii*- Direct control of voltage magnitude using On Load Tap Changer (OLTC) Mohaammedian, (2011).

The first method is believed to be the fastest method however very expensive. The second technique, being the cheapest, involves the use of tap in one or more windings of the transformer to adjust its turns-ratio thereby altering the voltage magnitudes, and eventually regulate the reactive power. The Tap Changer (TC) is a connection point selection mechanism along a power transformer winding that allows a variable number of turns to be selected (turns-ratio adjustment) in discrete steps. TCs are vital components of the transformer for stabilizing the output voltage Alam and Pant, (2020). Generally, this tap selection can be carried using an automatic or manual tap changing mechanism which can operated off-load (off-line) or on-load (on-line). The off-load tap changing transformers are disconnected from the system when the tap setting is to be adjusted. This type of tap-change operation is normally applied where the need to adjust the turns-ratio is occasional because of load pattern and seasonal changes, hence manual operation is commonly used. While in the on-load tap-changing, the tap adjustment is carried out with the transformers connected. This kind of operation is normally applied where it is undesirable to de-energize the transformer.

Moreover, the manual tap changing mechanisms use mechanical components for the adjustment of the tap, while the automatic ones use solid state electronic components for its operation. TCs are

generally liable to develop mechanical faults, which are the most serious, alongside electrical and dielectric faults, which can cause catastrophic damage to transformers. Some 33% of faults with transformers with OLTCs have been ascribed to the tap changer mechanisms Liu, *et al.,* (2019). In addition, mechanical TCs produce audible acoustic emissions when they operate and these are likely to vary when they malfunction. It is evident that they are quite slower compared to their solid-state counterparts and is devoid of friction. Moreover, if the tap-settings (tap position on the transformer winding) is not carefully selected, the power quality can be adversely affected instead of improving it Efkarpidis, *et al*., (2016). This is why a lot of research works focus on determining the optimal tap-settings with a one or more objectives using heuristic or meta-heuristic optimization algorithms.

For instance, Millano (2011) presented a hybrid control model of on-load tap changers. The proposed model was based on the well-known discrete and continuous control models designed to preserves the discrete behavior of the tap ratio while allowing small signal stability and Eigen value analysis of the entire system. Abdollah *et al*., (2013) presented the use of Artificial Bee Colony Algorithm to determine the OLTC with a view of improving voltage regulation. In a similar research work, Shirvani *et al*., (2014) presented the application of on-load tap changer for voltage control. The research aimed at showing the effects of on-load tap changers for voltage control as well as showing OLTC on power system performance. The effect of tap-changing transformer on voltage stability is evaluated in El-Sadek, et al., (1999). Influence of tap-changing transformer on maximum transmitted power and nodes critical voltages, from the point of view of voltage stability, are clarified. Zhu, *et al*., (2000) addresses the effects of OLTC operation on voltage collapse from the point of view of how the limit of power transfer from the generation to the load center can be affected by OLTC operation. In another study in Li, *et al.,* (2018), an optimal tap control method is proposed to regulate OLTCs by minimizing the maximum deviation of the voltage profile from 1 p.u. on the entire feeder and at the same time reducing the number of tap operations (TOs), which is implemented for the optimization horizon based on voltage forecasts derived from high resolution Photovoltaic (PV) generation forecasts.

Moreover, Ratra, *et al*., (2018) proposes a Taguchi based method to determine the optimal tap settings of OLTCs including critical transformer to improve the voltage stability margin and decrease the real power loss of the system. The proposed method is tested on IEEE 30-bus system to validate its applicability.

Despite these research works carried out and some ongoing ones, there is need to apply a fast and reliable optimization technique to determine the optimal tap-settings with the view of improving the voltage stability (reduce bus voltage deviations) and reactive power regulation (reduce reactive power loss) devoid of violating the system constraints. Hence, in this research work, Grey Wolf Optimization (GWO) algorithm is applied to determine the optimal On-Load Tap Changing (OLTC) of the available

transformers in the system in order to improve the voltage stability and regulate reactive power. The constraints considered in the formulation of the problem are demand-generation balance, bus voltage limits, line thermal overloading limits and tap-changer adjustment limits. The technique is implemented on IEEE 14-bus, IEEE 30-bus and 57-bus Nigerian Transmission systems.

### 1.2 Problem Statement

Present power systems are operated under overstretch condition. This make voltage stability issue to be one of the major concerns in the operation and planning of power systems. Voltage stability problems normally occur in heavily overstretch systems and can be attributed to the weakness of the transmission lines. Other factors contributing to voltage instability are the generator reactive power limits, load characteristics and characteristics of reactive compensation devices. With aid of OLTC, the voltage stability of the system can be improved. However, with each tap changing operation, the line current would increase, thereby increasing the reactive power loss of the system. As a result, the reactive power output of the generators increases gradually and generators may reach to their reactive power capability limit. Beyond that generator loses their capability to support the system voltages. So, there is compromise between voltage stability improvements (reducing bus voltage deviation in this regard) and reactive loss minimization. Therefore, operation of OLTCs is critical for voltage stability and line losses of the system. As such, there is need to apply a recently developed meta-heuristic optimization algorithm to determine the OLTC of the available transformers in the system in order to minimize the voltage deviation and reactive power loss simultaneously. In this research work, Grey Wolf Optimization (GWO) algorithm is employed for this application subject to some system constraints.

### 1.3 Significance Contribution of the Research

**Comment [u1]:** Read the meaning of 'significance' in the dictionary and then re-write this section. generally speaking, this section will be better written at the end of th work.

The main contribution of this research is to develop a technique of determining an optimal OLTC of transformers in order to minimize voltage deviation and reactive power loss simultaneously in transmission network. The minimization is carried out subject to number of constraints like demand-generation balance, bus voltage limits, line thermal overloading limits and tap-changer adjustment limits (0.85 – 1.15p.u) according to IEEE C57.131 2012 requirements. In addition, applying the technique on real 57-bus, 330kV Nigerian transmission systems makes the research quite noteworthy. Another key contribution is the application of a recently developed meta-heuristic, swarm intelligent optimization algorithm for optimal tuning of OLTC transformer; GWO. The algorithm has a lot of advantages over the rest of its counterparts. Due to its ability to mimics the natural leadership of grey wolves, GWO rarely traps in local minima unlike other optimization algorithms. In addition, GWO algorithm is based on few parameters and easy to implement.

### 1.4 Aim and Objectives of the Study

The aim of this research is to determine the optimal On-Load Tap Changing (OLTC) of the transformers in transmission network with a view to minimize voltage deviation and reactive power loss simultaneously using Grey Wolf Optimization (GWO) algorithm. In order to achieve this aim, the following objectives are follows: -

*i-* Determination of the network's inherent voltage deviation, reactive power loss, admittance active power loss and impedances using Newton-Raphson power flow algorithm.

*ii-* Grey Wolf Optimization algorithm will be applied to the solution obtained from the formulation of the multi-objective function and constraints for the minimization of the voltage deviation and reactive power loss.

*iii-* Implementing the developed technique on IEEE 14-bus, IEEE 30-bus and 57-bus 330kV Nigerian transmission network and comparing the new systems operating conditions with those in *i*, using reactive power loss and voltage deviation as performance metrics.

### 1.5 Scope and Limitation

The main limitation of the assumption that OLTCs are adjusted in a continuous pattern instead of discrete steps. This assumption is far from reality. It is therefore recommended carrying out similar studies with discrete OLTC positions.

**Comment [u2]:** How does this affect the realization of any or all of your objectives?

# CHAPTER TWO

# LITERATURE REVIEW

## 2.1 Introduction

This chapter presents review of literature which comprises of the overview of fundamental concepts as well as the review of similar works. In the review of fundamental concepts, fundamentals of power system, transformer operation and related theories are reviewed, while in the review of similar works, literature survey on recent similar works was presented.

## 2.2 Review of Fundamental Concepts

In this subsection, fundamental concepts related to the study are reviewed. It covers overview of transformer on Load Tap-changer, power flow algorithms, and optimization techniques.

### 2.2.1 Power Quality

Power quality is a set of parameters that define the characteristics of the power supply as delivered to the consumers in normal operating conditions in terms of continuity of supply and characteristics of voltage such as, frequency, magnitude, waveform and symmetry. Recently, power quality is not only a technical problem but also a problem that leads to financial issues. Many surveys have been shown that poor power quality causes large economic losses to industrial sectors. Moreover, large amount of power is wasted due to poor power quality in the services. Determining the exact problems requires sophisticated electronic test equipment but the symptoms such as equipment failure during lightning and thunder storm, tripping of circuit breakers without being overloaded, automated system stopping for no apparent reason, electronic system failure on a frequent basis and also working of electronic system in one location but not in another location, help us to identify the PQ problems Pandu, (2009).

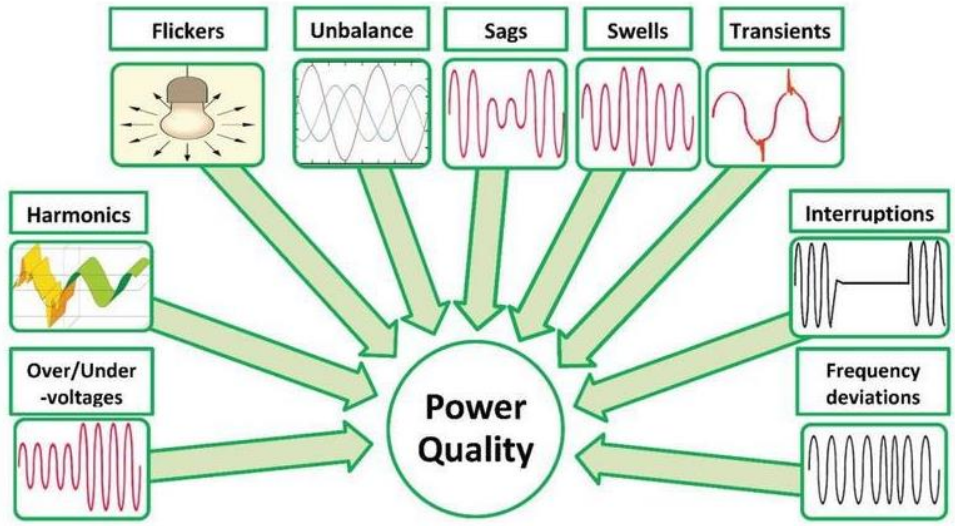


Fig. 2.1: Power Quality Sinik *et al.*, (2019)

*2.2.1.1 Classification of Power Quality Problem*

Power quality is a combination of voltage and current quality. In most cases the utility is responsible for voltage quality at the point of common coupling (PCC) while the consumers often influence the current quality at the PCC Bhattacharyya *et al.,* (2007).

*2.2.1.2 Power Quality Improvement Techniques and Solutions*

Power quality problems can be defined as the difference between the quality of power supplied and the quality of power required for reliable operation of the load equipment. Several types of power enhancement devices have been developed over the years to protect equipment from power disturbances. Some of the effective and economic measures can be identified as following:

1. Power conditioning devices
2. Custom power devices

### 2.2.2 Transformer On-Load Tap-changer

A tap changer is a mechanism in power transformer windings that allows adjustment of the transformer turns ratio in discrete steps. A transformer with a variable primary to secondary turns' ratio is formed, allowing stepped voltage regulation of the output. The mechanism of tap-changing can be made on-load or off-load Deakin, (2017).

An On-Load Tap Changer (OLTC) mechanism of power transformers is mainly applied voltage regulation. The tap changing process entails a transformer can be changed by addition and removal of the part of the windings from the transformer circuitry in order to adjust the turn ratio. As the name implies, tap changing is carried out when the power transformer is energized. With transformers equipped with OLTC the voltage can be controlled within acceptable range. Although the OLTC can be placed on any of the transformer windings, it is always recommended that the OLTC is placed on the high voltage (HV) side. This is due to the fact that the current on the HV winding is lower than the low voltage (LV) windings and as such the commutation is easier as the tap changer contacts, leads can be smaller. Another reason for placing OLTC on HV winding is that there is higher number of turns available on the HV side than the LV. It therefore gives more room for tap position thereby increasing the precision and accuracy of the voltage regulation Zhu, *et al.,* (2000).

Figure 2.2 shows the connections for an on-load tap changer that operates on the HV winding of the transformer.

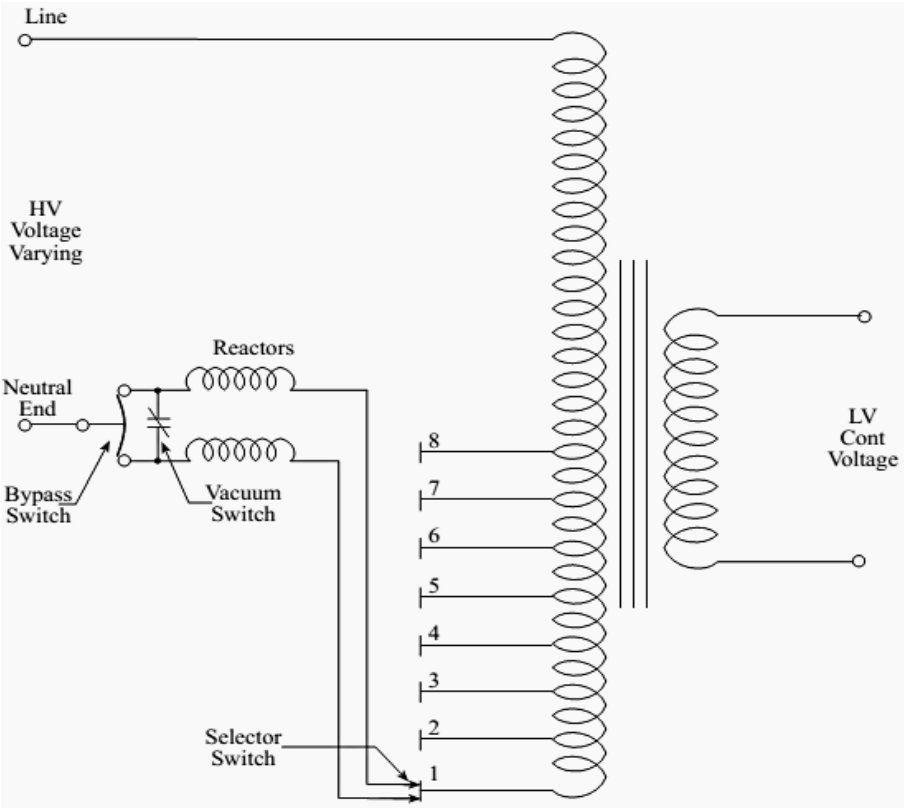


Figure 2.2 On-Load Tap Changer Circuit Viawan, (2008).

The tap changer mechanism has four essential features:

*1. Selector Switches*

These switches select the physical tap position on the transformer winding and, because of their construction, cannot and must not make or break the load current.

*2. Reactors*

The load current must never be interrupted during a tap change. Therefore, during each tap change, there is an interval where two voltage taps are spanned. Reactors (inductors) are used in the circuit to increase the impedance of the selector circuit and limit the amount of current circulating due to this voltage difference. Under normal load conditions, equal load current flows in both halves of the reactor windings and the fluxes balance out giving no resultant flux in the core. During the tap change, the selector switches are selected to different taps (see Figure 2) and a circulating current will flow in the reactor circuit. This circulating current will create a flux and the resulting inductive reactance will limit the flow of circulating current.

*3. Vacuum Switch*

This device performs the duty of a circuit breaker that makes and breaks current during the tap changing sequence Kothari and Nagrath, (2003).

*4. Bypass Switch*

This switch operates during the tap changing sequence but, at no time, does it make or break load current, though it does make before break each connection. Changing to any other tap position is done similarly with the selector switch always moving sequentially. The operating mechanism for the on-load tap changer is motor driven. Manual operation is used in the event of motor failure. The sequence of operation is mechanically linked, or interlocked, to ensure that all contacts always operate in their correct order. Any failure of the operating mechanism can result in severe damage to the transformers and tap changers Kothari and Nagrath, (2003).

### 2.2.3 Transmission Line Model with Tap-changing Transformer

A transformer with off nominal turns ratios can be represented by its impedance, or admittance, connected in series with an ideal autotransformer. With an off-nominal ratio, it is necessary to modify the admittance to include the effect of changing turns ratio. Consider a transmission line tapped at both ends with a view of compensating voltage drop as shown in Figure 2.3

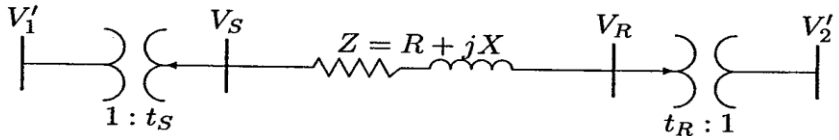

Figure 2.3 Transmission Line with tap changing transformers at both ends Saadat, (1999).

By placing at one phase of the three-phase transmission line a sep-up transformer at the sending end and a step-down transformer at the receiving end of the line. Referring to the single line representation of the set-up shown in Figure 2.3, where $t_s$ and $t_r$ are the tap settings in per-unit, $V_1'$ represent the supply phase voltage referred to the HV side and $V_2'$ is the load phase voltage, also referred to the HV side. The impedance shown comprises of the both the line impedance and the referred impedances of the sending end and the receiving end transformers to the HV side.

With the source and receiving end voltages $V_s$ and $V_r$ in phase, the phasor diagram describing the voltages and line current is shown in Figure 2.4

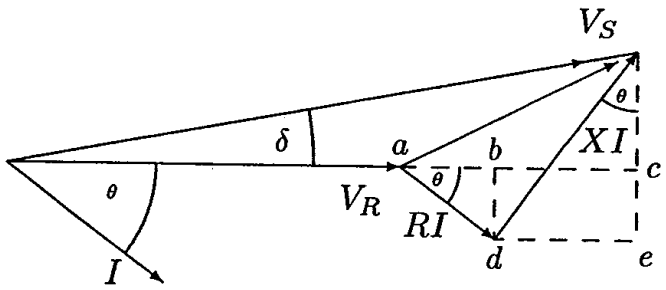


Figure 2.4 Voltage phasor diagram Saadat, (1999).

Thus,

$$V_R = V_S + (R + jX)I \tag{2.1}$$

The phase shift $\delta$ between the two ends of the line is usually small, as such the vertical component of $V_s$ can be neglected. Approximating the $V_s$ with its horizontal component results in

$$|V_S| = |V_R| + \overline{ab} + \overline{de} \tag{2.2}$$

$$= |V_R| + |I|Rcos\theta + |I|Xsin\theta \tag{2.3}$$

Substituting $|I|$ for $P_\phi = |V_R||I|cos\theta$ and $Q_\phi = |V_R||I|sin\theta$, (2.3) is modified to

$$|V_S| = |V_R| + \frac{RP_\phi + XQ_\phi}{|V_R|} \tag{2.4}$$

Where $P_\phi$ and $Q_\phi$ are the active and reactive power on the phase under consideration.

Since

$$V_S = t_S V_1' \tag{2.5}$$

And

$$V_R = t_R V_2' \tag{2.6}$$

Rearranging (2.4) – (2.6),

$$t_S|V_1'| = t_R|V_2'| + \frac{RP_\phi + XQ_\phi}{t_R|V_2'|} \tag{2.7}$$

Similarly,

$$t_S = \left(t_R|V_2'| + \frac{RP_\phi + XQ_\phi}{t_R|V_2'|}\right)|V_1'|^{-1} \tag{2.8}$$

By assuming the product of the sending and receing end tap setting, $t_s$ and $t_r$ to be unity

$$t_S = \sqrt{\frac{|V_2'|}{|V_1'|}\Big/\left(1 - \frac{RP_\phi + XQ_\phi}{|V_1'||V_2'|}\right)} \tag{2.9}$$

### 2.2.4 Power Flow Analysis of Power System Network

Power flow commonly known as load flow is one of the three major problems encountered in symmetrical steady state of power system (PS) operation. The other two are optimal load scheduling and systems control problems. Load Flow Analysis (LFA) in PS is the steady state solution of the system network.

#### *2.2.4.1 Advantages of LFA*

It has many advantages in maintaining stable and reliable operations of PS, among which are:-

*(i)* It helps in determining whether system parameters remain within specified limits under various contingency conditions, or equipment such as transformers, and conductors (transmission lines) are overloaded.

*(ii)* LF studies are used to identify the need for additional generation, capacitive, or inductive VAR support, or the placement of capacitors and/or reactors to maintain system voltages within specified limits.

*(iii)* It can be used to ascertain how efficient a system is by computing the losses on each branch and total system power losses.

*(iv)* It aids proper planning, economic scheduling, and control of an existing system as well as planning its future expansion.

*(v)* LFA is also required for transient stability and contingency studies.

The main information obtained from this study, under given load conditions comprises of the following (Saadat, 1999):-

*i.* voltage magnitude at *i*th bus, $|V_i|$

*ii.* voltage phase angle at *i*th bus, $\delta_i$

*iii.* active power at *i*th bus, $P_i$

*iv.* reactive power at *i*th bus, $Q_i$

*v.* active power flow between *i*th and *j*th bus, $P_{ij}$

*vi.* reactive power flow between *i*th and *j*th bus, $Q_{ij}$

The first four information are associated with buses while the last two are for lines (branches).

*2.2.4.2 Bus Classification*

Usually two variables (out of the four) at each bus are assumed known, while the other two variables are treated as state variables to be solved. According to the original data, the buses can be classified into three types; load (P-Q) buses, regulator (PV) buses and slack (reference) bus.

*A. Load (P-Q) Nodes*

Load buses (also known as P-Q buses) are substation buses where customers are being supplied. They are the most predominant buses in real PS. At these buses, load powers are known (from load forecasting) and are given constants. Hence for LFA, active and reactive power (*P* and *Q*) are specified as known parameters, and the voltage magnitudes, $|V|$ and their respective phase angles, $\delta$ are to be resolved. *P* and *Q* at load buses remain constant throughout the LFA Saadat, (1999).

*B. Regulator (P-V) buses*

Regulator buses (also known as P-V buses) are buses that are equipped with controllable reactive power resources like capacitors and FACTS devices (like STATCOM, SVC, DVR, UPFC) and can thus maintain bus voltage magnitude at a desirable value. There are usually many voltages regulator buses in typical PS network but certainly not as much as load buses. At these buses, active power, *P* and voltage magnitude, $|V|$ are specified as known variables, while reactive power *Q* and voltage phase angle, $\delta$ are to be calculated. Generally, buses of power plants are taken as P-V nodes (except slack bus), because voltages at these buses can be controlled with reactive power capacity of their generators Saadat, (1999).

*C. Slack (Swing) bus*

Among the set of power plant buses, one is chosen as slack, reference or swing bus. This bus is always characterized by specified constant phasor voltage ($|V|$ and $\delta$). Therefore, the active and reactive power (*P* and *Q*) variables to be solved. The effective generator at this node supplies the losses to the network. This is necessary because the magnitude of losses will not be known until the calculation of currents is complete, and this cannot be achieved unless one node has no power constraint and can feed the required losses into the system. The location of the slack node can significantly influence the complexity of the calculations; the bus most closely approaching a large AGC power station should be used. Table 2.1 summarizes the buses classification Saadat, (1999).

Table 2.1: Bus Classification Tiwari, *et al*., (2018 )

| **Bus type** | Quantities/ Variables | | | |
|---|---|---|---|---|
| | *P* | *Q* | $\|V\|$ | *Δ* |
| Slack/ Swing | Not specified | Not specified | Specified | Specified |
| Regulated (P-V) | Specified | Not specified | Specified | Not specified |
| Load (P-Q) | Specified | Specified | Not specified | Not specified |

*2.2.4.3 Power Flow Equations*

PS comprises several buses which are interconnected by means of transmission lines. Power is injected into a bus from generators while loads supplied with power from the same or another bus. Of course, there may be buses with only generators and no-loads, and there may be others with only loads and no generator. In addition, VAR generators may also be connected to some buses. The surplus power at some of the buses is transported via transmission lines to deficient buses. LFA provides a balanced steady operation state of the PS, without considering system transient processes. Hence, the mathematical model of load flow problem is a nonlinear algebraic equation system without differential equations. Consider a typical bus, *i* connected to *n* number of buses as shown in Figure 2.5 Saadat, (1999).

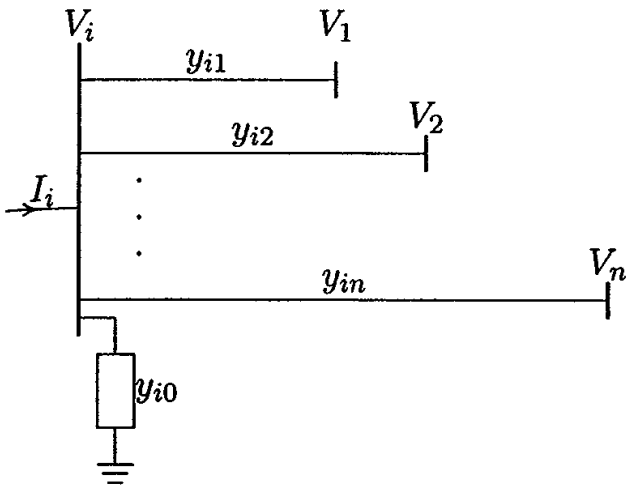


Figure 2.5 Typical bus in power system Saadat, (1999)

The injection current at *i*th bus, $I_i$ is obtained by applying KCL at the bus.

$$I_i = y_{i0}V_i + y_{i1}(V_i - V_1) + y_{i2}(V_i - V_2) + \cdots + y_{im}(V_i - V_m) \tag{2.10}$$

$$= V_i \sum_{j=0}^{m} y_{ij} - \sum_{j=1}^{m} y_{i1}V_j\,; \qquad j \neq i \tag{2.11}$$

The net active and reactive power at the bus is

$$S_i = P_i + jQ_i = V_i I_i^* \tag{2.12}$$

where $P_i$, $Q_i$ are the injected active and reactive power at bus *i*, respectively. While $I_i^*$ is the complex conjugate of the injection current at bus *i.* Thus,

$$I_i = \frac{P_i - jQ_i}{V_i^*} \tag{2.13}$$

Substituting for $I_i$ in the power equation,

$$\frac{P_i - jQ_i}{V_i^*} = V_i \sum_{j=0}^{m} y_{ij} - \sum_{j=1}^{m} y_{i1}V_j; \quad j \neq i \tag{2.14}$$

Mathematical formulation of LFA leads to a system of algebraic non-linear equations that requires iterative techniques for its solution Kiusalaas, (2005).

*2.2.4.4 Power Flow Solution*

Mathematically, load flow is a problem of solving a system of nonlinear algebraic equations. Its solution usually cannot avoid some iterative process. Thus, reliable convergence becomes the prime criterion for a load flow calculation method.

With the scale of real power system continually expanding, the dimension of load flow equations now becomes very high (several thousands to tens of thousands). For the equations with such high dimensions, it cannot be guaranteed that any mathematical method can converge to an exact solution. The most common techniques used for iterative solution of non-linear algebraic equations are Gauss-Seidel, Newton-Raphson and Fast Decoupled method Kiusalaas, (2005).

### *A. Gauss-Seidel Solution of LFA*

Gauss-Seidel iterative (indirect) method for solving non-linear simultaneous equations. To start with, an initial solution vector is assumed, based on practical experience in a physical situation. One of the equations is then used to obtain the revised value of a particular variable by substituting in it the present values of the remaining variables. The solution vector is immediately updated in respect of this variable. The process is then repeated for all the variables thereby completing one iteration. The process is then repeated until the iteration solution converges. The convergence is quite sensitive to the initial values assumed.

By solving (2.14) for $V_i$, the iterative sequence resolves to

$$V_i^{(k+1)} = \frac{\frac{P_i - jQ_i}{V_i^{*(k)}} + \sum y_{ij} V_j^{(k)}}{\sum y_{ij}} \quad j \neq i \tag{2.15}$$

where $y_{ij}$'s are the actual line admittances in *per unit.* Using Kirchhoff current law, it is assumed that the current injected into bus *i* is positive, then the real and the reactive powers supply into the buses, such as generator buses have a positive value. The real and the reactive powers flowing away from the buses, such as load buses have a negative value. *Pi* and *Qi* are solved from (2.14) which gives (for $j \neq i$) Kiusalaas, (2005).

$$P_i^{(k+1)} = real\left\{V_i^{*(k)}[V_i^{(k)}\sum_{j=0}^{n} y_{ij} - \sum_{j=0}^{n} y_{ij}V_j^{(k)}]\right\} \quad (2.16)$$

$$Q_i^{(k+1)} = -Im\left\{V_i^{*(k)}\left[V_i^{(k)}\sum_{j=0}^{n} y_{ij} - \sum_{j=0}^{n} y_{ij}V_j^{(k)}\right]\right\} \quad (2.17)$$

The complex powers from bus *i→j,* $S_{ij}$ and from bus *j→i,* $S_{ji}$ are

$$S_{ij} = V_i I_{ij}^{*(k)} \quad (2.18)$$

$$S_{ji} = V_j I_{ji}^{*(k)} \quad (2.19)$$

The power loss along line *ij,* is the algebraic sum of the complex apparent powers

$$S_{Lij} = S_{ij} + S_{ji} \quad (2.20)$$

Due to its linear convergence, Gauss-Siedel iterative technique is quite slow. Hence, the need to speed it up arises. An acceleration factor, $\alpha$ is used to accelerate the iteration. Instead of using the newly calculated solution in each iteration, it is updated using (2.21) Kiusalaas, (2005).

$$V_{i\,(acc)}{}^{(k+1)} = V_i{}^{(k)} + \alpha\left(V_i{}^{(k+1)} - V_i{}^{(k)}\right) \quad (2.21)$$

A suitable value of $\alpha$ for any system can be obtained by trial load flow studies. It is generally recommended to take the value of $\alpha$ as 1.6. A wrong choice of acceleration factor may indeed slow down convergence or even lead to divergence Kiusalaas, (2005).

### *B. Newton Raphson Solution of LFA*

The Newton-Raphson (N-R). method is a powerful and fast technique of solving non-linear algebraic equations. It is mathematically superior to Gauss-Siedel due to its quadratic convergence. It is less susceptible to divergence with ill-conditioned problems. It is indeed the most practical technique of load flow solution of large power networks imbedded in SCADA systems. The number of iterations

required to obtain a solution is independent of the system size unlike Gauss-Siedel (Kothari & Nagrath, 2003; Elgard, 1976). The N-R load flow is central to many recently developed methods for the optimization of power system operation, sensitivity analysis, system-state estimation, linear-network modelling, security evaluation and transient stability analysis, and it is well suited to online computation Li, *et al.*, (2018). Its main drawback is the requirement of more functional evaluation which costs for more computer memory.

For an arbitrary bus *i*, the injection current $I_i$ is resolved in terms of bus admittance matrix as;

$$I_i = \sum_{j=1}^{m} Y_{ij} V_j \qquad j = 1,2, \dots, i, \dots, m \tag{2.22}$$

$$I_i = \sum_{j=1}^{m} |Y_{ij}||V_j| \angle \theta_{ij} + \delta_j \tag{2.23}$$

Where $\theta_{ij}$ is the phase difference between bus *i* and *j.* substituting (2.23) in (2.14) leads to,

$$P_i - jQ_i = |V_i| \angle -\delta_i \sum_{j=1}^{m} |Y_{ij}||V_j| \angle \theta_{ij} + \delta_j \tag{2.24}$$

Separating the active and imaginary part,

$$P_i = \sum_{j=1}^{m} |V_i||V_j||Y_{ij}| cos(\theta_{ij} - \delta_i + \delta_j) \tag{2.25}$$

$$Q_i = -\sum_{j=1}^{m} |V_i||V_j||Y_{ij}| \sin(\theta_{ij} - \delta_i + \delta_j) \tag{2.26}$$

Equations (2.25) and (2.26) forms a set of non-linear algebraic equations in terms of the independent variables; $|V|$, $\delta$ (in radians). Based on the known and unknown variables at each bus, it can be seen that there are two equations for each PQ bus and one equation for each PV bus. By neglecting all the higher Taylor series expansion of (2.25) and (2.26) about initial estimate, the following system of equation is obtained Kiusalaas, (2005).

$$\begin{bmatrix} \Delta P_2^{(k)} \\ \vdots \\ \Delta P_n^{(k)} \\ \Delta Q_2^{(k)} \\ \vdots \\ \Delta Q_n^{(k)} \end{bmatrix} = \begin{bmatrix} \frac{\partial P_2}{\partial \delta_2}^{(k)} & \cdots & \frac{\partial P_2}{\partial \delta_n}^{(k)} & \frac{\partial P_2}{\partial |V_2|}^{(k)} & \cdots & \frac{\partial P_2}{\partial |V_2|}^{(k)} \\ \vdots & \ddots & \vdots & \vdots & \ddots & \vdots \\ \frac{\partial P_n}{\partial \delta_2}^{(k)} & \cdots & \frac{\partial P_n}{\partial \delta_n}^{(k)} & \frac{\partial P_n}{\partial |V_2|}^{(k)} & \cdots & \frac{\partial P_n}{\partial |V_n|}^{(k)} \\ \frac{\partial Q_2}{\partial \delta_2}^{(k)} & \cdots & \frac{\partial Q_2}{\partial \delta_n}^{(k)} & \frac{\partial Q_2}{\partial |V_2|}^{(k)} & \cdots & \frac{\partial Q_2}{\partial |V_n|}^{(k)} \\ \vdots & \ddots & \vdots & \vdots & \ddots & \vdots \\ \frac{\partial Q_n}{\partial \delta_2}^{(k)} & \cdots & \frac{\partial Q_n}{\partial \delta_n}^{(k)} & \frac{\partial Q_n}{\partial |V_2|}^{(k)} & \cdots & \frac{\partial Q_n}{\partial |V_n|}^{(k)} \end{bmatrix} \begin{bmatrix} \Delta \delta_2^{(k)} \\ \vdots \\ \Delta \delta_n^{(k)} \\ \Delta \left| V_2^{(k)} \right| \\ \vdots \\ \Delta \left| V_n^{(k)} \right| \end{bmatrix} \tag{2.27}$$

Bus 1 assumed to be the swing bus, hence is not included in the system of equations. The system is represented as (Saadat, 1999);

$$\begin{bmatrix} \Delta P \\ \Delta Q \end{bmatrix} = \begin{bmatrix} J_1 & J_2 \\ J_3 & J_4 \end{bmatrix} \begin{bmatrix} \Delta \delta \\ |V| \end{bmatrix} \tag{2.28}$$

The solution is extracted from the elements of the Jacobian matrices, $J_1$, $J_2$, $J_3$ and $J_4$.

- The diagonal elements of $J_1$ are:-

$$\frac{\partial P_i}{\partial \delta_i} = \sum_{j \neq i} |V_i||V_j||Y_{ij}| sin(\theta_{ij} - \delta_i + \delta_j) \tag{2.29}$$

- The off-diagonal elements of $J_1$ are:-

$$\frac{\partial P_i}{\partial \delta_j} = -|V_i||V_j||Y_{ij}| sin(\theta_{ij} - \delta_i + \delta_j) \quad j \neq i \tag{2.30}$$

- The diagonal elements of $J_2$ are:-

$$\frac{\partial P_i}{\partial |V_i|} = 2|V_i||Y_{ii}| cos\theta_{ii} + \sum_{j \neq i} |V_j||Y_{ij}| cos(\theta_{ij} - \delta_i + \delta_j) \tag{2.31}$$

- The off-diagonal elements of $J_2$ are:-

$$\frac{\partial P_i}{\partial |V_j|} = |V_j||Y_{ij}| cos(\theta_{ij} - \delta_i + \delta_j) \quad j \neq i \tag{2.32}$$

Saadat, (1999).

- The diagonal elements of $J_3$ are:-

$$\frac{\partial Q_i}{\partial \delta_i} = \sum_{j \neq i} |V_i||V_j||Y_{ij}|cos(\theta_{ij} - \delta_i + \delta_j) \tag{2.34}$$

- The off-diagonal elements of $J_3$ are:-

$$\frac{\partial Q_i}{\partial \delta_j} = -|V_i||V_j||Y_{ij}|cos(\theta_{ij} - \delta_i + \delta_j) \quad j \neq i \tag{2.35}$$

- The diagonal elements of $J_4$ are:-

$$\frac{\partial Q_i}{\partial |V_i|} = -2|V_i||Y_{ii}|sin\theta_{ii} - \sum_{j \neq i} |V_j||Y_{ij}|\, sin(\theta_{ij} - \delta_i + \delta_j) \tag{2.36}$$

- The off-diagonal elements of $J_4$ are:-

$$\frac{\partial Q_i}{\partial |V_i|} = -|V_j||Y_{ij}|\, sin(\theta_{ij} - \delta_i + \delta_j) \quad j \neq i \tag{2.37}$$

At each iteration, *k*, the power residuals are calculated as

$$\Delta P_i^{(k)} = P_i - P_i^{(k)} \tag{2.38}$$

$$\Delta Q_i^{(k)} = Q_i - Q_i^{(k)} \tag{2.39}$$

While the voltage magnitude and phase angles are updated as;

$$\delta_i^{(k+1)} = \delta_i^{(k)} - \Delta\delta_i^{(k)} \tag{2.40}$$

$$\left|V_i^{(k+1)}\right| = \left|V_i^{(k)}\right| + \Delta\left|V_i^{(k)}\right| \tag{2.41}$$

Saadat, (1999).

### 2.2.5 Optimization Algorithm

An optimization algorithm is a procedure which is executed iteratively by comparing various solutions till an optimum or a satisfactory solution is found. A simple optimal design is achieved by comparing a few (limited up to ten or so) alternative solutions created by using a priori problem knowledge. In this method feasibility of each design solution is first investigated. Thereafter an estimate of underlying objective of each solution is compared and best solution is adopted. Figure 2.6 shows an outline of the steps usually involved in an optimal design formulation.

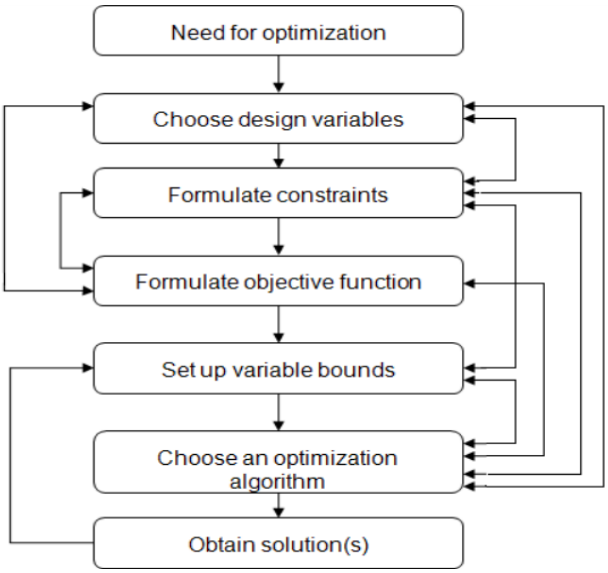


Figure 2.6: Flowchart of Optimal Design Procedure Das *et al*., (2009)

There are numerous heuristic and meta-heuristic optimization algorithms available for solving different engineering problems. This includes Genetic Algorithm, particle swarm optimization, Evolution Strategies, Simulated Annealing, Shuffled Frog-Leaping Algorithm, firefly algorithm, Bat Algorithm, Ant Colony Optimization, Cuckoo Search Algorithm, Ant Colony Optimization, Artificial Bee Colony, Fish Swarm Algorithm, Glowworm Swarm Optimization, Grey Wolf Optimizer (GWO), Fruit Fly Optimization Algorithm, Bat Algorithm, Novel Bat Algorithm, Dragonfly Algorithm, Cat Swarm Optimization, Cuckoo Search Algorithm, Cuckoo Optimization Algorithm, and Spider Monkey Optimization (SMO) Algorithm, among others (Mirjalili, et al., 2014; Mittal, et al., 2016; Rajabioun, 2011). The nature of the problem and the required solution inform the choice of the algorithm to be used. These algorithms are broadly classified as heuristic and meta-heuristic. Those in the latter class are further classified as evolutionary, swarm based and trajectory algorithms as shown in Figure 2.7 Das *et al*., (2009)

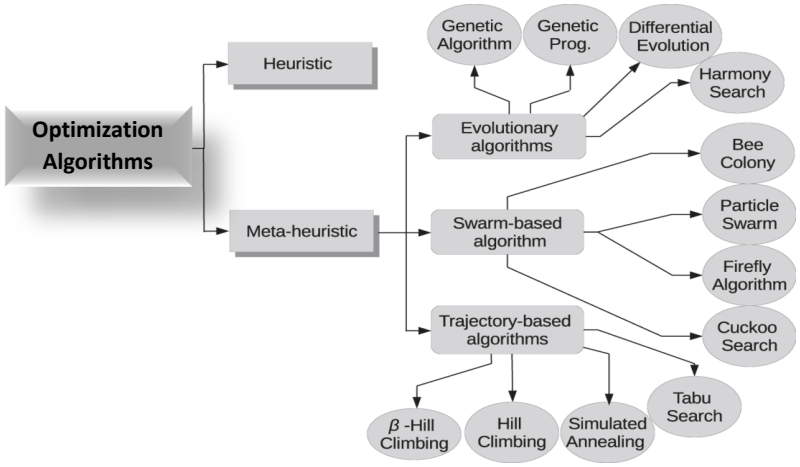


Figure 2.7 Classification of optimization algorithms Das, *et al.*, (2009)

Among these algorithms, GWO stands out due to some features, hence it is chosen for this study.

*2.2.5.1 Grey Wolf Optimizer*

GWO is a recently developed swarm-intelligence meta-heuristics inspired from the leadership hierarchy and hunting mechanism of grey wolves in nature and has been successfully applied for solving economic dispatch problems, feature subset selection, optimal design of double later grids, time forecasting, flow shop scheduling problem and optimal power flow problem. Grey wolves are considered as apex predators; they have average group size of 5–12. In the hierarchy of GWO, alpha ($\alpha$) is considered the most dominating member among the group. The rest of the subordinates to α are beta ($\beta$) and delta ($\delta$) which help to control the majority of wolves in the hierarchy that are considered as omega ($\omega$). The wolves are of lowest ranking in the hierarchy.

The mathematical model of hunting mechanism of grey wolves consists of these processes:

(i) Tracking, chasing, and approaching the prey.

(ii) Pursuing, encircling, and harassing the prey until it stops moving.

(iii)Attacking the prey.

***Encircling Prey***

Grey wolves encircle the prey during the hunt which can be mathematically written as follows:

$$\vec{D} = \left|\vec{C} \odot \vec{X}^*(t) - \vec{X}^*(t)\right| \quad (2.42)$$

$$\vec{X}^*(t+1) = \vec{X}^*(t) - \vec{A} \odot \vec{D} \quad (2.43)$$

where *D* describes the distance between the position vector of both the prey $X(t)^*$ and a whale *X(t)*, and t denotes the current iteration number. A and C are coefficient vectors, and defined as follows:

$$\overrightarrow{A} = 2\vec{a} \odot \vec{r} - \vec{a} \quad (2.44)$$

$$\vec{C} = 2\overrightarrow{r} \quad (2.45)$$

where *a* is linearly decreased from 2 to 0 over the course of iterations (in both exploration and exploitation phases) and *r* is a random vector in [0,1]. The position *(X, Y)* of a search agent can be updated according to the position of the current best record ( $X^*$, $Y^*$). Different places around the best agent can be achieved with respect to the current position by adjusting the value of *A* and *C* vector. The same concept can be extended to a search space with *n* dimensions, and the search agents will move in hyper-cubes around the best solution obtained so far.

***Hunting***

Hunting of prey is usually guided by $\alpha$ and $\beta$, and $\delta$ will participate occasionally. The best candidate solutions, that is, $\alpha$, $\beta$, and $\delta$, have better knowledge about the potential location of prey. The other search agents ($\omega$) update their positions according to the position of three best search agents.

The GWO algorithm is described briefly with the following steps: -

- *Step 1:* Initialize the GWO parameters such as search agents, design variable size, vectors and maximum number of iterations.
- *Step 2:* Generate wolves randomly based on size of the pack.
- *Step 3:* Estimate the fitness value of each hunt agent
- *Step 4:* identify the best hunt agent, the second-best hunt agent and the third best hunt agent,
- *Step 5:* Renew the location of the current hunt agent

*Step 6:* Estimate the fitness value of all hunts.

*Step 7:* Update the value of best hunt agent, the second-best hunt agent and the third best hunt agent,

*Step 8:* Check for stopping condition i.e., whether the Iter reaches Itermax, if yes, print the best value of solution otherwise go to *step* 5.

Figure 2.8 shows the flowchart of the GWO algorithm.

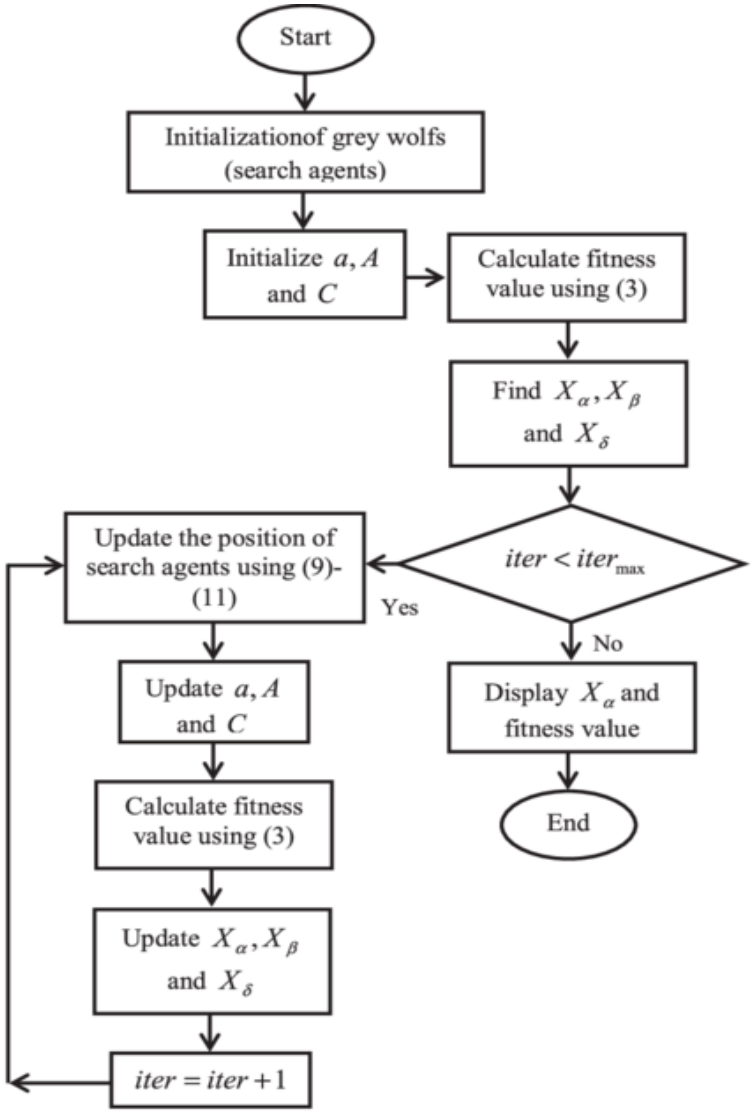


Figure 2.8 Flowchart of GWO Agarwal, *et al*., (2018)

**2.3 Review of Similar Works**

This sub-section presents a review of some relevant works carried out and published by other researchers. This gives an indication of the extent of the work in this area of research and the techniques or mechanisms used to resolve the same problem. It also covers some limitations of the reviewed works.

**El-Sadek, *et al.,* (1999)** evaluated the effect of tap-changing transformers on voltage stability of power systems. In addition, impact of tap-changing transformers on maximum transmitted power and nodes critical voltages, from the point of view of voltage stability, are also clarified. Based on the simulation results obtained, at off-nominal tap ratio of 0.79 in the studied system, voltage stability is at its maximum state. Below or over this value, degree of voltage stability will decrease and can go to a state of instability. Once more, off nominal tap ratios less than 0.45 will lead to unstable operations of the power system. However, the tap settings used for the evaluation of the impact of tap-changing transformers on maximum transmitted power and nodes critical voltages is not optimized. As such, the conclusion drawn on the degree of voltage stability is quite weak.

**Mohammadian, *et al*., (2011)** proposes a novel strategy based on Ant Colony Optimization algorithm to improve the voltage stability of the power systems with respect to minimum real power loss and proper voltages profile. The algorithm uses optimum settings of On-Line Tap Changer transformer (OLTC) and minimum number of Reactive Power Compensation Equipment (RPCE). The proposed algorithm is programmed on MATLAB and examine on IEEE 30-bus Test System to demonstrate the validity and the convenience of ACO approach with promising results. The voltage stability improvement and loss minimization in a power system are two objects considered by ACO. According to the results, the values of OLTCs and RPCEs proposed by the ACO have successfully improved the voltage stability of system. Also, the loss of active power has been decreased. Despite the improvement obtained, some voltages are outside allowable range of ±5% *pu*.

**Efkarpidis, *et al*., (2016)** proposes an optimization scheme to control both voltage magnitudes and voltage unbalances of LV distribution grids, OLTC distribution transformers, photovoltaic (PV) inverters, and batteries. Both the technical and cost models are taken into account for each of the aforementioned components, while the total cost function is constructed from the perspective of both distribution system operators' and domestic consumers' cost. The performance of the approach is investigated on a typical rural Flemish feeder. In addition, the violations of both voltage and voltage unbalance statutory limits, as well as the OLTC positions and the power utilization of both PV inverters and batteries are also examined. From the result analysis, it is concluded that the method could fully eliminate any existing violations of both under-voltage and 450 over-voltage statutory limits. Nevertheless, the applied method might increase the voltage unbalance of the grid, because of the

individual tap-change control of each phase. It was also noticed that the energy capacity of the batteries, the reactive power utilized by PVs, as well as the OLTC range are only partially exploited.

**Deakin, *et al.*, (2017)** studied the rationale, basis, and potential for continuous and event-driven online chromatic acoustic monitoring of transformers and their OLTCs. The feasibility has been demonstrated and system capabilities outlined, with large, complex, dynamic online data sources for using noninvasive, retrofittable, RF immune fiber-optic acoustic monitors incorporating chromatic analysis software and 3G communications to enable transformers and their OLTC equipment to be continuously monitored over relatively long periods for evaluating normal and potentially emerging abnormal behavior. However, overall acoustic transformer behavior trends can be monitored as well as trends in individual TC events, surges, level changes, and other events plus, at a deeper third level, details of the internal aspects of TCs.

**Morina, et al., (2017)** presents an original procedure to embed the OLTC nonlinearities in a predictive real-time Volt Var Control (VVC) for distribution systems. These commonly disregarded nonlinearities are namely the OLTC time-delays, the dead-band and the discrete nature of tap change. It is shown that using a continuous approximation can lead to control failures. The proposed nonlinear controller accurately anticipates the response of the system and the costs associated with control efforts. Demonstrations are performed in a 20 kV network to assess the performance of such a procedure compared to a predictive VVC using an OLTC continuous approximation. The resolution of the MPC turns into a problem with both integer and real values which calls for the use of a MINLP solver. In the study, solver BNB of the MATLAB toolbox YALMIP based on an implementation of a standard branch and bound algorithm for mixed integer programming is chosen. As acknowledged in the paper, the sensitivity of the proposed procedure with respect to errors and inaccuracies in the model is not analyzed.

**Tareen, *et al.*, (2017)** the inverter connects the renewable energy sources and power distribution network systems for the conversion of power. Therefore, this review would potentially help industrial researchers improve power quality in PV and WT energies and power distribution network systems.

**Kay & Khaing, (2018)** presents the co-operation of OLTC and shunt capacitor for power quality improvement in order to be convenient both at substation and at each load bus, various locations and various ratings of SC were considered for different load conditions in daily load cycle. In order to be convenient at both substation and loads, locations and ratings of SC to install are considered with different cases for various load conditions at OLTC Gauss-Sidel iterative algorithm and MATLAB software were used for simulations of power flow solutions. The study set tap movement of OLTC at a fixed position, to get voltage within ±5% and power factor between 0.9 and 1 both at OLTC's terminal

and at each bus for all conditions of daily load cycle. After installing SC, pf is improved and OLTC can generate more real power. At that state, more loads can be extended at the system. Then, SC reduced reactive power from source of the system to its location. Despite the reduction obtained in the reactive power, the technique is quite slow due to the use of Gauss-Siedel iterative algorithm for the power flow solution.

**Li, *et al.,* (2018)** proposed an Optimal Tap Control (OTC) to regulate OLTCs by minimizing the maximum deviation of the voltage profile from 1 p.u. on the entire feeder. A secondary objective is to reduce the number of tap operations (TOs), which is implemented for the optimization horizon based on voltage forecasts derived from high resolution PV generation forecasts. A linearization technique is applied to make the optimization problem convex and able to be solved at operational timescales. Simulations on a PC show the solution time for one time step is only 1.1 s for a large feeder with 4 OLTCs and 1623 buses. OTC results are compared against existing methods through simulations on two feeders in the Californian network. OTC is firstly compared against an advanced rule-based Voltage Level Control (VLC) method. OTC and VLC achieve the same reduction of voltage violations, but unlike VLC, OTC is capable of coordinating multiple OLTCs. Scalability to multiple OLTCs is therefore demonstrated against a basic conventional rule-based control method called Autonomous Tap Control (ATC). Comparing to ATC, the test feeder under control of OTC can accommodate around 67% more PV without over-voltage issues. However, since OTC relies on accurate solar and power demand forecast to optimize tap positions of the OLTCs, its effectiveness of voltage regulation has been dreadfully compromised by forecasts with low accuracy.

**Ratra, *et al.,* (2018)** proposes a Taguchi optimization-based method to find optimal tap settings of OLTCs including critical transformer to improve the voltage stability margin and decrease the real power loss of the system. The proposed method tested on IEEE 30-bus system to validate its applicability. The behavior of tap setting of OLTCs is investigated, and critical transformer and its allowed range of tap settings is identified. The technique has two objectives. First objective of real loss minimization while the second is the enhancement of voltage stability margin (VSM). Above critical tap ratio, the critical transformer loses its effectiveness. If tapping are raised above critical value, the voltage is pulled down, voltage stability margin decreases, line current and real power loss of the system increases. Optimal tap settings based upon proposed method for a given load optimizes the overall performance of the system, thereby minimizing the active power loss and improving the voltage stability. However, Taguchi optimization algorithm is trajectory-based, as such the effectiveness of the technique decreases with the increase in the system size.

**Liu, *et al.,* (2019)** proposed an OLTC & inverter coordinated regulation method. In the study, fuzzy controller is implemented to coordinate the OLTC and power allocation optimization (PAO) Module.

The PAO Module coordinates all inverters on a feeder to maintain terminal voltage of this feeder in rated range while maximizing the active power output of the inverters. By means of the state estimation, the fuzzy logic gathers voltage information from different feeder terminals, to decide whether to maintain voltage stability via adjusting OLTC or PAOs. Thus, the efficiency of PV generations can be improved greatly. A typical distribution network with high penetration of PV distributed generations is built to validate the results. The simulation results show that, when the terminal voltage fluctuation trends of different feeders have the same condition (all terminal voltages are in the high voltage or low voltage condition), the voltages can be maintained in the rated range by adjusting the tap of OLTC. However, with this master-slave arrangement, the coordination of the OLTC and PAO module is liable to fail when the central fuzzy logic controller fail, hence lacks reliability.

proposes a robust protection coordination scheme of directional overcurrent relays for multiple network topologies in the presence of on-load tap changers (OLTCs). The robust protection coordination scheme provides single settings of DOCRs which will be valid for all N−1 contingencies created after outage of a line, transformer or generator. An efficient constraint reduction strategy is introduced to reduce the number of coordination constraints caused by consideration of multiple topologies. The impact of tap positions of the OLTCs has been incorporated in the required steady-state and short-circuit current calculations. The robust protection coordination scheme has been posed as an optimization problem and solved using an interior point method-based algorithm. The feasibility and the effectiveness of the proposed formulation and solution algorithm has been demonstrated on the IEEE 14-bus power system network. From the simulation result, it is concluded that tap positions of on-load tap changers affect settings of DOCRs and must be considered while obtaining the settings for practical implementation. In spite of the improvement obtained, the developed approach is only applicable to networks with mesh structure as against radial distribution networks. This is because in radial network, there is only one DOCR on each feeder section and the DOCR in one-line acts as a backup relay for the next downstream line.

In conclusion, it can be understood from the reviewed literature that a lot has been done on optimal OLTC either alone or in conjunction other services and techniques. Nevertheless, there are still research gaps that need to be filled in. Among which is the development of the optimal OLTC technique using a recently developed meta-heuristic optimization algorithm like Grey Wolf Optimization (GWO) algorithm, in order to minimize the voltage deviation and reactive power loss simultaneously. Based on the literature survey, GWO has not been applied to optimal tuning of OLTCs, despite its numerous advantages.

**Ebeed, *et al*., (2019)** Optimal allocation of these controllers in the distribution networks is an important task for researchers for power loss minimizing, voltage profile improvement, voltage stability

enhancement, reducing the overall system costs and maximizing the system load ability and reliability. Several analytical and optimization methods have been presented to find the optimal siting and sizing of capacitors and shunt compensators in electric distribution networks.

**Razavi, *et al*., (2019)** another key point which needs to be considered relates to specific DG technologies based on Renewable Energy Sources (RESs), such as wind and solar, due to their uncertain power generation.

**Thakur**, ***et al*., (2019**) This paper contributes the adaptive whale optimization algorithm (AWOA) algorithm to solve the power quality issues under deregulated sector, which enhances available transfer capability, maintains voltage stability, minimizes loss and mitigates congestions. Through the performance analysis, the convergence of the final fitness of AWOA algorithm is 5 per cent better than artificial bee colony (ABC), 3.79 per cent better than genetic algorithm (GA), 2,081 per cent better than particle swarm optimization (PSO) and fire fly (FF) and 2.56 per cent better than whale optimization algorithm (WOA) algorithms at 400 per cent load condition for IEEE 30 test bus system, and the fitness convergence of AWOA algorithm for IEEE 57 test bus system is 4.44, 4.86, 5.49, 7.52 and 9.66 per cent better than FF, ABC, WOA, PSO and GA, respectively.

**دويكات, & ايمن براء. (2020).** The Maithaloon electrical grid (Jenin-Palestine) grid fed from Israeli Electrical Company at the far end of long distribution transmission line operated at 33 kV and have rated capacity of about 5 MVA, the penetration due to the DG's connected either on MV or LV side on the grid is very high (about 45-50%) compared to the standard recommendations. The research based on FACTS devices specially the UPFC which designed and integrated to the real model of Maithaloon electrical grid and operated as adaptive device in MATLAB simulation model to eliminate the harmonics, improve the voltage levels and reduce the electrical losses.

**Pal & Gupta (2020)** A prominent custom power device DVR is apparently suggested in the literature for the mitigation of voltage sag and swells, with the benefit of active or/and reactive power control. This review article presents a detailed study on DVR with the different possible configurations of its power circuit and control techniques encircling major power quality issues.

**Kala, *et al*., (2021)** the rising penetration of intermittent renewable energy systems into the grid further prompted not only the bulk use of power electronics converters in power system but also rise in several power quality issues. The switching operation of power converter devices and harmonic generated by the nonlinear load in power system raises the issues of power quality such as voltage distortion, poor power factor, voltage sag and swells, flicker, and voltage imbalance. The various conventional methods to tackle these issues related to power quality are to utilize the active and passive filter, flexible alternating current transmission (FACTs), Dynamic voltage restorer (DVR), unified

power quality controller (UPQC), PWM controllers, multilevel inverters (MLIs) in distribution network of power system.

**Shaheen, *et al*., (2021)** This research provides an application of the hybrid Grey Wolf Optimization and Particle Swarm Optimization (GWO-PSO) method to reach a solution to the optimal reactive power dispatch (ORPD) problem in the scope of electric power networks. The hybrid GWO-PSO is proven as an effective optimization technique when seeking the global best solution to an optimization problem.

# CHAPTER THREE

# METHODOLOGY

## 3.1 Research Methodology

In order to implement the above-mentioned objectives, the following steps are followed: -

*i-* Determination of the network's inherent voltage deviation, reactive power loss, and other network parameters using Newton-Raphson power flow algorithm.

- *a)* Formulation of network's line data matrix, bus data matrix, bus admittance matrix, and classifying the buses types,
- *b)* Compute the injection current and phase difference from the bus admittance matrix,
- *c)* Determining the active and reactive powers at each bus using the admittances, line currents and phase angles,
- *d)* Update the voltage magnitude and phase angles and line losses.

*ii-* Formulation of the multi-objective function and constraints for the minimization of the voltage deviation and reactive power loss.

- *a)* Formulation of the objective function for the minimization of the voltage deviation.
- *b)* Formulation of the objective function for the minimization of the reactive power loss.
- *c)* Formulation of the weighted multi-objective function by combining weighted functions in *iia* and *iib.*
- *d)* Formulation of the system constraints functions consisting of demand-generation balance, bus voltage limits, line thermal overloading limits and tap-changer adjustment limits.

*iii-* Application of Grey Wolf Optimization algorithm for the solution of the problem formulated in *ii* above.

- *a)* Initialize the GWO parameters such as search agents, design variable size vectors and maximum number of iterations,
- *b)* Generate wolves randomly based on size of the pack,
- *c)* Estimate the fitness value of each hunt agent and identify the best hunt agent, the second-best hunt agent and the third best hunt agent,
- *d)* Estimate the fitness value of all hunts and update the best, second best and the third best hunt agent
- *e)* Check for stopping condition and evaluate the best value of solution otherwise repeat.

*iv-* Implementing the developed technique on IEEE 14-bus, IEEE 30-bus and 57-bus 330kV Nigerian transmission network and comparing the new systems operating conditions with those in *i.*

*a)* Compute the optimal OLTCs and update the transformers TC settings.

*b)* Run the power flow of each network as described in *i* above, but with the optimal TC settings.

*c)* Compute the new voltage deviation, reactive power loss, and other network parameters of each network.

*d)* Carry comparative analysis on the network conditions with and without the optimal OLTCs.

*e)* Carry comparative analysis on the new voltage deviation and reactive power loss with those obtained in (Ratra, et al., 2018).

### 3.2 Test Systems Description

To ascertain the effectiveness of the applied technique, it is implemented on IEEE 14-bus, IEEE 30-bus and 57-bus Nigerian Transmission systems. This is among the standard IEEE test systems made available for carrying different simulation studies of power system. The systems structure and size are described below

#### 3.2.1 IEEE 14-Bus Test System

The IEEE 14-bus test case represents a simple approximation of the American Electric Power system as of February 1962 (Saadat, 1999). It has 14 buses, 5 generators, and 11 loads. The system has three transformers all equipped with OLTCs. Single line diagram of the system is shown in Figure 3.1. The system bus and line data are given in Appendix A1 & A2 respectively. The transformer between bus 4 and 9 is OLTC transformer and it aims at controlling the voltage at bus 9 (Efkarpidis, et al., 2016).

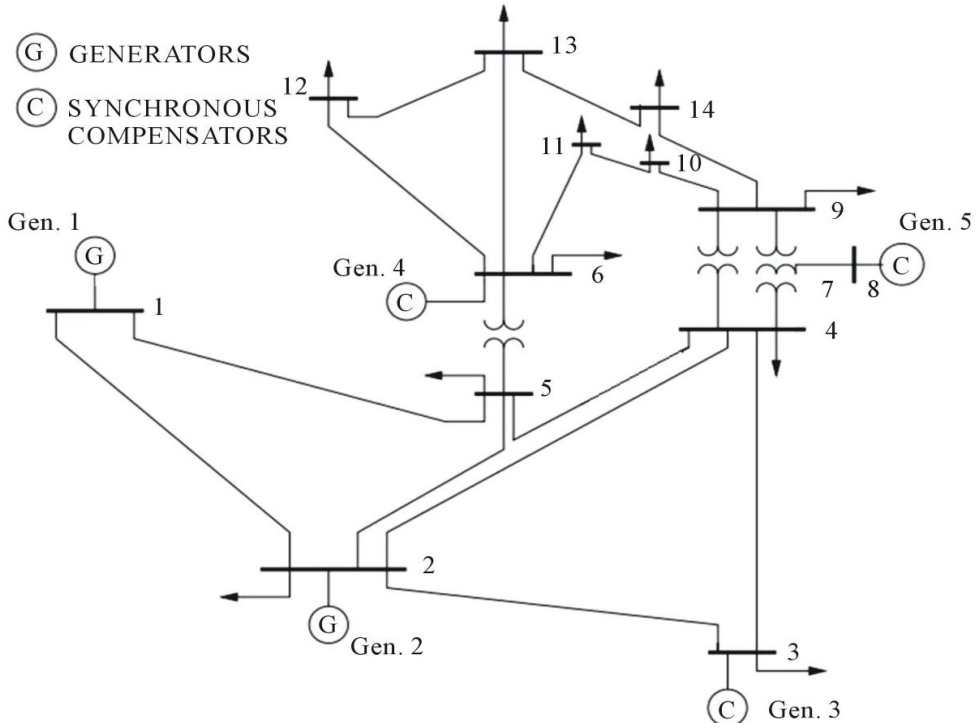


Figure 3.1 Single Line Diagram of IEEE 14 Bus (Tiwari, et al., 2018 )

### 3.2.2 IEEE 30-Bus Test System

The second test system is IEEE 30-bus system. It is part of old American Electric Service Corporation Network which is being made available to the electric utility as a standard test case for evaluating various analytical methods regarding power system. The system has six generator buses and twenty-five load buses with forty-one interconnected lines. The single line diagram of

IEEE 30-bus system is illustrated in Figure 3.2. Discrete tap positions of transformers are placed within 4 – 12, 6 – 9, 6 – 10 and 28 – 27 with predefined tap settings of 0.932, 0.978, 0.969, and 0.968 respectively. The system bus and line data are given in Appendix B1 & B2 respectively

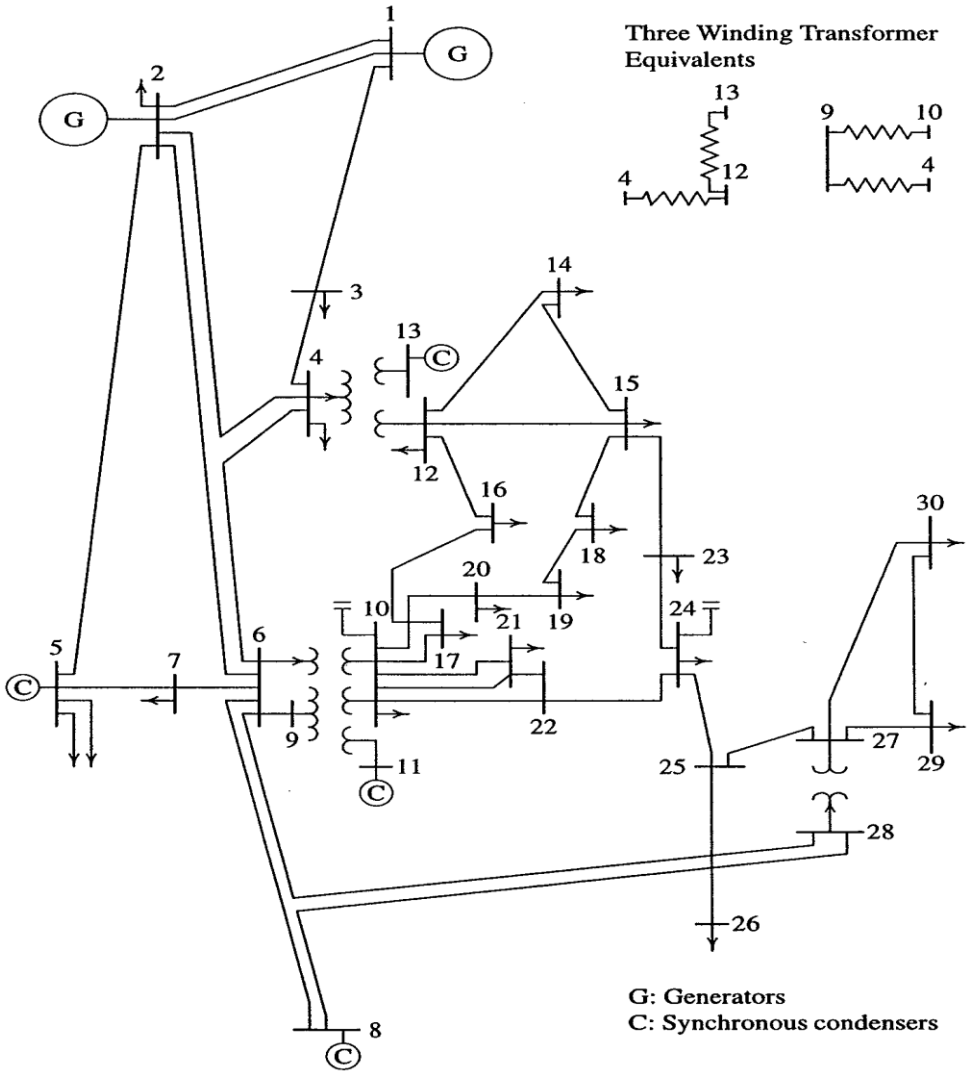


Figure 3.2 Single Line Diagram of IEEE 30 Bus (Saadat, 1999)

### 3.2.3 Nigeria 330kV Transmission System

The real system used for the validation of this work is Nigerian 57-bus, 330kV transmission network. The network is made up of 5000km of 330kV lines, about 6000km of 132kV lines, 23km of 330/132kV substations and 91km of 132/33kV substations. The system has 57 buses and 80 interconnected lines within which 15 has transformers equipped with OLTCs. The tap positions of transformers with their respective predefined tap settings are summarized in Table 3.1. Figure 3.3 shows the single line diagram of the system. The system bus and line data are given in Appendix C1 & C2 respectively.

Table 4.3: OLTCs of the Transformers in Nigerian 57-Bus System

| Transformers OLTC | Tap settings |
|---|---|
| T4 ~18 | 0.9600 |
| T4 ~18 | 0.9880 |
| T20 ~21 | 0.9950 |
| T24 ~ 26 | 1.0130 |
| T7 ~ 29 | 0.9970 |
| T34 ~ 32 | 0.9650 |
| T11 ~ 41 | 0.9850 0.9750 |
| T15 ~ 45 | 0.9500 |
| T14 ~ 46 | 0.9300 |
| T10 ~ 51 | 0.9250 |
| T13 ~ 49 | 0.9280 |
| T11 ~ 43 | 0.9380 |
| T40 ~ 56 | 0.9400 |
| T39 ~ 57 | 0.9700 |
| T9 ~ 55 | |

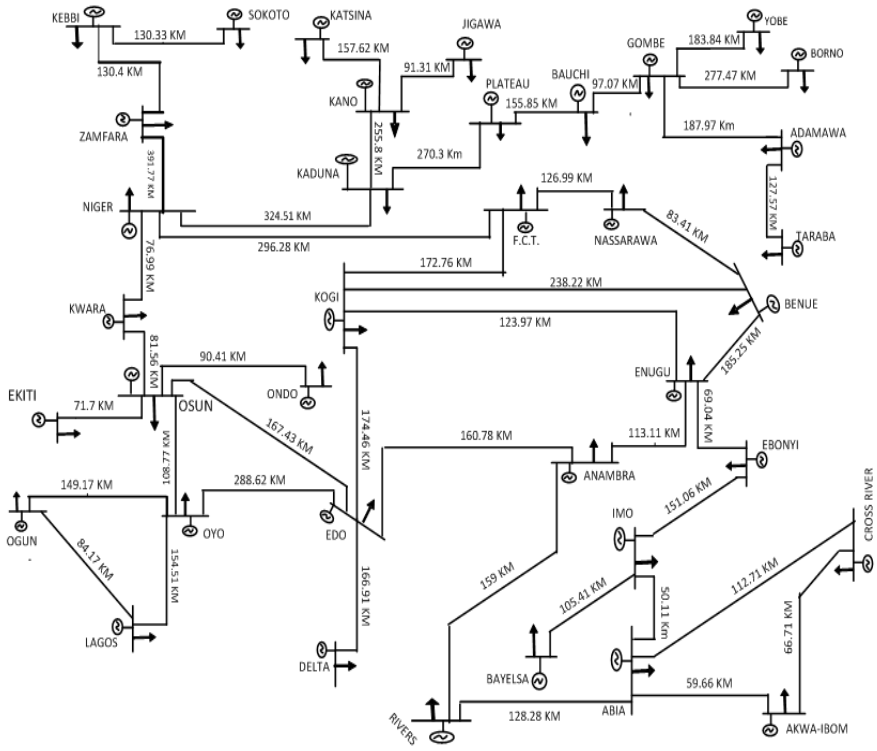


Figure 3.3 Single-line diagram of Nigerian Transmission Network.

### 3.3 Methodology

In this subsection, the methodology followed to accomplish this research work is presented. It covered the formulation of objective function and constraints.

### 3.3.2 Objective Function

The aim of the research is to minimize the voltage deviation and reactive power loss simultaneously by optimizing the OLTC of the available transformers in the system. As such, the objective function is formulated to have two components as shown in (3.1):

$$min\, F$$

where

$$F = \psi f_1 + \beta f_2 \tag{3.1}$$

Where $\psi$ and $\beta$ are the weighing coefficients of the voltage deviation and reactive power loss respectively.

#### *3.3.2.1 Minimization of Voltage Deviation*

The first component of the objective function is the minimization of voltage deviation from 1 *pu*. It is obtained by normalizing its minimized value, $V_{dev}$ with its initial value, $V_{dev.}^{initial}$ as in (3.2).

$$f_1 = \frac{V_{dev}}{V_{dev}^{initial}} \tag{3.2}$$

The total inherent voltage deviation is computed as;

$$\Delta V_{total}^{initial} = \sum_{j=1}^{n_b} \left| V_{ref,j} - V_j \right| \quad for\ j = 1,2, \dots n_b \tag{3.3}$$

$V_{ref,j}$ is the nominal voltage magnitude of load bus *j*.

#### *3.3.2.1 Minimization of Reactive Power Loss*

The second component of the objective function is the minimization of reactive power loss. It is obtained by normalizing the reactive power loss with its original value as expressed in (3.3).

$$f_2 = \frac{Q_{loss}}{Q_{loss}^{initial}} \tag{3.3}$$

where $Q_{loss}$ is the power loss experienced in the optimized DN, while $Q_{loss}^{initial}$ is its inherent power loss calculated as;

$$Q_{loss} = \sum_{j=1}^{m} G_{ij}\left(V_i^2 + V_j^2 - 2V_iV_j\sin\left(\theta_{ij} - \delta_i + \delta_j\right)\right) \tag{3.4}$$

### 3.3.3 Constraints

The proposed minimization of the voltage deviation and reactive power loss is solved by considering the following constraints: -

1. *Voltage limit*: the bus voltage magnitudes are constrained within lower and upper limits as in (3.5),

$$V_i^{min} \le V_i \le V_i^{max}, \qquad i = 1,2,\dots,n_b \tag{3.5}$$

2. *Maximum permissible line current carrying capacity*: to avoid exceeding the current capacity of the branches, the current in *k*th branch, $I_k$ is limited to a maximum permissible current, $I_k^{min}$ as in (3.6),

$$I_k \le I_k^{min}, \quad k = 1,2,\dots,n_l \tag{3.6}$$

Where

$$I_k^2 = \alpha_k\left[A_{ij}V_i^2 + B_{ij}V_i^2 - 2V_iV_j\left(C_{ij}\cos\beta_{ij} - D_{ij}\sin\beta_{ij}\right)\right] \tag{3.7}$$

$$A_{ij} = g_{ij}^2 + \left(b_{ij} + \frac{b_{shij}}{2}\right)^2 \tag{3.8}$$

$$B_{ij} = g_{ij}^2 + b_{ij}^2 \tag{3.9}$$

$$C_{ij} = g_{ij}^2 + b_{ij}\left(b_{ij} + \frac{b_{shij}}{2}\right)^2 \tag{3.10}$$

$$D_{ij} = g_{ij}^2\frac{b_{shij}}{2} \tag{3.11}$$

Where $V_i$ is *i*th bus voltage, $\beta_{ij}$ is the phase difference between buses *i* and *j*. While $b_{ij}$, $g_{ij}$ and $b_{shij}$ are the susceptance, conductance and shunt susceptance of the line linking *i*th and *j*th buses.

3. *Active and reactive power generation limits*: to avoid exceeding the generation capacity of the generators, the power generation from the generators are constrained as in (3.12),

$$P_k^{min} \leq P_k^G \leq P_k^{max}, \quad k = 1,2,\dots,G \tag{3.12}$$

And

$$Q_k^{min} \leq Q_k^G \leq Q_k^{max}, \quad k = 1,2,\dots,G \tag{3.13}$$

Where $P_k^{min}$ and $P_k^{max}$ are the minimum and maximum active power generation capacity of generator *k*. $Q_k^{min}$ and $Q_k^{max}$ are the minimum and maximum reactive power generation capacity of generator *k.*

4. *Tap-changer adjustment limits*

   The OLTCs are constrained within (0.85 – 1.15p.u). This is according to IEEE C57.131 2012 requirement.

### 3.3.4 GWO Parameters Selection

The objective function formulated in (3.1) and further defined in (3.2) and (3.3) is solved using GWO. For this purpose, the initialization and user-defined parameters for the GWO are presented in table 3.1.

Table 3.1 Initialization Parameters of the GWO

| Parameter | Value |
|---|---|
| Search agents (population size) | 50 |
| Max number of iteration | 100 |
| ***A*** | Decreased from 2 to 0 |
| Jumping rate jr = 0.3; | 0.4 |
| Design variable size | Size of the network |
| Random vectors | [0, 1] |
| distance between the position vector, D | 0.3 |
| The probability that each wolf will be trapped, *P* | 0.25 |

# CHAPTER FOUR

# RESULTS AND DISCUSSION

## 4.1 Introduction

In this chapter, the results obtained from the simulation carried out on the test systems are discussed. It also provides the detailed discussions and inference on the system condition before and after optimizing the transformers' OLTCs. All the simulations are carried out in MATLAB environment.

## 4.2 Optimizing OLTCs of the IEEE 14-Bus System

The OLTC of the transformers in the IEEE 14-bus system are optimized by minimizing the objective function formulated and discussed in subsection 3.3.2 subject to the constraints formulated in subsection 3.3.3. The results obtained with the optimized OLTCs are compared with the base case.

### 4.2.1 Base Case of the IEEE 14-Bus System

To determine the original condition of the system, load flow analysis of the system is carried prior to optimizing the OLTCs. The original OLTC of the three transformers in the system are 0.9680, 0.9530 and 0.9880 of transformers T4~7, T4~9 and T5~6 respectively, as shown in Table 4.1. The inherent voltage deviation of the system is calculated to be 2.0892*pu* while the reactive power loss is 277.2988MVar. The other network parameters are summarized in Appendix D.

Table 4.1: OLTCs of the Transformers in IEEE 14-Bus System

| Transformers OLTC | Base Case | Optimized OLTC |
|---|---|---|
| T4~7 | 0.9680 | 0.9780 |
| T4~9 | 0.9530 | 0.9690 |
| T5~6 | 0.9880 | 0.9320 |

### 4.2.2 IEEE 14-Bus System with Optimized OLTCs

The developed GWO-based technique is then applied on the IEEE 14-Bus system by minimizing the objective function. The optimal settings of the OLTCs are computed to be 0.9780, 0.9690 and 0.9320 of

transformers T4~7, T4~9 and T5~6 respectively, as shown in Table 4.1. With this optimized OLTCs (based on GWO), the voltage deviation reduces to 1.0153*pu*. Figure 4.1 shows the voltage profile of IEEE 14-bus with optimized OLTCs.

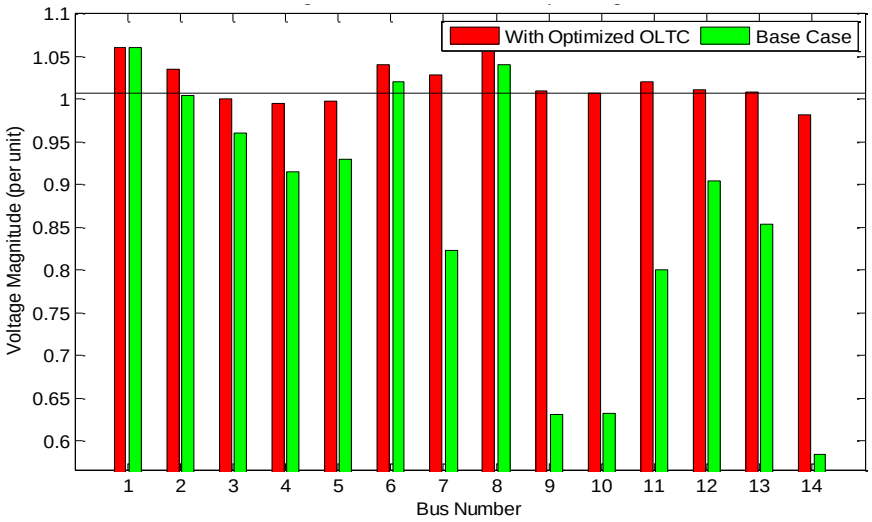


Figure 4.1: Voltage profile of IEEE 14-bus Optimized with GWO

It can be seen that none of the voltages of the 14 buses violate the IEEE voltage limits of ±5% *pu* apart from the bus 1 which is generator bus chosen as the swing. This is a significant improvement compared to the original network voltage profile which only 3 buses within the range.

To establish the superiority of the applied GWO-based OLTCs, its performance is compared with those obtained using the Particle Swarm Optimization (PSO). From Figure 4.2, the improvement obtained on the voltage deviation (VD) when the GWO is applied compared to the base case and PSO can be clearly observed. Table 4.2 summarizes the improvement.

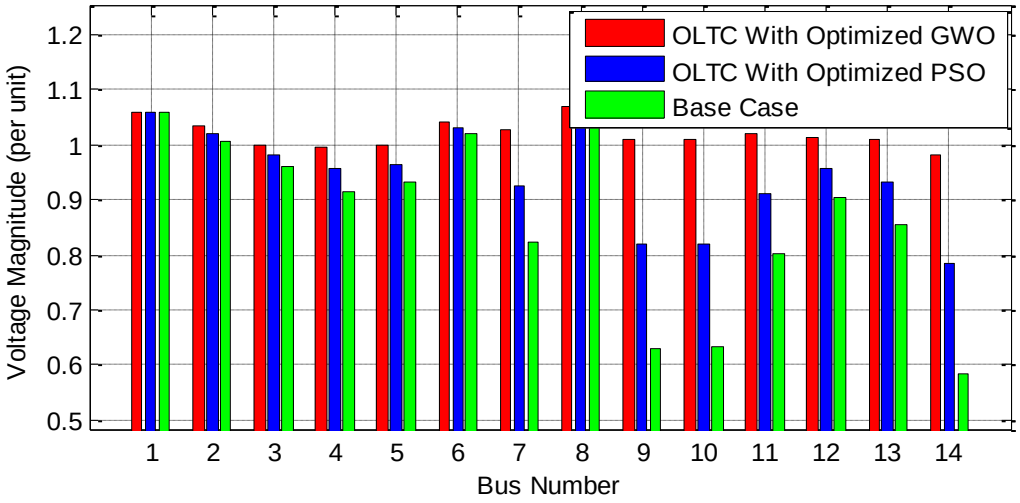


Figure 4.2: Improvement of GWO over the PSO on the Voltage Profile of IEEE 14-bus

Table 4.2: Summary of the voltage deviation in IEEE 14-Bus System

| **Scenario** | **Total VD** (***pu***) | **Improvement** | |
|---|---|---|---|
| | | ***Over the Base Case*** | ***GWO over the PSO*** |
| **Base Case** | 2.0892 | – | – |
| **OLTC Optimized with PSO** | 1.4783 | 29.24% | – |
| **OLTC Optimized with GWO** | 1.0153 | 51.40% | 31.32% |

Similarly, the reactive power loss is found to have reduced to 156.542*MVar* due to the optimal tuning of the OLCTs using GWO and 206.591*MVar* when PSO was applied as shown Figure 4.3. This represents 43.54% performance of the GWO compared with the base case and 24.23% compared with the PSO.

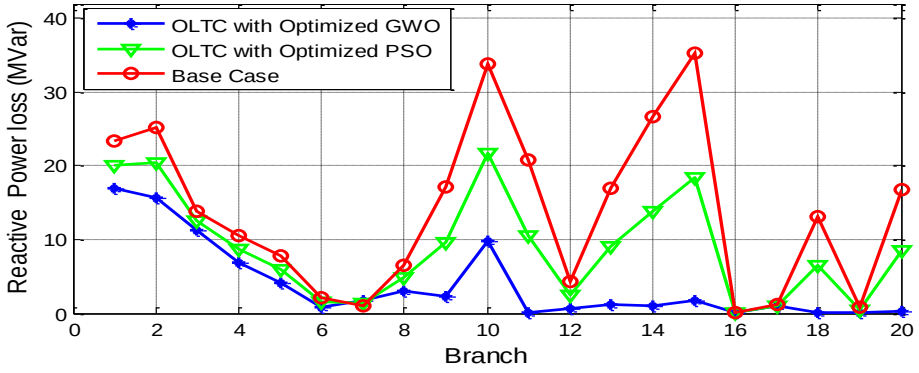


Figure 4.3: Improvement of GWO over the PSO on the Reactive Power of IEEE 14-bus

Table 4.3: Summary of the Reactive Power in IEEE 14-Bus System

| Scenario | Total Reactive (*MVar*) | Improvement of GWO | |
|---|---|---|---|
| | | ***Over the Base Case*** | ***Over the PSO*** |
| **Base Case** | 277.298 | – | – |
| OLTC Optimized with PSO | 206.591 | 25.49% | – |
| OLTC Optimized with GWO | 156.542 | 43.54% | 24.23% |

Not only the voltage profile and reactive power the GWO-optimized OLTCs improved but also the total active power in the network as depicted in Figure 4.4

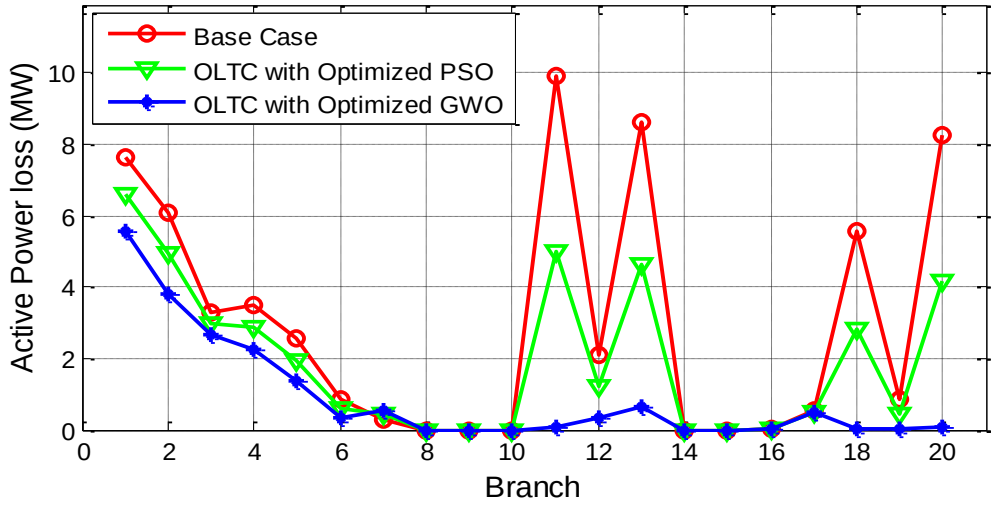


Figure 4.4: Improvement of GWO over the PSO on the Active Power of IEEE 14-bus

### 4.3 Optimizing OLTCs of the IEEE 30-Bus System

Unlike the IEEE 14-bus system with three transformers, the IEEE 30-bus system is equipped with four transformers between buses 6-9, 6-10, 4-12 and 28-27 whose OLTCs are also optimized. The results obtained with the optimized OLTCs are compared with the base case and those obtained using PSO.

#### 4.3.1 Base Case of the IEEE 30-Bus System

To determine the original condition of the system, load flow analysis of the system is carried prior to optimizing the OLTCs. The original tap settings of the three transformers in the system are 0.9580, 0.9889, 0.9520 and 0.9780 of transformers T6-9, T6-10, T4-12 and T28-27 respectively, as summarized

in Table 4.4 Ratra *et al*., (2009). The inherent voltage deviation of the system is calculated to be 1.7926*pu* while the reactive power loss is 89.9340*MVar*. The other network parameters are summarized in Appendix E.

Table 4.4: OLTCs of the Transformers in IEEE 30-Bus System

| Transformers OLTC | Base Case | Optimal OLTC |
|---|---|---|
| T6-9 | 0.9580 | 0.9780 |
| T6-10 | 0.9889 | 0.9690 |
| T4-12 | 0.9520 | 0.9320 |
| T28-27 | 0.9780 | 0.9680 |

### 4.3.2 IEEE 30-Bus System with Optimized OLTCs

The developed GWO-based technique is also applied on the IEEE 30-Bus system to optimize the system OLTCs. The optimal OLTCs are computed to be 0.9780, 0.9690, 0.9320 and 0.9680 of transformers T6-9, T6-10, T4-12 and T28-27 respectively, as summarized in Table 4.2. After optimizing the OLTCs (based on GWO), the voltage deviation has reduced to 0.9140*pu*. Figure 4.5 shows the voltage profile of IEEE 30-bus with optimized OLTCs which clearly shows the improvement obtained on the voltage deviation (VD) when the GWO is applied compared to the base case and PSO. Table 4.4 summarizes the improvement obtained on the voltage profile.

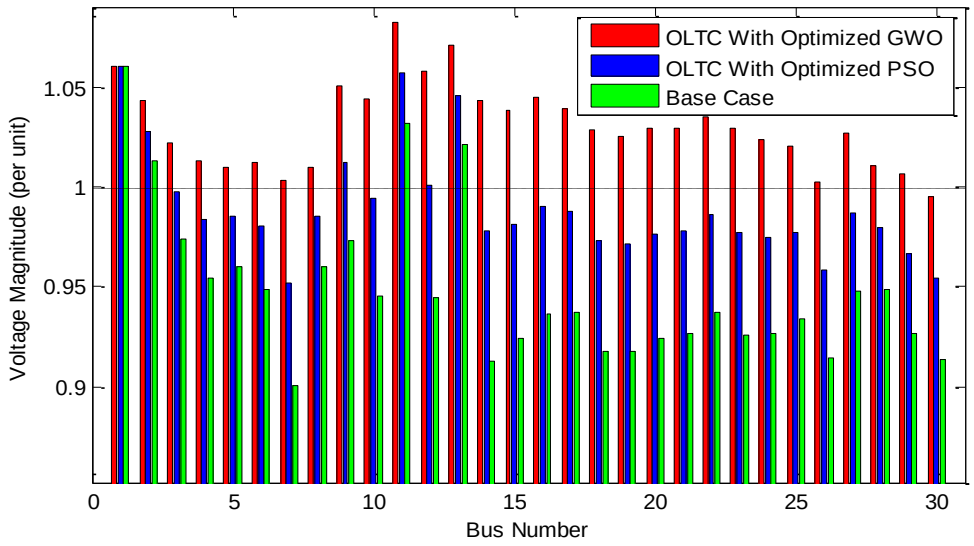


Figure 4.5: Improvement of GWO over the PSO on the Voltage Profile of IEEE 30-bus

Table 4.5: Summary of the Voltage Deviation in IEEE 30-Bus System

| Scenario | Total VD (*pu*) | Improvement | |
|---|---|---|---|
| | | ***Over the Base Case*** | ***GWO over the PSO*** |
| **Base Case** | 1.7926 | – | – |
| **OLTC Optimized with PSO** | 1.3215 | 26.278% | – |
| **OLTC Optimized with GWO** | 0.9826 | 45.185% | 25.646% |

In the same way, the reactive power loss of the IEEE 30 is found to have reduced to 52.664*MVar* due to the optimal tuning of the OLCTs using GWO and 67.904*MVar* when PSO was applied as shown Figure 4.6. This represents 41.44% performance of the GWO compared with the base and 22.42% compared with the PSO.

Table 4.6: Summary of the Reactive Power in IEEE 30-Bus System

| Scenario | Total Reactive (*MVar*) | Improvement of GWO | |
|---|---|---|---|
| | | ***Over the Base Case*** | ***Over the PSO*** |
| **Base Case** | 89.934 | – | – |
| OLTC Optimized with PSO | 67.904 | 24.49% | – |
| OLTC Optimized with GWO | 52.664 | 41.44% | 22.42% |

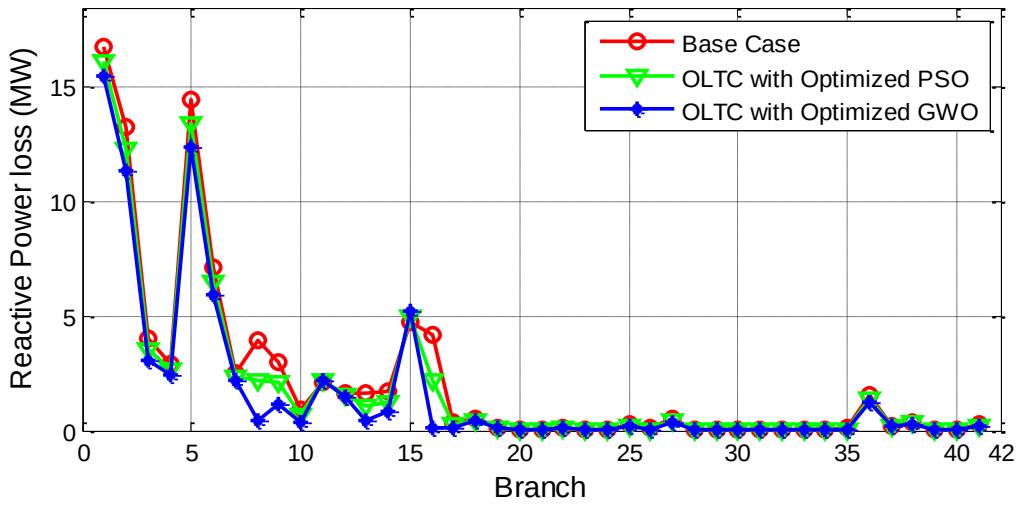

Figure 4.6: Improvement of GWO over the PSO on the Reactive Power of IEEE 30-bus

In addition to reducing the reactive power losses, optimizing OLTCs also reduced the active power losses along the transmission lines as shown Figure 4.7.

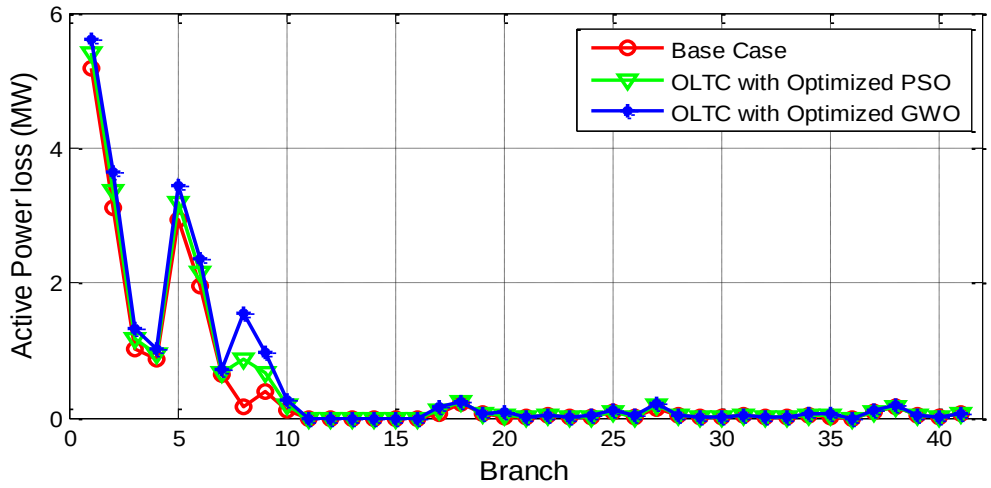


Figure 4.7: Improvement of GWO over the PSO on the Active Power of IEEE 30-bus

### 4.4 Optimizing OLTCs of the Nigerian 57-Bus Transmission System

Having establish the applicability of the GWO and its superiority over PSO in optimizing the OLTCs in the IEEE 14-bus and 30-bus systems, it is applied on real transmission network; Nigerian 57-bus, 330kV transmission network to establish its practicability. The network has 15 transformers equipped with OLTCs. As applied in the previous cases, the results obtained with the optimized OLTCs are analyzed and compared with the base case.

#### 4.4.1 Base Case of the Nigerian 57-Bus System

The adopted N-R load analysis is used to determine the original operating condition of the system prior to optimizing the OLTCs. The original OLTCs of the fifteen transformers in the system are summarized in Table 4.5. The inherent voltage deviation of the system is calculated to be 6.7808*pu* while the reactive power loss is 185.4685*MVar*. The other network parameters are summarized in Appendix F.

Table 4.7: OLTCs of the Transformers in Nigerian 57-Bus System

| Transformers OLTC | Base Case | Optimal OLTC |
|---|---|---|
| T4~18 T4~18 | 0.9600 | 0.9700 |
| T20~21 | 0.9880 | 0.9780 |
| T24~26 T7~29 | 0.9950 | 1.0430 |
| T34~32 | 1.0130 | 1.0430 |
| T11~41 T15~45 | 0.9970 | 0.9670 |
| T14~46 | 0.9650 | 0.9750 |
| T10~51 | 0.9850 0.9750 | 0.9550 0.9550 |
| T13~49 | 0.9500 | 0.9000 |
| T11~43 | 0.9300 | 0.9300 |
| T40~56 | 0.9250 | 0.8950 |
| T39~57 T9~55 | 0.9280 | 0.9580 |
| | 0.9380 | 0.9580 |
| | 0.9400 | 0.9800 |
| | 0.9700 | 0.9400 |

### 4.4.2 Nigerian 57-Bus System with Optimized OLTCs

The developed GWO-based technique is also applied on the Nigerian 57-Bus System to optimize the system OLTCs. The optimal OLTCs are computed and summarized in Table 4.5. After optimizing the OLTCs (based on GWO), the voltage deviation has reduced to 4.4519*pu*. Figure 4.58 shows the voltage profile of the Nigerian 57-Bus System with optimized OLTCs which clearly shows the improvement obtained on the VD when the GWO is applied compared to the base case. Table 4.6 summarizes the improvement obtained on the voltage profile and the reactive power loss.

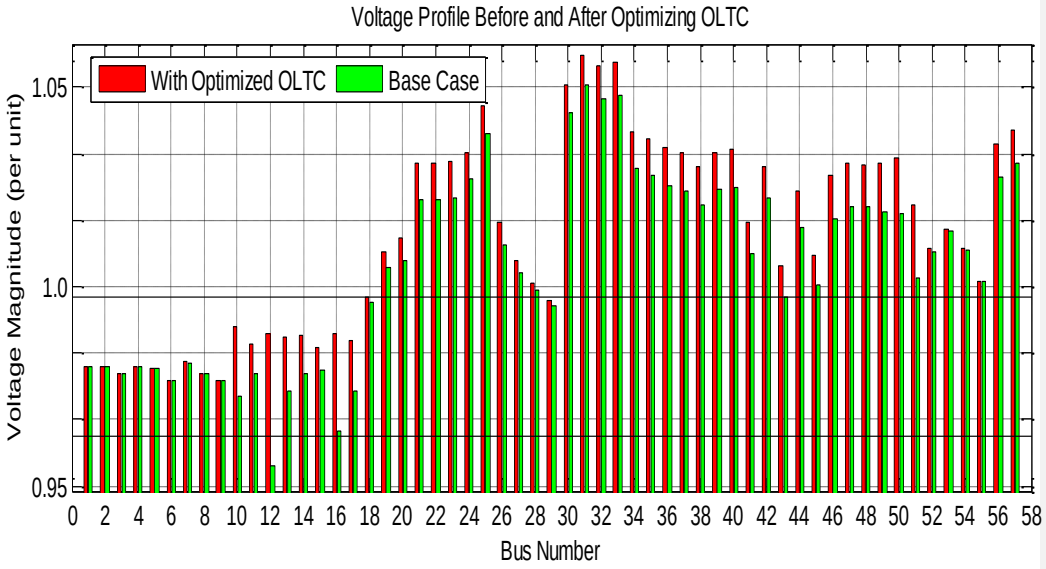


Figure 4.8: Voltage profiles of Nigerian 57-bus system

Table 4.8: Summary of the Voltage Deviation in IEEE 30-Bus System

| Scenario | Total VD (*pu*) | Reactive Power (*MVar*) |
|---|---|---|
| **Base Case** | 6.7808 | 185.4685 |
| **OLTC Optimized with GWO** | 4.4519 | 117.8465 |
| **Improvement** | 34.36% | 36.46% |

It can be seen that none of the voltages of the 57 buses violate the IEEE voltage limits of ±5% *pu*. This has confirmed the ability of the developed technique to determine the OLTCs settings in the systems with higher number of buses devoid of violating the constraints.

Likewise, the reactive power loss in the system is found to have reduced to 117.8465*MVar* due to the optimal tuning of the OLCTs using GWO. This represents 36.46% performance of the GWO compared with the base case. This can be seen by observing the reactive power losses along the individual transmission lines as shown in Figure 4.9.

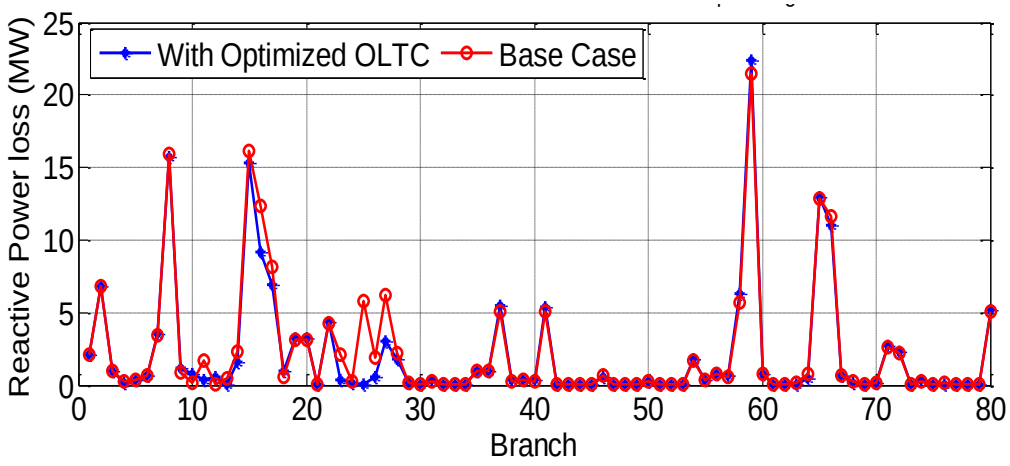


Figure 4.8 Reactive Power Profiles of the Nigerian 57-bus system

In addition to reducing the reactive power losses, optimizing OLTCs also reduced the active power losses along the transmission lines from 27.3611MW in the original system to 22.7030MW as shown in Figure 4.10.

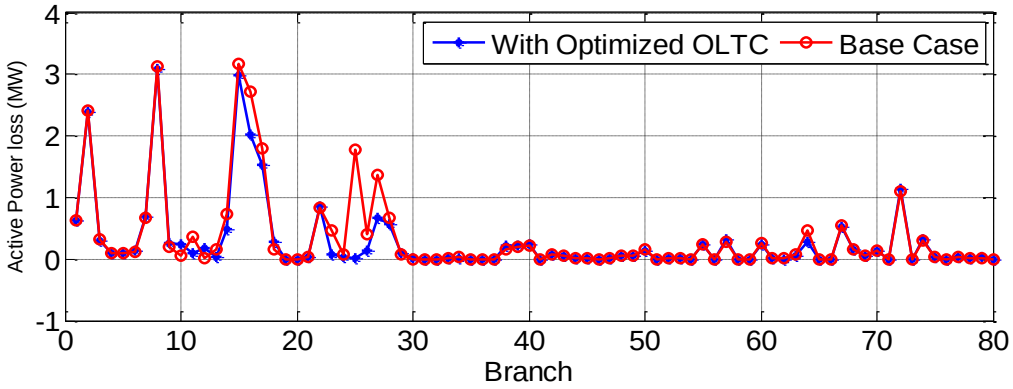


Figure 4.10: Active Power Profiles of Nigerian 57-bus system

# CHAPTER FIVE

# CONCLUSION AND RECOMMENDATION

## 5.1 Conclusion

This chapter summarizes the key findings of this research work. It also covers the limitations of the research and possible ways of improvement the research. In the presented work, GWO algorithm is applied to determine the optimal OLTC of the available transformers in transmission system with the view of improving the voltage profile and minimizing reactive power. To ascertain the effectiveness of the developed technique, it was implemented on IEEE 14-bus, IEEE 30-bus and 57-bus Nigerian Transmission systems.

The performances of the proposed technique is compared with those obtained using Particle Swarm Optimization (PSO). It is observed there is significant reductions in the overall voltage deviation (VD) as well as the reactive power loss (RPL) when the OLTCs are optimized.

For instance, in the IEEE 14-bus system, the VD was reduced from 2.0892*pu* (base case) to 1.0153*pu* due to the optimal tuning of the OLCTs using GWO and 1.4783*pu* when PSO was applied.

This represents 51.40% improvement of the developed GWO compared with the base case and 31.32% compared with the PSO. Similarly, the RPL was reduced to 156.542*MVar* due to the optimal tuning of the OLCTs using GWO and 206.591*MVar* when PSO was applied representing 43.54% and 25.49% improvements respectively.

While in the Nigerian 57-bus system, by applying the GWO, the total VD was reduced from 6.7808*pu* (base case) to 4.4519*pu* representing 34.35% improvement. Likewise, the RPL was reduced by 36.56% from its original value of 185.4685*Mvar.*

These have demonstrated the applicability of the GWO, its superiority over PSO and also revealed its practicability in optimizing the OLTCs in real-life systems.

## 5.2 Significant Contributions

The key contribution of this research work is

Comment [u3]: These contributions have be re-worked to give percentages of improvements

*i-* Reduction of the IEEE 14 bus system reactive power loss to 156.542MVar due to the optimal tuning of the OLCTs using GWO and 206.591MVar when PSO was applied representing 43.54% and 25.49% improvements respectively.

*ii-* Improvement of voltage profile of transmission in the IEEE 14 bus system by optimizing OLTCs of transformers, with improvement of 51.40% when compared with the base case and 31.32% compared with the PSO.

*iii-* Demonstration of the practicability of Grey Wolf Optimization (GWO) for optimizing the OLTCs of transformers in real system (Nigerian 57-bus transmission system), thereby improving the voltage profile by 34.35% and reducing the RPL by 36.56%.

### 5.4 Recommendation for Further Work

The possible areas are recommended for further research:

1. The algorithm should be use on power quality improvement on PV
2. Another metaheuristic algorithm should be use for the improvement of power Quality.

## REFERENCES


Agarwal, A., Chandra, A., Shalivahan, S. & Singh, R. K., (2018). Grey Wolf Optimizer: a new strategy to invert geophysical data sets. Geophysical Prospecting, Vol. 3, pp. 1215-1221.

Alam, M. N., Das, B. & Pant, V., (2020). Protection coordination scheme for directional overcurrent relays considering change in network topology and OLTC tap position. Electric Power Systems Research, Volume 185, pp. 1-10.

Bhattacharyya, S, Myrzik, JAM, Cobben, JFG, Kling, WL & Didden, M 2007, 'Need of voltage quality regulation in the future electricity infrastructure', Ninth international conference on electrical power quality and utilization, pp. 1-6.

Das, S., Biswas, A., Dasgupta, S. & Abraham, A., (2009). Bacterial foraging optimization algorithm: theoretical foundations, analysis, and applications. Studies in Computational Intelligence, Volume 203, pp. 23-55.

Deakin, A. G. (2017). Chromatic Optoacoustic Monitoring of Transformers and Their Onload Tap Changers. IEEE TRANSACTIONS ON POWER DELIVERY, 29(1), pp. 207 - 214.

Efkarpidis, N., Rybel, T. D. & Driesen, J., (2016). Optimization control scheme utilizing small-scale distributed generators and OLTC distribution transformers. Sustainable Energy, Grids and Networks, Volume 12, pp. 1-35.

Elgard, O. I. (., 1976. Electric Energy System Theorys: An Introduction. Newyork: Tata McGraw-Hill Publising Company..

El-Sadek, M., Mahmoud, G., Dessouky, M. & Rashe, W., (1999). Tap changing transformer role in voltage stability enhancement. Electric Power Systs Research, Vol. 50, pp. 115-118.

Ebeed, M., Kamel, S., Aleem, S. H. A., & Abdelaziz, A. Y. (2018). Optimal allocation of compensators. In *Electric distribution network planning* (pp. 321-353). Springer, Singapore.

Kay, M. & Khaing, T., (2018). Co-operation of On-Load Tap Changing Transformer and Shunt Capacitor for Power Quality Improvement in Large Industrial Load. Mandalay, Myanmar, IEEE.

Kala, P., Joshi, P., Joshi, M., Agarwal, S., & Yadav, L. K. (2021). Tackling Power Quality Issues Using Metaheuristics. In *Metaheuristic and Evolutionary Computation: Algorithms and Applications* (pp. 63-85). Springer, Singapore.

Kiusalaas, J., (2005). Numerical Methods in Engineering with MATLAB. 2nd ed. Cambridge, UK: Cambridge University Press.

Kothari, D. & Nagrath, I. J., (2003). Modern Power System Analysis. New Delhi, India: Tata McGraw Hill Educ..

Li, C. (2018). Optimal OLTC voltage control scheme to enable high solar penetrations. Electric Power Systems Research, Volume 160, p. 318–326.

Liu, J. (2019). An OLTC-inverter coordinated voltage regulation method for distribution network with high penetration of PV generations. Electrical Power and Energy Systems, Volume 113, p. 991–1001.

Mirjalili, S., Mirjalili, S. M. & Lewis, A., (2014). Grey Wolf Optimizer. Advances in Engineering Software, Volume 69, pp. 46-61.

Mittal, N., Singh, U. & Sohi, B. S., (2016). Modified Grey Wolf Optimizer for Global Engineering Optimization. Applied Computational Intelligence and Soft Comp, Vol. 2, pp. 1-16.

Mohammadian, M., Khaleghi, M., Azimi, R. & Gharaveisi, A., (2011). Optimal Tuning Of OLTC And RPCE To Improve Power System Voltage Stability Based on Ant Colony. Jordan, IEEE Jordan Conference on Applied Electrical Engineering and Computing Technologies.

Morina, J. (2017). Embedding OLTC nonlinearities in predictive Volt Var Control for active distribution networks. Electric Power Systems Research, Volume 143, p. 225–234.

Nasar, S., (1998). Synchronous Machine. In: Schaum's Outline; Electric Machine and Electromechanics. Newyork: McGraw-Hill, pp. 123-130.

Pal, R., & Gupta, S. (2020). Topologies and control strategies implicated in dynamic voltage restorer (DVR) for power quality improvement. *Iranian Journal of Science and Technology, Transactions of Electrical Engineering*, *44*(2), 581-603.

Pandu Sathish Babu Nagappan Kamaraj, 'Quality Enhancement using Dynamic Voltage Restorer', Lambert Academic Publishing, chapter-1, pp.1-16.

Rajabioun, R., (2011). Cuckoo optimiza) . Load Flow Analysis of IEEE 14 Bus System Using ANN Technique. Noida, India, International Conference on Sustainable Energy, Electronics & computing Systems (SEEMS) .

Razavi, S. E., Rahimi, E., Javadi, M. S., Nezhad, A. E., Lotfi, M., Shafie-khah, M., & Catalão, J. P. (2019). Impact of distributed generation on protection and voltage regulation of distribution systems: A review. *Renewable and Sustainable Energy Reviews*, *105*, 157-167.

Shaheen, M. A., Hasanien, H. M., & Alkuhayli, A. (2021). A novel hybrid GWO-PSO optimization technique for optimal reactive power dispatch problem solution. *Ain Shams Engineering Journal*, *12*(1), 621-630.

Sinik, V., Despotovic, D. Z., Radovanovic, L., Đurđev, M., Novaković, B., Tolmač, J., & Palinkaš, I. (2019). *SOME ASPECTS OF THE ELECTRICAL POWER QUALITY*.

Tareen, W. U., Mekhilef, S., Seyed mahmoudian, M., & Horan, B. (2017). Active power filter

(APF) for mitigation of power quality issues in grid integration of wind and photovoltaic energy conversion system. *Renewable and Sustainable Energy Reviews*, *70*, 635-655.

Thakur, N., Awasthi, Y. K., Hooda, M., & Siddiqui, A. S. (2019). Adaptive whale optimization

for intelligent multi-constraints power quality improvement under deregulated environment. Journal of Engineering, Design and Technology.

Zhu, T. X., lso, S. K. & Lo, K. L., (2000). An lnvestigation into the OLTC effects on Voltage

Collapse,"Vol. 15,. IEEE Transaction on Power System, 15(2), pp. 21 - 32.

كاتدوي, & ايد من بد راء. (2020). *Design Unified Power Flow Compensator to Solve Power Quality*

*for Maithaloon-Jenin's Medium Voltage Network* (Doctoral dissertation, An-Najah National University).

## APPENDIX A

### Appendix A1: Line Data for IEEE 14-Bus Network

```
%          |  From |  To   |   R      |   X      |     B/2   |  X'mer   | Power|
%          |  Bus  | Bus   |  pu      |  pu      |     pu    | TAP (a)  | Limit|
linedat14 = [1       2       0.01938   0.05917    0.0264         1
             1       5       0.05403   0.22304    0.0246         1
             2       3       0.04699   0.19797    0.0219         1
             2       4       0.05811   0.17632    0.0170         1
             2       5       0.05695   0.17388    0.0173         1
             3       4       0.06701   0.17103    0.0064         1
             4       5       0.01335   0.04211    0.0            1
             4       7       0.0       0.20912    0.0        0.978
             4       9       0.0       0.55618    0.0        0.969
             5       6       0.0       0.25202    0.0        0.932
             6      11       0.09498   0.19890    0.0            1
             6      12       0.12291   0.25581    0.0            1
             6      13       0.06615   0.13027    0.0            1
             7       8       0.0       0.17615    0.0            1
             7       9       0.0       0.11001    0.0            1
             9      10       0.03181   0.08450    0.0            1
             9      14       0.12711   0.27038    0.0            1
            10      11       0.08205   0.19207    0.0            1
            12      13       0.22092   0.19988    0.0            1
            13      14       0.17093   0.34802    0.0            1 ];
```

**Appendix A2: Line Data for IEEE 14-Bus Network**

```
%          |Bus | Type | Vsp | theta | PGi | QGi | PLi | QLi |  Qmin | Qmax |

busdat14 = [1     1    1.060   0       0     0     0     0       0       0;
            2     2    1.045   0      40   42.4  21.7  12.7     -40      50;
            3     2    1.010   0       0   23.4  94.2  19.0       0      40;
            4     3    1.0     0       0     0  47.8  -3.9       0       0;
            5     3    1.0     0       0     0   7.6   1.6       0       0;
            6     2    1.070   0       0  12.2  11.2   7.5      -6      24;
            7     3    1.0     0       0     0   0.0   0.0       0       0;
            8     2    1.090   0       0  17.4   0.0   0.0      -6      24;
            9     3    1.0     0       0     0  29.5  16.6       0       0;
            10    3    1.0     0       0     0   9.0   5.8       0       0;
            11    3    1.0     0       0     0   3.5   1.8       0       0;
            12    3    1.0     0       0     0  16.1   1.6       0       0;
            13    3    1.0     0       0     0  23.5   5.8       0       0;
            14    3    1.0     0       0     0  24.9   5.0       0       0;];
```

## APPENDIX B

### Appendix B1: Line Data for IEEE 30-Bus Network

```
%          |  From |  To   |   R     |   X     |     B/2  |  X'mer  |
%          |  Bus  | Bus   |  pu     |  pu     |     pu   | TAP (a) |
linedat30 = [1      2       0.0192    0.0575     0.0264         1
             1      3       0.0452    0.1652     0.0204         1
             2      4       0.0570    0.1737     0.0184         1
             3      4       0.0132    0.0379     0.0042         1
             2      5       0.0472    0.1983     0.0209         1
             2      6       0.0581    0.1763     0.0187         1
             4      6       0.0119    0.0414     0.0045         1
             5      7       0.0460    0.1160     0.0102         1
             6      7       0.0267    0.0820     0.0085         1
             6      8       0.0120    0.0420     0.0045         1
             6      9       0.0       0.2080     0.0         0.978
             6     10       0.0       0.5560     0.0         0.969
             9     11       0.0       0.2080     0.0            1
             9     10       0.0       0.1100     0.0            1
             4     12       0.0       0.2560     0.0         0.932
            12     13       0.0       0.1400     0.0            1
            12     14       0.1231    0.2559     0.0            1
            12     15       0.0662    0.1304     0.0            1
            12     16       0.0945    0.1987     0.0            1
            14     15       0.2210    0.1997     0.0            1
            16     17       0.0824    0.1923     0.0            1
            15     18       0.1073    0.2185     0.0            1
            18     19       0.0639    0.1292     0.0            1
            19     20       0.0340    0.0680     0.0            1
            10     20       0.0936    0.2090     0.0            1
            10     17       0.0324    0.0845     0.0            1
            10     21       0.0348    0.0749     0.0            1
            10     22       0.0727    0.1499     0.0            1
            21     23       0.0116    0.0236     0.0            1
            15     23       0.1000    0.2020     0.0            1
            22     24       0.1150    0.1790     0.0            1
            23     24       0.1320    0.2700     0.0            1
```

```
    24     25       0.1885    0.3292     0.0            1
    25     26       0.2544    0.3800     0.0            1
    25     27       0.1093    0.2087     0.0            1
    28     27       0.0       0.3960     0.0        0.968
    27     29       0.2198    0.4153     0.0            1
    27     30       0.3202    0.6027     0.0            1
    29     30       0.2399    0.4533     0.0            1
     8     28       0.0636    0.2000     0.0214         1
     6     28       0.0169    0.0599     0.065          1 ];
```

**Appendix B2: Bus Data for IEEE 30-Bus Network**

```
%          |Bus | Type | Vsp | theta | PGi | QGi | PLi | QLi |  Qmin | Qmax |
busdat30 = [1     1    1.06    0       0     0     0     0       0       0;
            2     2    1.043   0      40    50.0  21.7   12.7    -40     50;
            3     3    1.0     0       0     0    2.4    1.2     0       0;
            4     3    1.06    0       0     0    7.6    1.6     0       0;
            5     2    1.01    0       0    37.0  94.2   19.0    -40     40;
            6     3    1.0     0       0     0    0.0    0.0     0       0;
            7     3    1.0     0       0     0   22.8   10.9     0       0;
            8     2    1.01    0       0    37.3  30.0   30.0    -10     40;
            9     3    1.0     0       0     0    0.0    0.0     0       0;
            10    3    1.0     0       0    19.0   5.8    2.0     0       0;
            11    2    1.082   0       0    16.2   0.0    0.0    -6      24;
            12    3    1.0     0       0     0   11.2    7.5     0       0;
            13    2    1.071   0       0    10.6   0.0    0.0    -6      24;
            14    3    1.0     0       0     0    6.2    1.6     0       0;
            15    3    1.0     0       0     0    8.2    2.5     0       0;
```

```
16    3    1.0    0      0      0    3.5    1.8    0      0;
17    3    1.0    0      0      0    9.0    5.8    0      0;
18    3    1.0    0      0      0    3.2    0.9    0      0;
19    3    1.0    0      0      0    9.5    3.4    0      0;
20    3    1.0    0      0      0    2.2    0.7    0      0;
21    3    1.0    0      0      0   17.5   11.2    0      0;
22    3    1.0    0      0      0    0.0    0.0    0      0;
23    3    1.0    0      0      0    3.2    1.6    0      0;
24    3    1.0    0      0    4.3    8.7    6.7    0      0;
25    3    1.0    0      0      0    0.0    0.0    0      0;
26    3    1.0    0      0      0    3.5    2.3    0      0;
27    3    1.0    0      0      0    0.0    0.0    0      0;
28    3    1.0    0      0      0    0.0    0.0    0      0;
29    3    1.0    0      0      0    2.4    0.9    0      0;
30    3    1.0    0      0      0   10.6    1.9    0      0 ];
```

## APPENDIX C

### Appendix C1: Line Data for Nigerian 57-Bus Network

```
%          |  From |  To   |   R     |   X     |     B/2   |  X'mer   |
%          |  Bus  | Bus   |  pu     |  pu     |     pu    | TAP (a)  |
linedat57 = [   1     2     0.0083    0.0280      0.0645         1
                2     3     0.0298    0.0850      0.0409         1
                3     4     0.0112    0.0366      0.0190         1
                4     5     0.0625    0.1320      0.0129         1
                4     6     0.0430    0.1480      0.0174         1
                6     7     0.0200    0.1020      0.0138         1
                6     8     0.0339    0.1730      0.0235         1
                8     9     0.0099    0.0505      0.0274         1
                9    10     0.0369    0.1679      0.0220         1
                9    11     0.0258    0.0848      0.0109         1
                9    12     0.0648    0.2950      0.0386         1
                9    13     0.0481    0.1580      0.0203         1
               13    14     0.0132    0.0434      0.0055         1
               13    15     0.0269    0.0869      0.0115         1
                1    15     0.0178    0.0910      0.0494         1
                1    16     0.0454    0.2060      0.0273         1
                1    17     0.0238    0.1080      0.0143         1
                3    15     0.0162    0.0530      0.0272         1
                4    18     0.0       0.5550      0.0         0.970
                4    18     0.0       0.4300      0.0         0.978
                5     6     0.0302    0.0641      0.0062         1
                7     8     0.0139    0.0712      0.0097         1
               10    12     0.0277    0.1262      0.0164         1
               11    13     0.0223    0.0732      0.0094         1
               12    13     0.0178    0.0580      0.0302         1
               12    16     0.0180    0.0813      0.0108         1
               12    17     0.0397    0.1790      0.0238         1
               14    15     0.0171    0.0547      0.0074         1
               18    19     0.4610    0.6850      0.0            1
               19    20     0.2830    0.4340      0.0            1
               21    20     0.0       0.7767      0.0         1.043
               21    22     0.0736    0.1170      0.0            1
```

| | | | | | |
|---|---|---|---|---|---|
| 22 | 23 | 0.0099 | 0.0152 | 0.0 | 1 |
| 23 | 24 | 0.1660 | 0.2560 | 0.0042 | 1 |
| 24 | 25 | 0.0 | 1.1820 | 0.0 | 1 |
| 24 | 25 | 0.0 | 1.2300 | 0.0 | 1 |
| 24 | 26 | 0.0 | 0.0473 | 0.0 | 1.043 |
| 26 | 27 | 0.1650 | 0.2540 | 0.0 | 1 |
| 27 | 28 | 0.0618 | 0.0954 | 0.0 | 1 |
| 28 | 29 | 0.0418 | 0.0587 | 0.0 | 1 |
| 7 | 29 | 0.0 | 0.0648 | 0.0 | 0.967 |
| 25 | 30 | 0.1350 | 0.2020 | 0.0 | 1 |
| 30 | 31 | 0.3260 | 0.4970 | 0.0 | 1 |
| 31 | 32 | 0.5070 | 0.7550 | 0.0 | 1 |
| 32 | 33 | 0.0392 | 0.0360 | 0.0 | 1 |
| 34 | 32 | 0.0 | 0.9530 | 0.0 | 0.975 |
| 34 | 35 | 0.0520 | 0.0780 | 0.0016 | 1 |
| 35 | 36 | 0.0430 | 0.0537 | 0.0008 | 1 |
| 36 | 37 | 0.0290 | 0.0366 | 0.0 | 1 |
| 37 | 38 | 0.0651 | 0.1009 | 0.0010 | 1 |
| 37 | 39 | 0.0239 | 0.0379 | 0.0 | 1 |
| 36 | 40 | 0.0300 | 0.0466 | 0.0 | 1 |
| 22 | 38 | 0.0192 | 0.0295 | 0.0 | 1 |
| 11 | 41 | 0.0 | 0.7490 | 0.0 | 0.955 |
| 41 | 42 | 0.2070 | 0.3520 | 0.0 | 1 |
| 41 | 43 | 0.0 | 0.4120 | 0.0 | 1 |
| 38 | 44 | 0.0289 | 0.0585 | 0.0010 | 1 |
| 15 | 45 | 0.0 | 0.1042 | 0.0 | 0.955 |
| 14 | 46 | 0.0 | 0.0735 | 0.0 | 0.900 |
| 46 | 47 | 0.0230 | 0.0680 | 0.0016 | 1 |
| 47 | 48 | 0.0182 | 0.0233 | 0.0 | 1 |
| 48 | 49 | 0.0834 | 0.1290 | 0.0024 | 1 |
| 49 | 50 | 0.0801 | 0.1280 | 0.0 | 1 |
| 50 | 51 | 0.1386 | 0.2200 | 0.0 | 1 |
| 10 | 51 | 0.0 | 0.0712 | 0.0 | 0.930 |
| 13 | 49 | 0.0 | 0.1910 | 0.0 | 0.895 |
| 29 | 52 | 0.1442 | 0.1870 | 0.0 | 1 |
| 52 | 53 | 0.0762 | 0.0984 | 0.0 | 1 |

```
    53    54    0.1878    0.2320      0.0           1
    54    55    0.1732    0.2265      0.0           1
    11    43    0.0       0.1530      0.0       0.958
    44    45    0.0624    0.1242      0.0020        1
    40    56    0.0       1.1950      0.0       0.958
    56    41    0.5530    0.5490      0.0           1
    56    42    0.2125    0.3540      0.0           1
    39    57    0.0       1.3550      0.0       0.980
    57    56    0.1740    0.2600      0.0           1
    38    49    0.1150    0.1770      0.0015        1
    38    48    0.0312    0.0482      0.0           1
     9    55    0.0       0.1205      0.0       0.940];
```

**Appendix B2: Bus Data for Nigerian 57-Bus Network**

```
%          |Bus | Type | Vsp | theta | PGi |  QGi | PLi |  QLi |  Qmin |  Qmax |
busdat57 = [1     1     1.040    0     0.0    0.0   0.0     0.0    0.0     0.0;
            2     2     1.010    0     3.0   88.0   0.0    -0.8   50.0   -17.0;
            3     2     0.985    0    41.0   21.0  40.0    -1.0   60.0   -10.0;
            4     3     1.000    0     0.0    0.0   0.0     0.0    0.0     0.0;
            5     3     1.000    0    13.0    4.0   0.0     0.0    0.0     0.0;
            6     2     0.980    0    75.0    2.0   0.0     0.8   25.0    -8.0;
            7     3     1.000    0     0.0    0.0   0.0     0.0    0.0     0.0;
            8     2     1.005    0   150.0   22.0 450.0    62.1  200.0  -140.0;
            9     2     0.980    0   121.0   26.0   0.0     2.2    9.0    -3.0;
           10     3     1.000    0     5.0    2.0   0.0     0.0    0.0     0.0;
           11     3     1.000    0     0.0    0.0   0.0     0.0    0.0     0.0;
           12     2     1.015    0   377.0   24.0 310.0   128.5  155.0  -150.0;
           13     3     1.000    0    18.0    2.3   0.0     0.0    0.0     0.0;
           14     3     1.000    0    10.5    5.3   0.0     0.0    0.0     0.0;
           15     3     1.000    0    22.0    5.0   0.0     0.0    0.0     0.0;
           16     3     1.000    0    43.0    3.0   0.0     0.0    0.0     0.0;
           17     3     1.000    0    42.0    8.0   0.0     0.0    0.0     0.0;
           18     3     1.000    0    27.2    9.8   0.0     0.0    0.0     0.0;
           19     3     1.000    0     3.3    0.6   0.0     0.0    0.0     0.0;
           20     3     1.000    0     2.3    1.0   0.0     0.0    0.0     0.0;
           21     3     1.000    0     0.0    0.0   0.0     0.0    0.0     0.0;
           22     3     1.000    0     0.0    0.0   0.0     0.0    0.0     0.0;
```

```
23    3    1.000    0    6.3    2.1    0.0    0.0    0.0    0.0;
24    3    1.000    0    0.0    0.0    0.0    0.0    0.0    0.0;
25    3    1.000    0    6.3    3.2    0.0    0.0    0.0    0.0;
26    3    1.000    0    0.0    0.0    0.0    0.0    0.0    0.0;
27    3    1.000    0    9.3    0.5    0.0    0.0    0.0    0.0;
28    3    1.000    0    4.6    2.3    0.0    0.0    0.0    0.0;
29    3    1.000    0   17.0    2.6    0.0    0.0    0.0    0.0;
30    3    1.000    0    3.6    1.8    0.0    0.0    0.0    0.0;
31    3    1.000    0    5.8    2.9    0.0    0.0    0.0    0.0;
32    3    1.000    0    1.6    0.8    0.0    0.0    0.0    0.0;
33    3    1.000    0    3.8    1.9    0.0    0.0    0.0    0.0;
34    3    1.000    0    0.0    0.0    0.0    0.0    0.0    0.0;
35    3    1.000    0    6.0    3.0    0.0    0.0    0.0    0.0;
36    3    1.000    0    0.0    0.0    0.0    0.0    0.0    0.0;
37    3    1.000    0    0.0    0.0    0.0    0.0    0.0    0.0;
38    3    1.000    0   14.0    7.0    0.0    0.0    0.0    0.0;
39    3    1.000    0    0.0    0.0    0.0    0.0    0.0    0.0;
40    3    1.000    0    0.0    0.0    0.0    0.0    0.0    0.0;
41    3    1.000    0    6.3    3.0    0.0    0.0    0.0    0.0;
42    3    1.000    0    7.1    4.4    0.0    0.0    0.0    0.0;
43    3    1.000    0    2.0    1.0    0.0    0.0    0.0    0.0;
44    3    1.000    0   12.0    1.8    0.0    0.0    0.0    0.0;
45    3    1.000    0    0.0    0.0    0.0    0.0    0.0    0.0;
46    3    1.000    0    0.0    0.0    0.0    0.0    0.0    0.0;
47    3    1.000    0   29.7   11.6    0.0    0.0    0.0    0.0;
48    3    1.000    0    0.0    0.0    0.0    0.0    0.0    0.0;
49    3    1.000    0   18.0    8.5    0.0    0.0    0.0    0.0;
50    3    1.000    0   21.0   10.5    0.0    0.0    0.0    0.0;
51    3    1.000    0   18.0    5.3    0.0    0.0    0.0    0.0;
52    3    1.000    0    4.9    2.2    0.0    0.0    0.0    0.0;
53    3    1.000    0   20.0   10.0    0.0    0.0    0.0    0.0;
54    3    1.000    0    4.1    1.4    0.0    0.0    0.0    0.0;
55    3    1.000    0    6.8    3.4    0.0    0.0    0.0    0.0;
56    3    1.000    0    7.6    2.2    0.0    0.0    0.0    0.0;
57    3    1.000    0    6.7    2.0    0.0    0.0    0.0    0.0];
```

Appendix D1: Base Case Load flow Analysis of IEEE 14-Bus Network

Newton Raphson Load flow Analysis

| Bus No | V pu | Angle Degree | Injection MW | Injection MVar | Generation MW | Generation Mvar | Load MW | Load MVar |
|---|---|---|---|---|---|---|---|---|
| PF_Result = | | | | | | | | |
| 1.0000 | 1.0600 | 0 | 267.1561 | 4.6836 | 267.1561 | 4.6836 | 0 | 0 |
| 2.0000 | 1.0350 | -5.6082 | 18.3000 | 31.3969 | 40.0000 | 44.0969 | 21.7000 | 12.7000 |
| 3.0000 | 1.0000 | -14.0398 | -94.2000 | 13.4740 | 0.0000 | 32.4740 | 94.2000 | 19.0000 |
| 4.0000 | 0.9956 | -11.7725 | -47.8000 | 3.9000 | 0.0000 | 0.0000 | 47.8000 | -3.9000 |
| 5.0000 | 0.9983 | -10.1821 | -7.6000 | -1.6000 | -0.0000 | 0.0000 | 7.6000 | 1.6000 |
| 6.0000 | 1.0400 | -18.3781 | -11.2000 | 13.4312 | -0.0000 | 20.9312 | 11.2000 | 7.5000 |
| 7.0000 | 1.0284 | -15.8833 | -0.0000 | -0.0000 | -0.0000 | -0.0000 | 0 | 0 |
| 8.0000 | 1.0700 | -15.8833 | 0 | 25.2570 | 0 | 25.2570 | 0 | 0 |
| 9.0000 | 1.0101 | -18.0614 | -29.5000 | -16.6000 | -0.0000 | -0.0000 | 29.5000 | 16.6000 |
| 10.0000 | 1.0077 | -18.4183 | -9.0000 | -5.8000 | -0.0000 | -0.0000 | 9.0000 | 5.8000 |
| 11.0000 | 1.0202 | -18.5238 | -3.5000 | -1.8000 | 0.0000 | 0.0000 | 3.5000 | 1.8000 |
| 12.0000 | 1.0117 | -20.3917 | -16.1000 | -1.6000 | 0.0000 | 0.0000 | 16.1000 | 1.6000 |
| 13.0000 | 1.0087 | -20.1782 | -23.5000 | -5.8000 | 0.0000 | 0.0000 | 23.5000 | 5.8000 |
| 14.0000 | 0.9826 | -20.9607 | -24.9000 | -5.0000 | 0.0000 | 0 | 24.9000 | 5.0000 |
| 0 | 0 | 0 | 18.1561 | 53.9427 | 307.1561 | 127.4427 | 289.0000 | 73.5000 |

Line Flow and Losses

| From Bus | To Bus | P MW | Q MVar | From Bus | To Bus | P MW | Q MVar | Line Loss MW | Line Loss MVar |
|---|---|---|---|---|---|---|---|---|---|
| LF_Result = | | | | | | | | | |
| 1.0000 | 2.0000 | 179.5160 | -5.1357 | 2.0000 | 1.0000 | -173.9531 | 22.1202 | 5.5629 | 16.9845 |
| 1.0000 | 5.0000 | 87.6401 | 15.5497 | 5.0000 | 1.0000 | -83.8304 | 0.1770 | 3.8097 | 15.7267 |
| 2.0000 | 3.0000 | 77.9506 | 5.4465 | 3.0000 | 2.0000 | -75.2721 | 5.8377 | 2.6784 | 11.2842 |
| 2.0000 | 4.0000 | 64.4902 | 5.2747 | 4.0000 | 2.0000 | -62.2190 | 1.6167 | 2.2712 | 6.8913 |

```
    2.0000    5.0000   49.8124    7.4038    5.0000    2.0000  -48.4641   -3.2872    1.3483    4.1166
    3.0000    4.0000  -18.9279   10.4663    4.0000    3.0000   19.2413   -9.6662    0.3135    0.8001
    4.0000    5.0000  -61.1484   13.7467    5.0000    4.0000   61.6775  -12.0778    0.5291    1.6689
    4.0000    7.0000   35.8870  -14.7067    7.0000    4.0000  -35.8870   17.8105   -0.0000    3.1038
    4.0000    9.0000   20.4390   -1.5561    9.0000    4.0000  -20.4390    3.8408         0    2.2847
    5.0000    6.0000   63.0170  -13.1953    6.0000    5.0000  -63.0170   22.9644         0    9.7691
    6.0000   11.0000    5.1325    7.9088   11.0000    6.0000   -5.0544   -7.7453    0.0781    0.1635
    6.0000   12.0000   16.3273    3.9034   12.0000    6.0000  -16.0071   -3.2369    0.3202    0.6665
    6.0000   13.0000   30.3572    9.9676   13.0000    6.0000  -29.7328   -8.7380    0.6244    1.2296
    7.0000    8.0000   -0.0000  -24.2755    8.0000    7.0000    0.0000   25.2570         0    0.9815
    7.0000    9.0000   35.8870   17.8420    9.0000    7.0000  -35.8870  -16.1714         0    1.6707
    9.0000   10.0000    7.4928   -0.0291   10.0000    9.0000   -7.4753    0.0756    0.0175    0.0465
    9.0000   14.0000   19.3332    1.6281   14.0000    9.0000  -18.8642   -0.6305    0.4690    0.9976
   10.0000   11.0000   -1.5247   -5.8756   11.0000   10.0000    1.5544    5.9453    0.0298    0.0697
   12.0000   13.0000   -0.0929    1.6369   13.0000   12.0000    0.0987   -1.6316    0.0058    0.0052
   13.0000   14.0000    6.1341    4.5696   14.0000   13.0000   -6.0358   -4.3695    0.0983    0.2001
         0         0         0         0         0         0         0         0   18.1561   78.6607
```

---

## Appendix D2: Load flow Analysis of IEEE 14-Bus Network with Optimized OLTCs

---

Newton Raphson Load flow Analysis

---

| Bus | V | Angle | Injection | | Generation | | Load | |
|---|---|---|---|---|---|---|---|---|
| No | pu | Degree | MW | MVar | MW | Mvar | MW | MVar |

---

```
PF_Result =
    1.0000    1.0600         0  309.1147   81.7422  309.1147   81.7422         0         0
    2.0000    1.0050   -6.1531   18.3000   40.1940   40.0000   52.8940   21.7000   12.7000
    3.0000    0.9600  -15.7560  -94.2000   32.7334   -0.0000   51.7334   94.2000   19.0000
    4.0000    0.9152  -12.8415  -47.8000   33.1500   -0.0000   -0.0000   47.8000  -33.1500
    5.0000    0.9306  -11.9310   -7.6000  -13.6000    0.0000   -0.0000    7.6000   13.6000
    6.0000    1.0200  -27.6849  -11.2000  265.1303    0.0000  328.8803   11.2000   63.7500
    7.0000    0.8229  -17.3468    0.0000   -0.0000    0.0000   -0.0000         0         0
```

| | | | | | | | | |
|---|---|---|---|---|---|---|---|---|
| 8.0000 | 1.0400 | -17.3468 | 0.0000 | 128.1696 | 0.0000 | 128.1696 | 0 | 0 |
| 9.0000 | 0.6307 | -20.8618 | -29.5000 | -141.1000 | 0.0000 | -0.0000 | 29.5000 | 141.1000 |
| 10.0000 | 0.6329 | -21.2381 | -9.0000 | -49.3000 | -0.0000 | -0.0000 | 9.0000 | 49.3000 |
| 11.0000 | 0.8003 | -24.5617 | -3.5000 | -15.3000 | -0.0000 | -0.0000 | 3.5000 | 15.3000 |
| 12.0000 | 0.9046 | -28.9544 | -16.1000 | -13.6000 | -0.0000 | -0.0000 | 16.1000 | 13.6000 |
| 13.0000 | 0.8535 | -27.2034 | -23.5000 | -49.3000 | -0.0000 | -0.0000 | 23.5000 | 49.3000 |
| 14.0000 | 0.5852 | -24.9545 | -24.9000 | -42.5000 | -0.0000 | 0 | 24.9000 | 42.5000 |
| 0 | 0 | 0 | 60.1147 | 256.4196 | 349.1147 | 643.4196 | 289.0000 | 387.0000 |

Line Flow and Losses

| From Bus | To Bus | P MW | Q MVar | From Bus | To Bus | P MW | Q MVar | Line Loss MW | Line Loss MVar |
|---|---|---|---|---|---|---|---|---|---|
| LF_Result = | | | | | | | | | |
| 1.0000 | 2.0000 | 206.4929 | 41.2688 | 2.0000 | 1.0000 | -198.8447 | -17.9176 | 7.6482 | 23.3512 |
| 1.0000 | 5.0000 | 102.6218 | 46.2038 | 5.0000 | 1.0000 | -96.5312 | -21.0611 | 6.0907 | 25.1427 |
| 2.0000 | 3.0000 | 83.6303 | 9.8229 | 3.0000 | 2.0000 | -80.3316 | 4.0749 | 3.2988 | 13.8978 |
| 2.0000 | 4.0000 | 71.0800 | 31.3313 | 4.0000 | 2.0000 | -67.6085 | -20.7977 | 3.4716 | 10.5336 |
| 2.0000 | 5.0000 | 62.4343 | 25.3003 | 5.0000 | 2.0000 | -59.8755 | -17.4877 | 2.5588 | 7.8126 |
| 3.0000 | 4.0000 | -13.8684 | 31.2666 | 4.0000 | 3.0000 | 14.7191 | -29.0954 | 0.8507 | 2.1712 |
| 4.0000 | 5.0000 | -38.7780 | -20.9501 | 5.0000 | 4.0000 | 39.0877 | 21.9269 | 0.3097 | 0.9768 |
| 4.0000 | 7.0000 | 28.9249 | 42.4160 | 7.0000 | 4.0000 | -28.9249 | -35.9795 | 0 | 6.4364 |
| 4.0000 | 9.0000 | 14.9425 | 49.3537 | 9.0000 | 4.0000 | -14.9425 | -32.2428 | 0.0000 | 17.1109 |
| 5.0000 | 6.0000 | 109.7189 | -20.2492 | 6.0000 | 5.0000 | -109.7189 | 54.0135 | -0.0000 | 33.7643 |
| 6.0000 | 11.0000 | 25.8378 | 100.9349 | 11.0000 | 6.0000 | -15.9277 | -80.1818 | 9.9101 | 20.7530 |
| 6.0000 | 12.0000 | 24.4915 | 34.3428 | 12.0000 | 6.0000 | -22.3895 | -29.9680 | 2.1020 | 4.3748 |
| 6.0000 | 13.0000 | 48.1897 | 105.9595 | 13.0000 | 6.0000 | -39.5746 | -88.9938 | 8.6151 | 16.9657 |
| 7.0000 | 8.0000 | 0 | -101.4158 | 8.0000 | 7.0000 | 0 | 128.1696 | 0 | 26.7538 |
| 7.0000 | 9.0000 | 28.9249 | 144.6798 | 9.0000 | 7.0000 | -28.9249 | -109.3158 | 0 | 35.3640 |
| 9.0000 | 10.0000 | 2.1716 | -2.4718 | 10.0000 | 9.0000 | -2.1629 | 2.4948 | 0.0087 | 0.0230 |
| 9.0000 | 14.0000 | 12.1958 | 5.2183 | 14.0000 | 9.0000 | -11.6335 | -4.0222 | 0.5623 | 1.1961 |
| 10.0000 | 11.0000 | -6.8371 | -51.7948 | 11.0000 | 10.0000 | 12.4277 | 64.8818 | 5.5906 | 13.0870 |
| 12.0000 | 13.0000 | 6.2895 | 16.3680 | 13.0000 | 12.0000 | -5.4594 | -15.6169 | 0.8301 | 0.7511 |

| | | | | | | | | | |
|---|---|---|---|---|---|---|---|---|---|
| 13.0000 | 14.0000 | 21.5340 | 55.3107 | 14.0000 | 13.0000 | -13.2665 | -38.4778 | 8.2675 | 16.8329 |
| 0 | 0 | 0 | 0 | 0 | 0 | 0 | 0 | 60.1147 | 277.2988 |

## Appendix E1: Base Case Load flow Analysis of IEEE 30-Bus Network

Newton Raphson Load flow Analysis

| Bus No | V pu | Angle Degree | Injection MW | Injection MVar | Generation MW | Generation Mvar | Load MW | Load MVar |
|---|---|---|---|---|---|---|---|---|
| PF_Result= | | | | | | | | |
| 1.0000 | 1.0600 | 0 | 265.9490 | 65.2903 | 265.9490 | 65.2903 | 0 | 0 |
| 2.0000 | 1.0130 | -5.1117 | 18.3000 | 27.7451 | 40.0000 | 40.4451 | 21.7000 | 12.7000 |
| 3.0000 | 0.9742 | -7.1843 | -2.4000 | -1.2000 | -0.0000 | 0.0000 | 2.4000 | 1.2000 |
| 4.0000 | 0.9543 | -8.9059 | -7.6000 | -13.6000 | -0.0000 | -0.0000 | 7.6000 | 13.6000 |
| 5.0000 | 0.9600 | -14.7698 | -94.2000 | 52.4883 | 0.0000 | 213.9883 | 94.2000 | 161.5000 |
| 6.0000 | 0.9488 | -10.8958 | 0.0000 | 0.0000 | 0.0000 | 0.0000 | 0 | 0 |
| 7.0000 | 0.9008 | -12.1756 | -22.8000 | -92.6500 | 0.0000 | 0.0000 | 22.8000 | 92.6500 |
| 8.0000 | 0.9600 | -11.9435 | -30.0000 | 37.8072 | 0.0000 | 67.8072 | 30.0000 | 30.0000 |
| 9.0000 | 0.9733 | -14.5315 | 0.0000 | 0 | 0.0000 | 0 | 0 | 0 |
| 10.0000 | 0.9454 | -16.5036 | -5.8000 | 2.0000 | -0.0000 | 19.0000 | 5.8000 | 17.0000 |
| 11.0000 | 1.0320 | -14.5315 | -0.0000 | 29.1431 | -0.0000 | 29.1431 | 0 | 0 |
| 12.0000 | 0.9444 | -15.2835 | -11.2000 | -63.7500 | 0.0000 | 0.0000 | 11.2000 | 63.7500 |
| 13.0000 | 1.0210 | -15.2835 | -0.0000 | 55.8804 | -0.0000 | 55.8804 | 0 | 0 |
| 14.0000 | 0.9127 | -15.6861 | -6.2000 | -13.6000 | -0.0000 | 0.0000 | 6.2000 | 13.6000 |
| 15.0000 | 0.9242 | -16.5082 | -8.2000 | -2.5000 | 0.0000 | -0.0000 | 8.2000 | 2.5000 |
| 16.0000 | 0.9367 | -16.1516 | -3.5000 | -1.8000 | -0.0000 | -0.0000 | 3.5000 | 1.8000 |
| 17.0000 | 0.9369 | -16.6575 | -9.0000 | -5.8000 | 0.0000 | -0.0000 | 9.0000 | 5.8000 |
| 18.0000 | 0.9180 | -17.3756 | -3.2000 | -0.9000 | -0.0000 | 0.0000 | 3.2000 | 0.9000 |
| 19.0000 | 0.9179 | -17.6500 | -9.5000 | -3.4000 | 0.0000 | -0.0000 | 9.5000 | 3.4000 |
| 20.0000 | 0.9239 | -17.4355 | -2.2000 | -0.7000 | -0.0000 | -0.0000 | 2.2000 | 0.7000 |
| 21.0000 | 0.9268 | -17.0923 | -17.5000 | -11.2000 | -0.0000 | 0.0000 | 17.5000 | 11.2000 |
| 22.0000 | 0.9375 | -16.9076 | 0.0000 | 0.0000 | 0.0000 | 0.0000 | 0 | 0 |
| 23.0000 | 0.9258 | -17.0866 | -3.2000 | -1.6000 | -0.0000 | -0.0000 | 3.2000 | 1.6000 |
| 24.0000 | 0.9264 | -17.3555 | -8.7000 | -2.4000 | 0.0000 | 4.3000 | 8.7000 | 6.7000 |
| 25.0000 | 0.9340 | -16.9591 | -0.0000 | 0 | -0.0000 | 0 | 0 | 0 |
| 26.0000 | 0.9147 | -17.4587 | -3.5000 | -2.3000 | 0.0000 | -0.0000 | 3.5000 | 2.3000 |
| 27.0000 | 0.9481 | -16.3965 | 0.0000 | 0.0000 | 0.0000 | 0.0000 | 0 | 0 |
| 28.0000 | 0.9483 | -11.6901 | 0.0000 | 0.0000 | 0.0000 | 0.0000 | 0 | 0 |
| 29.0000 | 0.9265 | -17.8341 | -2.4000 | -0.9000 | 0.0000 | 0.0000 | 2.4000 | 0.9000 |
| 30.0000 | 0.9140 | -18.8717 | -10.6000 | -1.9000 | 0.0000 | -0.0000 | 10.6000 | 1.9000 |
| 0 | 0 | 0 | 22.5490 | 50.1543 | 305.9490 | 495.8543 | 283.4000 | 445.7000 |

---

Line Flow and Losses

---

| From Bus | To Bus | P MW | Q MVar | From Bus | To Bus | P MW | Q MVar | Line Loss MW | Line Loss MVar |
|---|---|---|---|---|---|---|---|---|---|

LF_Result =

| | | | | | | | | | |
|---|---|---|---|---|---|---|---|---|---|
| 1.0000 | 2.0000 | 177.9534 | 34.6494 | 2.0000 | 1.0000 | -172.3369 | -17.8293 | 5.6165 | 16.8201 |
| 1.0000 | 3.0000 | 87.9956 | 35.8993 | 3.0000 | 1.0000 | -84.3622 | -22.6198 | 3.6334 | 13.2795 |
| 2.0000 | 4.0000 | 43.7563 | 21.1174 | 4.0000 | 2.0000 | -42.4451 | -17.1217 | 1.3112 | 3.9957 |
| 3.0000 | 4.0000 | 81.9622 | 23.7544 | 4.0000 | 3.0000 | -80.9494 | -20.8462 | 1.0129 | 2.9082 |
| 2.0000 | 5.0000 | 85.5287 | 13.6677 | 5.0000 | 2.0000 | -82.0781 | 0.8293 | 3.4506 | 14.4970 |
| 2.0000 | 6.0000 | 61.3519 | 19.4501 | 6.0000 | 2.0000 | -59.0066 | -12.3333 | 2.3453 | 7.1167 |
| 4.0000 | 6.0000 | 73.8385 | -7.3013 | 6.0000 | 4.0000 | -73.1191 | 9.8043 | 0.7195 | 2.5030 |
| 5.0000 | 7.0000 | -12.1219 | 54.5252 | 7.0000 | 5.0000 | 13.6792 | -50.5982 | 1.5573 | 3.9270 |
| 6.0000 | 7.0000 | 37.4576 | 43.5390 | 7.0000 | 6.0000 | -36.4792 | -40.5342 | 0.9784 | 3.0048 |
| 6.0000 | 8.0000 | 30.0699 | -33.5477 | 8.0000 | 6.0000 | -29.7994 | 34.4946 | 0.2706 | 0.9470 |
| 6.0000 | 9.0000 | 28.7860 | -10.4994 | 9.0000 | 6.0000 | -28.7860 | 12.6210 | 0 | 2.1216 |
| 6.0000 | 10.0000 | 16.2699 | 1.3863 | 10.0000 | 6.0000 | -16.2699 | 0.2094 | -0.0000 | 1.5958 |
| 9.0000 | 11.0000 | 0.0000 | -27.4844 | 11.0000 | 9.0000 | -0.0000 | 29.1431 | 0 | 1.6587 |
| 9.0000 | 10.0000 | 28.7860 | 25.1077 | 10.0000 | 9.0000 | -28.7860 | -23.4133 | 0 | 1.6943 |
| 4.0000 | 12.0000 | 41.9559 | 6.2905 | 12.0000 | 4.0000 | -41.9559 | -1.5746 | 0 | 4.7159 |
| 12.0000 | 13.0000 | 0.0000 | -51.6867 | 13.0000 | 12.0000 | -0.0000 | 55.8804 | -0.0000 | 4.1937 |
| 12.0000 | 14.0000 | 6.4907 | 8.5732 | 14.0000 | 12.0000 | -6.3311 | -8.2415 | 0.1596 | 0.3318 |
| 12.0000 | 15.0000 | 17.3317 | 5.9594 | 15.0000 | 12.0000 | -17.0824 | -5.4682 | 0.2493 | 0.4911 |
| 12.0000 | 16.0000 | 6.9335 | 0.3968 | 16.0000 | 12.0000 | -6.8824 | -0.2894 | 0.0511 | 0.1075 |
| 14.0000 | 15.0000 | 0.1311 | -5.3585 | 15.0000 | 14.0000 | -0.0549 | 5.4274 | 0.0762 | 0.0689 |
| 16.0000 | 17.0000 | 3.3824 | -1.5106 | 17.0000 | 16.0000 | -3.3695 | 1.5407 | 0.0129 | 0.0301 |
| 15.0000 | 18.0000 | 5.7853 | -0.1891 | 18.0000 | 15.0000 | -5.7432 | 0.2748 | 0.0421 | 0.0857 |
| 18.0000 | 19.0000 | 2.5432 | -1.1748 | 19.0000 | 18.0000 | -2.5373 | 1.1869 | 0.0060 | 0.0120 |
| 19.0000 | 20.0000 | -6.9627 | -4.5869 | 20.0000 | 19.0000 | 6.9908 | 4.6430 | 0.0281 | 0.0561 |
| 10.0000 | 20.0000 | 9.3147 | 5.6197 | 20.0000 | 10.0000 | -9.1908 | -5.3430 | 0.1239 | 0.2767 |
| 10.0000 | 17.0000 | 5.6621 | 7.4231 | 17.0000 | 10.0000 | -5.6305 | -7.3407 | 0.0316 | 0.0824 |
| 10.0000 | 21.0000 | 18.9202 | 14.8515 | 21.0000 | 10.0000 | -18.6949 | -14.3667 | 0.2252 | 0.4848 |
| 10.0000 | 22.0000 | 5.3590 | 2.4529 | 22.0000 | 10.0000 | -5.3307 | -2.3946 | 0.0283 | 0.0583 |
| 21.0000 | 23.0000 | 1.1949 | 3.1667 | 23.0000 | 21.0000 | -1.1934 | -3.1635 | 0.0015 | 0.0031 |
| 15.0000 | 23.0000 | 3.1520 | -2.2701 | 23.0000 | 15.0000 | -3.1343 | 2.3057 | 0.0177 | 0.0357 |
| 22.0000 | 24.0000 | 5.3307 | 2.3946 | 24.0000 | 22.0000 | -5.2860 | -2.3251 | 0.0447 | 0.0696 |
| 23.0000 | 24.0000 | 1.1277 | -0.7422 | 24.0000 | 23.0000 | -1.1249 | 0.7479 | 0.0028 | 0.0057 |

| | | | | | | | | | |
|---|---|---|---|---|---|---|---|---|---|
| 24.0000 | 25.0000 | -2.2891 | -0.8229 | 25.0000 | 24.0000 | 2.3021 | 0.8456 | 0.0130 | 0.0227 |
| 25.0000 | 26.0000 | 3.5533 | 2.3797 | 26.0000 | 25.0000 | -3.5000 | -2.3000 | 0.0533 | 0.0797 |
| 25.0000 | 27.0000 | -5.8555 | -3.2252 | 27.0000 | 25.0000 | 5.9114 | 3.3321 | 0.0560 | 0.1069 |
| 28.0000 | 27.0000 | 19.2436 | 0.8363 | 27.0000 | 28.0000 | -19.2436 | 0.7453 | 0.0000 | 1.5816 |
| 27.0000 | 29.0000 | 6.2120 | 1.7114 | 29.0000 | 27.0000 | -6.1105 | -1.5195 | 0.1015 | 0.1918 |
| 27.0000 | 30.0000 | 7.1201 | 1.7148 | 30.0000 | 27.0000 | -6.9291 | -1.3552 | 0.1911 | 0.3596 |
| 29.0000 | 30.0000 | 3.7105 | 0.6195 | 30.0000 | 29.0000 | -3.6709 | -0.5448 | 0.0396 | 0.0747 |
| 8.0000 | 28.0000 | -0.2006 | 5.6995 | 28.0000 | 8.0000 | 0.2231 | -5.6289 | 0.0224 | 0.0706 |
| 6.0000 | 28.0000 | 19.5422 | -4.5393 | 28.0000 | 6.0000 | -19.4667 | 4.8071 | 0.0756 | 0.2678 |
| 0 | 0 | 0 | 0 | 0 | 0 | 0 | 0 | 22.5490 | 89.9340 |

## Appendix E2: Load flow Analysis of IEEE 30-Bus Network with Optimized OLTCs

Newton Raphson Loadflow Analysis

| Bus No | V pu | Angle Degree | Injection MW | Injection MVar | Generation MW | Generation Mvar | Load MW | Load MVar |
|---|---|---|---|---|---|---|---|---|
| PF_Result = | | | | | | | | |
| 1.0000 | 1.0600 | 0 | 260.9280 | -17.1183 | 260.9280 | -17.1183 | 0 | 0 |
| 2.0000 | 1.0430 | -5.3474 | 18.3000 | 35.0656 | 40.0000 | 47.7656 | 21.7000 | 12.7000 |
| 3.0000 | 1.0217 | -7.5448 | -2.4000 | -1.2000 | -0.0000 | 0.0000 | 2.4000 | 1.2000 |
| 4.0000 | 1.0129 | -9.2989 | -7.6000 | -1.6000 | 0.0000 | 0.0000 | 7.6000 | 1.6000 |
| 5.0000 | 1.0100 | -14.1542 | -94.2000 | 16.9651 | -0.0000 | 35.9651 | 94.2000 | 19.0000 |
| 6.0000 | 1.0121 | -11.0880 | 0.0000 | 0.0000 | 0.0000 | 0.0000 | 0 | 0 |
| 7.0000 | 1.0035 | -12.8734 | -22.8000 | -10.9000 | -0.0000 | -0.0000 | 22.8000 | 10.9000 |
| 8.0000 | 1.0100 | -11.8039 | -30.0000 | 0.6915 | 0.0000 | 30.6915 | 30.0000 | 30.0000 |
| 9.0000 | 1.0507 | -14.1363 | 0.0000 | 0.0000 | 0.0000 | 0.0000 | 0 | 0 |
| 10.0000 | 1.0438 | -15.7341 | -5.8000 | 17.0000 | -0.0000 | 19.0000 | 5.8000 | 2.0000 |
| 11.0000 | 1.0820 | -14.1363 | 0 | 16.2696 | 0 | 16.2696 | 0 | 0 |
| 12.0000 | 1.0576 | -14.9416 | -11.2000 | -7.5000 | 0.0000 | -0.0000 | 11.2000 | 7.5000 |
| 13.0000 | 1.0710 | -14.9416 | 0 | 10.2475 | 0 | 10.2475 | 0 | 0 |
| 14.0000 | 1.0429 | -15.8244 | -6.2000 | -1.6000 | -0.0000 | 0.0000 | 6.2000 | 1.6000 |
| 15.0000 | 1.0384 | -15.9101 | -8.2000 | -2.5000 | -0.0000 | 0.0000 | 8.2000 | 2.5000 |
| 16.0000 | 1.0445 | -15.5487 | -3.5000 | -1.8000 | -0.0000 | -0.0000 | 3.5000 | 1.8000 |
| 17.0000 | 1.0387 | -15.8856 | -9.0000 | -5.8000 | -0.0000 | 0.0000 | 9.0000 | 5.8000 |
| 18.0000 | 1.0282 | -16.5425 | -3.2000 | -0.9000 | -0.0000 | 0.0000 | 3.2000 | 0.9000 |
| 19.0000 | 1.0252 | -16.7273 | -9.5000 | -3.4000 | -0.0000 | 0.0000 | 9.5000 | 3.4000 |
| 20.0000 | 1.0291 | -16.5363 | -2.2000 | -0.7000 | 0.0000 | -0.0000 | 2.2000 | 0.7000 |

| | | | | | | | | |
|---|---|---|---|---|---|---|---|---|
| 21.0000 | 1.0293 | -16.2462 | -17.5000 | -11.2000 | -0.0000 | 0.0000 | 17.5000 | 11.2000 |
| 22.0000 | 1.0353 | -16.0738 | 0.0000 | -0.0000 | 0.0000 | -0.0000 | 0 | 0 |
| 23.0000 | 1.0291 | -16.2528 | -3.2000 | -1.6000 | 0.0000 | 0.0000 | 3.2000 | 1.6000 |
| 24.0000 | 1.0237 | -16.4409 | -8.7000 | -2.4000 | -0.0000 | 4.3000 | 8.7000 | 6.7000 |
| 25.0000 | 1.0202 | -16.0539 | 0.0000 | 0.0000 | 0.0000 | 0.0000 | 0 | 0 |
| 26.0000 | 1.0025 | -16.4712 | -3.5000 | -2.3000 | -0.0000 | -0.0000 | 3.5000 | 2.3000 |
| 27.0000 | 1.0265 | -15.5558 | 0.0000 | -0.0000 | 0.0000 | -0.0000 | 0 | 0 |
| 28.0000 | 1.0109 | -11.7436 | 0.0000 | 0.0000 | 0.0000 | 0.0000 | 0 | 0 |
| 29.0000 | 1.0067 | -16.7777 | -2.4000 | -0.9000 | -0.0000 | -0.0000 | 2.4000 | 0.9000 |
| 30.0000 | 0.9953 | -17.6546 | -10.6000 | -1.9000 | 0.0000 | 0.0000 | 10.6000 | 1.9000 |
| 0 | 0 | 0 | 17.5280 | 20.9210 | 300.9280 | 147.1210 | 283.4000 | 126.2000 |

---

Line FLow and Losses

---

| From Bus | To Bus | P MW | Q MVar | From Bus | To Bus | P MW | Q MVar | Line Loss MW | Line Loss MVar |
|---|---|---|---|---|---|---|---|---|---|

---

LF_Result =

| | | | | | | | | | |
|---|---|---|---|---|---|---|---|---|---|
| 1.0000 | 2.0000 | 173.1430 | -18.1076 | 2.0000 | 1.0000 | -167.9643 | 33.6169 | 5.1787 | 15.5092 |
| 1.0000 | 3.0000 | 87.7849 | 6.2478 | 3.0000 | 1.0000 | -84.6692 | 5.1398 | 3.1157 | 11.3876 |
| 2.0000 | 4.0000 | 43.6185 | 5.1943 | 4.0000 | 2.0000 | -42.6075 | -2.1133 | 1.0110 | 3.0810 |
| 3.0000 | 4.0000 | 82.2692 | -3.7720 | 4.0000 | 3.0000 | -81.4115 | 6.2346 | 0.8577 | 2.4626 |
| 2.0000 | 5.0000 | 82.2929 | 4.0325 | 5.0000 | 2.0000 | -79.3475 | 8.3418 | 2.9454 | 12.3743 |
| 2.0000 | 6.0000 | 60.3529 | 1.4034 | 6.0000 | 2.0000 | -58.4065 | 4.5029 | 1.9464 | 5.9063 |
| 4.0000 | 6.0000 | 72.2720 | -17.5214 | 6.0000 | 4.0000 | -71.6305 | 19.7528 | 0.6414 | 2.2315 |
| 5.0000 | 7.0000 | -14.8525 | 11.7958 | 7.0000 | 5.0000 | 15.0147 | -11.3867 | 0.1622 | 0.4091 |
| 6.0000 | 7.0000 | 38.1954 | -1.2007 | 7.0000 | 6.0000 | -37.8147 | 2.3697 | 0.3807 | 1.1690 |
| 6.0000 | 8.0000 | 29.4897 | -3.2137 | 8.0000 | 6.0000 | -29.3866 | 3.5745 | 0.1031 | 0.3608 |
| 6.0000 | 9.0000 | 27.7995 | -18.4846 | 9.0000 | 6.0000 | -27.7995 | 20.6979 | 0 | 2.2133 |
| 6.0000 | 10.0000 | 15.8822 | -5.3058 | 10.0000 | 6.0000 | -15.8822 | 6.7806 | -0.0000 | 1.4748 |
| 9.0000 | 11.0000 | -0.0000 | -15.7993 | 11.0000 | 9.0000 | 0.0000 | 16.2696 | 0.0000 | 0.4703 |
| 9.0000 | 10.0000 | 27.7995 | 7.0412 | 10.0000 | 9.0000 | -27.7995 | -6.2219 | 0 | 0.8194 |
| 4.0000 | 12.0000 | 44.1470 | -16.7948 | 12.0000 | 4.0000 | -44.1470 | 21.9829 | 0 | 5.1881 |
| 12.0000 | 13.0000 | -0.0000 | -10.1193 | 13.0000 | 12.0000 | 0.0000 | 10.2475 | 0.0000 | 0.1282 |
| 12.0000 | 14.0000 | 7.7900 | 2.3896 | 14.0000 | 12.0000 | -7.7169 | -2.2377 | 0.0731 | 0.1519 |
| 12.0000 | 15.0000 | 17.6394 | 6.7049 | 15.0000 | 12.0000 | -17.4287 | -6.2898 | 0.2108 | 0.4152 |
| 12.0000 | 16.0000 | 7.5176 | 3.4205 | 16.0000 | 12.0000 | -7.4600 | -3.2993 | 0.0576 | 0.1212 |
| 14.0000 | 15.0000 | 1.5169 | 0.6377 | 15.0000 | 14.0000 | -1.5114 | -0.6328 | 0.0055 | 0.0050 |

| | | | | | | | | | |
|---|---|---|---|---|---|---|---|---|---|
| 16.0000 | 17.0000 | 3.9600 | 1.4993 | 17.0000 | 16.0000 | -3.9464 | -1.4677 | 0.0135 | 0.0316 |
| 15.0000 | 18.0000 | 6.2913 | 1.8291 | 18.0000 | 15.0000 | -6.2486 | -1.7422 | 0.0427 | 0.0870 |
| 18.0000 | 19.0000 | 3.0486 | 0.8422 | 19.0000 | 18.0000 | -3.0425 | -0.8299 | 0.0060 | 0.0122 |
| 19.0000 | 20.0000 | -6.4575 | -2.5701 | 20.0000 | 19.0000 | 6.4731 | 2.6013 | 0.0156 | 0.0313 |
| 10.0000 | 20.0000 | 8.7492 | 3.4713 | 20.0000 | 10.0000 | -8.6731 | -3.3013 | 0.0761 | 0.1700 |
| 10.0000 | 17.0000 | 5.0669 | 4.3670 | 17.0000 | 10.0000 | -5.0536 | -4.3323 | 0.0133 | 0.0347 |
| 10.0000 | 21.0000 | 18.2856 | 11.7645 | 21.0000 | 10.0000 | -18.1346 | -11.4394 | 0.1510 | 0.3250 |
| 10.0000 | 22.0000 | 5.7799 | 3.1070 | 22.0000 | 10.0000 | -5.7512 | -3.0477 | 0.0287 | 0.0592 |
| 21.0000 | 23.0000 | 0.6346 | 0.2394 | 23.0000 | 21.0000 | -0.6345 | -0.2393 | 0.0001 | 0.0001 |
| 15.0000 | 23.0000 | 4.4488 | 2.5934 | 23.0000 | 15.0000 | -4.4242 | -2.5438 | 0.0246 | 0.0497 |
| 22.0000 | 24.0000 | 5.7512 | 3.0477 | 24.0000 | 22.0000 | -5.7057 | -2.9769 | 0.0455 | 0.0708 |
| 23.0000 | 24.0000 | 1.8588 | 1.1831 | 24.0000 | 23.0000 | -1.8527 | -1.1707 | 0.0061 | 0.0124 |
| 24.0000 | 25.0000 | -1.1415 | 1.7477 | 25.0000 | 24.0000 | 1.1494 | -1.7340 | 0.0078 | 0.0137 |
| 25.0000 | 26.0000 | 3.5444 | 2.3663 | 26.0000 | 25.0000 | -3.5000 | -2.3000 | 0.0444 | 0.0663 |
| 25.0000 | 27.0000 | -4.6938 | -0.6323 | 27.0000 | 25.0000 | 4.7173 | 0.6773 | 0.0236 | 0.0450 |
| 28.0000 | 27.0000 | 17.9976 | -3.5291 | 27.0000 | 28.0000 | -17.9976 | 4.7909 | 0 | 1.2618 |
| 27.0000 | 29.0000 | 6.1892 | 1.6673 | 29.0000 | 27.0000 | -6.1035 | -1.5054 | 0.0857 | 0.1619 |
| 27.0000 | 30.0000 | 7.0910 | 1.6610 | 30.0000 | 27.0000 | -6.9299 | -1.3576 | 0.1612 | 0.3034 |
| 29.0000 | 30.0000 | 3.7035 | 0.6054 | 30.0000 | 29.0000 | -3.6701 | -0.5424 | 0.0333 | 0.0630 |
| 8.0000 | 28.0000 | -0.6134 | -0.2410 | 28.0000 | 8.0000 | 0.6137 | 0.2418 | 0.0003 | 0.0009 |
| 6.0000 | 28.0000 | 18.6703 | -3.0943 | 28.0000 | 6.0000 | -18.6113 | 3.3038 | 0.0591 | 0.2094 |
| 0 | 0 | 0 | 0 | 0 | 0 | 0 | 0 | 17.5280 | 68.8881 |

## Appendix F1: Base Case Load flow Analysis of Nigerian 57-bus Network

Newton Raphson Loadflow Analysis

| Bus No | V pu | Angle Degree | Injection MW | Injection MVar | Generation MW | Generation Mvar | Load MW | Load MVar |
|---|---|---|---|---|---|---|---|---|
| PF_Result = 1.0e+03 * | | | | | | | | |
| 0.0010 | 0.0010 | 0 | -0.3684 | 0.1329 | -0.3684 | 0.1329 | 0 | 0 |
| 0.0020 | 0.0010 | 0.0014 | 0.0030 | 0.0034 | 0.0030 | 0.0026 | 0 | -0.0008 |
| 0.0030 | 0.0010 | 0.0059 | 0.0010 | -0.0318 | 0.0410 | -0.0328 | 0.0400 | -0.0010 |
| 0.0040 | 0.0010 | 0.0070 | 0.0000 | 0.0000 | 0.0000 | 0.0000 | 0 | 0 |
| 0.0050 | 0.0010 | 0.0080 | 0.0130 | 0.0040 | 0.0130 | 0.0040 | 0 | 0 |
| 0.0060 | 0.0010 | 0.0081 | 0.0750 | -0.0554 | 0.0750 | -0.0486 | 0 | 0.0068 |
| 0.0070 | 0.0010 | 0.0069 | 0 | -0.0000 | 0 | -0.0000 | 0 | 0 |
| 0.0080 | 0.0010 | 0.0038 | -0.3000 | 0.0665 | 0.1500 | 0.1286 | 0.4500 | 0.0621 |
| 0.0090 | 0.0010 | 0.0089 | 0.1210 | -0.0157 | 0.1210 | 0.0030 | 0 | 0.0187 |
| 0.0100 | 0.0010 | 0.0110 | 0.0050 | 0.0020 | 0.0050 | 0.0020 | 0 | 0 |
| 0.0110 | 0.0010 | 0.0095 | -0.0000 | -0.0000 | -0.0000 | -0.0000 | 0 | 0 |
| 0.0120 | 0.0010 | 0.0105 | 0.0670 | -0.2413 | 0.3770 | 0.8510 | 0.3100 | 1.0922 |
| 0.0130 | 0.0010 | 0.0093 | 0.0180 | 0.0023 | 0.0180 | 0.0023 | 0 | 0 |
| 0.0140 | 0.0010 | 0.0088 | 0.0105 | 0.0053 | 0.0105 | 0.0053 | 0 | 0 |
| 0.0150 | 0.0010 | 0.0068 | 0.0220 | 0.0050 | 0.0220 | 0.0050 | 0 | 0 |
| 0.0160 | 0.0010 | 0.0088 | 0.0430 | 0.0030 | 0.0430 | 0.0030 | 0 | 0 |
| 0.0170 | 0.0010 | 0.0053 | 0.0420 | 0.0080 | 0.0420 | 0.0080 | 0 | 0 |
| 0.0180 | 0.0011 | 0.0107 | 0.0272 | 0.0098 | 0.0272 | 0.0098 | 0 | 0 |
| 0.0190 | 0.0011 | 0.0119 | 0.0033 | 0.0006 | 0.0033 | 0.0006 | 0 | 0 |
| 0.0200 | 0.0011 | 0.0120 | 0.0023 | 0.0010 | 0.0023 | 0.0010 | 0 | 0 |
| 0.0210 | 0.0012 | 0.0116 | 0 | 0.0000 | 0 | 0.0000 | 0 | 0 |
| 0.0220 | 0.0012 | 0.0116 | 0.0000 | -0.0000 | 0.0000 | -0.0000 | 0 | 0 |
| 0.0230 | 0.0012 | 0.0116 | 0.0063 | 0.0021 | 0.0063 | 0.0021 | 0 | 0 |
| 0.0240 | 0.0012 | 0.0116 | 0.0000 | 0.0000 | 0.0000 | 0.0000 | 0 | 0 |
| 0.0250 | 0.0012 | 0.0149 | 0.0063 | 0.0032 | 0.0063 | 0.0032 | 0 | 0 |
| 0.0260 | 0.0011 | 0.0113 | -0.0000 | 0.0000 | -0.0000 | 0.0000 | 0 | 0 |
| 0.0270 | 0.0011 | 0.0102 | 0.0093 | 0.0005 | 0.0093 | 0.0005 | 0 | 0 |
| 0.0280 | 0.0011 | 0.0094 | 0.0046 | 0.0023 | 0.0046 | 0.0023 | 0 | 0 |
| 0.0290 | 0.0011 | 0.0088 | 0.0170 | 0.0026 | 0.0170 | 0.0026 | 0 | 0 |
| 0.0300 | 0.0012 | 0.0153 | 0.0036 | 0.0018 | 0.0036 | 0.0018 | 0 | 0 |
| 0.0310 | 0.0013 | 0.0157 | 0.0058 | 0.0029 | 0.0058 | 0.0029 | 0 | 0 |
| 0.0320 | 0.0012 | 0.0153 | 0.0016 | 0.0008 | 0.0016 | 0.0008 | 0 | 0 |

| | | | | | | | | |
|---|---|---|---|---|---|---|---|---|
| 0.0330 | 0.0012 | 0.0154 | 0.0038 | 0.0019 | 0.0038 | 0.0019 | 0 | 0 |
| 0.0340 | 0.0012 | 0.0128 | 0.0000 | 0.0000 | 0.0000 | 0.0000 | 0 | 0 |
| 0.0350 | 0.0012 | 0.0126 | 0.0060 | 0.0030 | 0.0060 | 0.0030 | 0 | 0 |
| 0.0360 | 0.0012 | 0.0124 | -0.0000 | 0.0000 | -0.0000 | 0.0000 | 0 | 0 |
| 0.0370 | 0.0012 | 0.0122 | -0.0000 | -0.0000 | -0.0000 | -0.0000 | 0 | 0 |
| 0.0380 | 0.0012 | 0.0115 | 0.0140 | 0.0070 | 0.0140 | 0.0070 | 0 | 0 |
| 0.0390 | 0.0012 | 0.0123 | -0.0000 | -0.0000 | -0.0000 | -0.0000 | 0 | 0 |
| 0.0400 | 0.0012 | 0.0125 | 0.0000 | -0.0000 | 0.0000 | -0.0000 | 0 | 0 |
| 0.0410 | 0.0011 | 0.0130 | 0.0063 | 0.0030 | 0.0063 | 0.0030 | 0 | 0 |
| 0.0420 | 0.0012 | 0.0136 | 0.0071 | 0.0044 | 0.0071 | 0.0044 | 0 | 0 |
| 0.0430 | 0.0011 | 0.0106 | 0.0020 | 0.0010 | 0.0020 | 0.0010 | 0 | 0 |
| 0.0440 | 0.0011 | 0.0109 | 0.0120 | 0.0018 | 0.0120 | 0.0018 | 0 | 0 |
| 0.0450 | 0.0011 | 0.0090 | -0.0000 | -0.0000 | -0.0000 | -0.0000 | 0 | 0 |
| 0.0460 | 0.0012 | 0.0100 | 0.0000 | 0.0000 | 0.0000 | 0.0000 | 0 | 0 |
| 0.0470 | 0.0012 | 0.0111 | 0.0297 | 0.0116 | 0.0297 | 0.0116 | 0 | 0 |
| 0.0480 | 0.0012 | 0.0113 | -0.0000 | -0.0000 | -0.0000 | -0.0000 | 0 | 0 |
| 0.0490 | 0.0012 | 0.0115 | 0.0180 | 0.0085 | 0.0180 | 0.0085 | 0 | 0 |
| 0.0500 | 0.0012 | 0.0122 | 0.0210 | 0.0105 | 0.0210 | 0.0105 | 0 | 0 |
| 0.0510 | 0.0011 | 0.0120 | 0.0180 | 0.0053 | 0.0180 | 0.0053 | 0 | 0 |
| 0.0520 | 0.0011 | 0.0100 | 0.0049 | 0.0022 | 0.0049 | 0.0022 | 0 | 0 |
| 0.0530 | 0.0011 | 0.0104 | 0.0200 | 0.0100 | 0.0200 | 0.0100 | 0 | 0 |
| 0.0540 | 0.0011 | 0.0103 | 0.0041 | 0.0014 | 0.0041 | 0.0014 | 0 | 0 |
| 0.0550 | 0.0011 | 0.0097 | 0.0068 | 0.0034 | 0.0068 | 0.0034 | 0 | 0 |
| 0.0560 | 0.0012 | 0.0135 | 0.0076 | 0.0022 | 0.0076 | 0.0022 | 0 | 0 |
| 0.0570 | 0.0012 | 0.0138 | 0.0067 | 0.0020 | 0.0067 | 0.0020 | 0 | 0 |
| 0 | 0 | 0 | 0.0274 | -0.0049 | 0.8274 | 1.1732 | 0.8000 | 1.1781 |

---

Line FLow and Losses

---

| From Bus | To Bus | P MW | Q MVar | From Bus | To Bus | P MW | Q MVar | Line Loss MW | Line Loss MVar |
|---|---|---|---|---|---|---|---|---|---|

LF_Result =

| | | | | | | | | | |
|---|---|---|---|---|---|---|---|---|---|
| 1.0000 | 2.0000 | -86.9957 | 26.9560 | 2.0000 | 1.0000 | 87.6323 | -24.8087 | 0.6365 | 2.1473 |
| 2.0000 | 3.0000 | -84.6323 | 39.6273 | 3.0000 | 2.0000 | 87.0383 | -32.7643 | 2.4061 | 6.8630 |
| 3.0000 | 4.0000 | -54.4304 | 4.0604 | 4.0000 | 3.0000 | 54.7419 | -3.0425 | 0.3115 | 1.0179 |
| 4.0000 | 5.0000 | -11.3943 | 6.6831 | 5.0000 | 4.0000 | 11.4952 | -6.4700 | 0.1009 | 0.2131 |
| 4.0000 | 6.0000 | -11.7835 | 10.3469 | 6.0000 | 4.0000 | 11.8813 | -10.0102 | 0.0978 | 0.3367 |
| 6.0000 | 7.0000 | 19.9664 | -16.5000 | 7.0000 | 6.0000 | -19.8400 | 17.1451 | 0.1265 | 0.6450 |
| 6.0000 | 8.0000 | 44.6125 | -9.9571 | 8.0000 | 6.0000 | -43.9448 | 13.3643 | 0.6677 | 3.4072 |
| 8.0000 | 9.0000 | -176.1327 | 53.0336 | 9.0000 | 8.0000 | 179.2597 | -37.0829 | 3.1270 | 15.9507 |
| 9.0000 | 10.0000 | -20.3579 | 12.8836 | 10.0000 | 9.0000 | 20.5598 | -11.9650 | 0.2019 | 0.9186 |
| 9.0000 | 11.0000 | -14.6060 | -1.2657 | 11.0000 | 9.0000 | 14.6583 | 1.4375 | 0.0523 | 0.1718 |
| 9.0000 | 12.0000 | -4.6241 | 23.8551 | 12.0000 | 9.0000 | 4.9847 | -22.2132 | 0.3606 | 1.6418 |
| 9.0000 | 13.0000 | -3.3592 | 6.3387 | 13.0000 | 9.0000 | 3.3825 | -6.2621 | 0.0233 | 0.0766 |
| 13.0000 | 14.0000 | 11.7596 | -32.1079 | 14.0000 | 13.0000 | -11.6118 | 32.5938 | 0.1478 | 0.4859 |
| 13.0000 | 15.0000 | 43.8461 | -30.0878 | 15.0000 | 13.0000 | -43.1177 | 32.4410 | 0.7284 | 2.3532 |
| 1.0000 | 15.0000 | -133.2813 | 37.9881 | 15.0000 | 1.0000 | 136.4422 | -21.8284 | 3.1609 | 16.1597 |
| 1.0000 | 16.0000 | -66.8988 | 44.9259 | 16.0000 | 1.0000 | 69.6246 | -32.5579 | 2.7258 | 12.3680 |
| 1.0000 | 17.0000 | -81.2631 | 39.8831 | 17.0000 | 1.0000 | 83.0662 | -31.7009 | 1.8031 | 8.1822 |
| 3.0000 | 15.0000 | -31.6079 | 6.2130 | 15.0000 | 3.0000 | 31.7648 | -5.6996 | 0.1569 | 0.5134 |
| 4.0000 | 18.0000 | -31.5642 | -20.6498 | 18.0000 | 4.0000 | 31.5642 | 23.7577 | 0 | 3.1078 |
| 4.0000 | 18.0000 | -31.5642 | -20.6498 | 18.0000 | 4.0000 | 31.5642 | 23.7577 | 0 | 3.1078 |
| 5.0000 | 6.0000 | 1.5048 | 12.5286 | 6.0000 | 5.0000 | -1.4602 | -12.4339 | 0.0446 | 0.0947 |
| 7.0000 | 8.0000 | 80.7569 | -2.2890 | 8.0000 | 7.0000 | -79.9225 | 6.5632 | 0.8344 | 4.2742 |
| 10.0000 | 12.0000 | 14.6383 | 38.7115 | 12.0000 | 10.0000 | -14.1796 | -36.6215 | 0.4587 | 2.0900 |
| 11.0000 | 13.0000 | 9.5437 | 15.3215 | 13.0000 | 11.0000 | -9.4759 | -15.0987 | 0.0679 | 0.2227 |
| 12.0000 | 13.0000 | 6.7242 | -96.3088 | 13.0000 | 12.0000 | -4.9426 | 102.1140 | 1.7816 | 5.8052 |
| 12.0000 | 16.0000 | 27.0369 | -37.4446 | 16.0000 | 12.0000 | -26.6246 | 39.3069 | 0.4123 | 1.8623 |
| 12.0000 | 17.0000 | 42.4337 | -37.5105 | 17.0000 | 12.0000 | -41.0662 | 43.6762 | 1.3675 | 6.1658 |
| 14.0000 | 15.0000 | 60.8660 | -23.2729 | 15.0000 | 14.0000 | -60.1869 | 25.4452 | 0.6791 | 2.1723 |
| 18.0000 | 19.0000 | -4.3642 | -1.1474 | 19.0000 | 18.0000 | 4.4433 | 1.2650 | 0.0792 | 0.1176 |
| 19.0000 | 20.0000 | -1.1433 | -0.6650 | 20.0000 | 19.0000 | 1.1473 | 0.6712 | 0.0040 | 0.0061 |
| 21.0000 | 20.0000 | -1.1527 | 6.6007 | 20.0000 | 21.0000 | 1.1527 | -6.3333 | 0 | 0.2675 |
| 21.0000 | 22.0000 | 1.1527 | 0.3200 | 22.0000 | 21.0000 | -1.1519 | -0.3187 | 0.0008 | 0.0012 |
| 22.0000 | 23.0000 | -9.1256 | -7.3565 | 23.0000 | 22.0000 | 9.1356 | 7.3719 | 0.0100 | 0.0154 |
| 23.0000 | 24.0000 | -2.8356 | -4.7000 | 24.0000 | 23.0000 | 2.8724 | 4.7567 | 0.0367 | 0.0567 |
| 24.0000 | 25.0000 | -13.8733 | -6.3262 | 25.0000 | 24.0000 | 13.8733 | 7.3306 | 0.0000 | 1.0044 |
| 24.0000 | 25.0000 | -13.8733 | -6.3262 | 25.0000 | 24.0000 | 13.8733 | 7.3306 | 0.0000 | 1.0044 |

| | | | | | | | | | |
|---|---|---|---|---|---|---|---|---|---|
| 24.0000 | 26.0000 | 11.0009 | 118.7472 | 26.0000 | 24.0000 | -11.0009 | -113.7183 | 0.0000 | 5.0289 |
| 26.0000 | 27.0000 | 11.0009 | 2.1091 | 27.0000 | 26.0000 | -10.8393 | -1.8602 | 0.1617 | 0.2489 |
| 27.0000 | 28.0000 | 20.1393 | 2.3602 | 28.0000 | 27.0000 | -19.9334 | -2.0425 | 0.2059 | 0.3178 |
| 28.0000 | 29.0000 | 24.5334 | 4.3425 | 29.0000 | 28.0000 | -24.3181 | -4.0402 | 0.2153 | 0.3023 |
| 7.0000 | 29.0000 | -60.9169 | -71.5142 | 29.0000 | 7.0000 | 60.9169 | 76.6003 | 0 | 5.0862 |
| 25.0000 | 30.0000 | -7.5733 | -4.1306 | 30.0000 | 25.0000 | 7.6413 | 4.2323 | 0.0680 | 0.1017 |
| 30.0000 | 31.0000 | -4.0413 | -2.4323 | 31.0000 | 30.0000 | 4.0892 | 2.5053 | 0.0479 | 0.0730 |
| 31.0000 | 32.0000 | 1.7108 | 0.3947 | 32.0000 | 31.0000 | -1.7008 | -0.3798 | 0.0100 | 0.0149 |
| 32.0000 | 33.0000 | -3.7954 | -1.8958 | 33.0000 | 32.0000 | 3.8000 | 1.9000 | 0.0046 | 0.0042 |
| 34.0000 | 32.0000 | -7.0963 | -6.6089 | 32.0000 | 34.0000 | 7.0963 | 7.2267 | -0.0000 | 0.6178 |
| 34.0000 | 35.0000 | 7.0963 | 2.9324 | 35.0000 | 34.0000 | -7.0746 | -2.8999 | 0.0217 | 0.0325 |
| 35.0000 | 36.0000 | 13.0746 | 6.2365 | 36.0000 | 35.0000 | -13.0102 | -6.1561 | 0.0643 | 0.0804 |
| 36.0000 | 37.0000 | 15.1252 | 1.6330 | 37.0000 | 36.0000 | -15.0768 | -1.5718 | 0.0485 | 0.0612 |
| 37.0000 | 38.0000 | 17.8559 | 1.3150 | 38.0000 | 37.0000 | -17.7041 | -1.0797 | 0.1518 | 0.2353 |
| 37.0000 | 39.0000 | -2.7792 | 0.3943 | 39.0000 | 37.0000 | 2.7805 | -0.3921 | 0.0014 | 0.0022 |
| 36.0000 | 40.0000 | -2.1150 | 4.6339 | 40.0000 | 36.0000 | 2.1206 | -4.6251 | 0.0056 | 0.0087 |
| 22.0000 | 38.0000 | 10.2775 | 7.6752 | 38.0000 | 22.0000 | -10.2543 | -7.6394 | 0.0233 | 0.0358 |
| 11.0000 | 41.0000 | -9.7985 | -12.7580 | 41.0000 | 11.0000 | 9.7985 | 14.4868 | 0 | 1.7287 |
| 41.0000 | 42.0000 | -8.8509 | -7.9801 | 42.0000 | 41.0000 | 9.0832 | 8.3751 | 0.2323 | 0.3950 |
| 41.0000 | 43.0000 | 12.4035 | 9.0222 | 43.0000 | 41.0000 | -12.4035 | -8.2564 | 0 | 0.7658 |
| 38.0000 | 44.0000 | 32.2799 | 17.2342 | 44.0000 | 38.0000 | -31.9930 | -16.6535 | 0.2869 | 0.5807 |
| 15.0000 | 45.0000 | -42.9024 | -66.0021 | 45.0000 | 15.0000 | 42.9024 | 71.7375 | 0 | 5.7354 |
| 14.0000 | 46.0000 | -38.7542 | -182.2383 | 46.0000 | 14.0000 | 38.7542 | 203.7140 | -0.0000 | 21.4757 |
| 46.0000 | 47.0000 | -38.7542 | -3.2698 | 47.0000 | 46.0000 | 39.0169 | 4.0464 | 0.2627 | 0.7765 |
| 47.0000 | 48.0000 | -9.3169 | 7.7692 | 48.0000 | 47.0000 | 9.3367 | -7.7438 | 0.0199 | 0.0254 |
| 48.0000 | 49.0000 | -1.1073 | 4.5930 | 49.0000 | 48.0000 | 1.1212 | -4.5716 | 0.0138 | 0.0214 |
| 49.0000 | 50.0000 | -8.2670 | 6.6245 | 50.0000 | 49.0000 | 8.3342 | -6.5171 | 0.0672 | 0.1074 |
| 50.0000 | 51.0000 | 12.6658 | 17.0171 | 51.0000 | 50.0000 | -12.1982 | -16.2748 | 0.4677 | 0.7423 |
| 10.0000 | 51.0000 | -30.1982 | -138.3429 | 51.0000 | 10.0000 | 30.1982 | 151.1797 | -0.0000 | 12.8367 |
| 13.0000 | 49.0000 | -26.5697 | -79.8925 | 49.0000 | 13.0000 | 26.5697 | 91.4971 | 0 | 11.6046 |
| 29.0000 | 52.0000 | -19.5988 | -7.8133 | 52.0000 | 29.0000 | 20.1428 | 8.5187 | 0.5440 | 0.7054 |
| 52.0000 | 53.0000 | -15.2428 | -6.3187 | 53.0000 | 52.0000 | 15.4064 | 6.5300 | 0.1636 | 0.2113 |
| 53.0000 | 54.0000 | 4.5936 | 3.4700 | 54.0000 | 53.0000 | -4.5459 | -3.4110 | 0.0477 | 0.0590 |
| 54.0000 | 55.0000 | 8.6459 | 4.8110 | 55.0000 | 54.0000 | -8.5125 | -4.6365 | 0.1334 | 0.1745 |
| 11.0000 | 43.0000 | -14.4035 | -40.9075 | 43.0000 | 11.0000 | 14.4035 | 43.4823 | 0 | 2.5747 |
| 44.0000 | 45.0000 | 43.9930 | 18.8467 | 45.0000 | 44.0000 | -42.9024 | -16.6760 | 1.0906 | 2.1707 |
| 40.0000 | 56.0000 | -2.1206 | -0.6652 | 56.0000 | 40.0000 | 2.1206 | 0.7061 | 0 | 0.0409 |
| 56.0000 | 41.0000 | 7.3595 | 4.8728 | 41.0000 | 56.0000 | -7.0511 | -4.5667 | 0.3084 | 0.3061 |
| 56.0000 | 42.0000 | 2.0140 | 4.0265 | 42.0000 | 56.0000 | -1.9832 | -3.9751 | 0.0308 | 0.0514 |
| 39.0000 | 57.0000 | -2.7805 | -1.7220 | 57.0000 | 39.0000 | 2.7805 | 1.8252 | 0 | 0.1033 |
| 57.0000 | 56.0000 | 3.9195 | 2.3175 | 56.0000 | 57.0000 | -3.8941 | -2.2796 | 0.0254 | 0.0379 |

| | | | | | | | | | |
|---|---|---|---|---|---|---|---|---|---|
| 38.0000 | 49.0000 | 1.4306 | 2.4025 | 49.0000 | 38.0000 | -1.4239 | -2.3923 | 0.0067 | 0.0103 |
| 38.0000 | 48.0000 | 8.2479 | -3.4455 | 48.0000 | 38.0000 | -8.2294 | 3.4741 | 0.0185 | 0.0285 |
| 9.0000 | 55.0000 | -15.3125 | -67.5248 | 55.0000 | 9.0000 | 15.3125 | 72.6433 | 0 | 5.1185 |
| 0 | 0 | 0 | 0 | 0 | 0 | 0 | 0 | 27.3611 | 185.4685 |

## Appendix F2: Load flow Analysis of Nigerian 57-bus Network with Optimized OLTCs

| Bus No | V pu | Angle Degree | Injection MW | Injection MVar | Generation MW | Generation Mvar | Load MW | Load MVar |
|---|---|---|---|---|---|---|---|---|

PF_Result =

| | | | | | | | | |
|---|---|---|---|---|---|---|---|---|
| 1.0000 | 1.0400 | 0 | -373.0970 | 37.5168 | -373.0970 | 37.5168 | 0 | 0 |
| 2.0000 | 1.0400 | 1.4067 | 3.0000 | 3.3941 | 3.0000 | 2.5941 | 0 | -0.8000 |
| 3.0000 | 1.0350 | 5.8615 | 1.0000 | -67.8724 | 41.0000 | -68.8724 | 40.0000 | -1.0000 |
| 4.0000 | 1.0400 | 6.9149 | 0.0000 | 0.0000 | 0.0000 | 0.0000 | 0 | 0 |
| 5.0000 | 1.0383 | 7.9008 | 13.0000 | 4.0000 | 13.0000 | 4.0000 | 0 | 0 |
| 6.0000 | 1.0300 | 8.0353 | 75.0000 | -56.8406 | 75.0000 | -56.0406 | 0 | 0.8000 |
| 7.0000 | 1.0440 | 6.7305 | 0.0000 | 0 | 0.0000 | 0 | 0 | 0 |
| 8.0000 | 1.0350 | 3.6456 | -300.0000 | 64.5442 | 150.0000 | 126.6442 | 450.0000 | 62.1000 |
| 9.0000 | 1.0300 | 8.6756 | 121.0000 | -136.4532 | 121.0000 | -134.2532 | 0 | 2.2000 |
| 10.0000 | 1.0703 | 9.8352 | 5.0000 | 2.0000 | 5.0000 | 2.0000 | 0 | 0 |
| 11.0000 | 1.0564 | 9.0009 | -0.0000 | -0.0000 | -0.0000 | -0.0000 | 0 | 0 |
| 12.0000 | 1.0650 | 8.7864 | 67.0000 | -9.4529 | 377.0000 | 119.0471 | 310.0000 | 128.5000 |
| 13.0000 | 1.0620 | 8.5663 | 18.0000 | 2.3000 | 18.0000 | 2.3000 | 0 | 0 |
| 14.0000 | 1.0640 | 8.2373 | 10.5000 | 5.3000 | 10.5000 | 5.3000 | 0 | 0 |
| 15.0000 | 1.0548 | 6.5271 | 22.0000 | 5.0000 | 22.0000 | 5.0000 | 0 | 0 |
| 16.0000 | 1.0644 | 7.5757 | 43.0000 | 3.0000 | 43.0000 | 3.0000 | 0 | 0 |
| 17.0000 | 1.0598 | 4.7206 | 42.0000 | 8.0000 | 42.0000 | 8.0000 | 0 | 0 |
| 18.0000 | 1.0922 | 10.6655 | 27.2000 | 9.8000 | 27.2000 | 9.8000 | 0 | 0 |
| 19.0000 | 1.1259 | 11.4934 | 3.3000 | 0.6000 | 3.3000 | 0.6000 | 0 | 0 |
| 20.0000 | 1.1364 | 11.4429 | 2.3000 | 1.0000 | 2.3000 | 1.0000 | 0 | 0 |
| 21.0000 | 1.1928 | 11.0236 | 0 | 0.0000 | 0 | 0.0000 | 0 | 0 |
| 22.0000 | 1.1931 | 10.9344 | 0 | 0.0000 | 0 | 0.0000 | 0 | 0 |
| 23.0000 | 1.1943 | 10.9695 | 6.3000 | 2.1000 | 6.3000 | 2.1000 | 0 | 0 |
| 24.0000 | 1.2007 | 11.0921 | -0.0000 | 0 | -0.0000 | 0 | 0 | 0 |
| 25.0000 | 1.2363 | 14.3136 | 6.3000 | 3.2000 | 6.3000 | 3.2000 | 0 | 0 |
| 26.0000 | 1.1488 | 10.8536 | 0.0000 | 0.0000 | 0.0000 | 0.0000 | 0 | 0 |
| 27.0000 | 1.1196 | 9.9570 | 9.3000 | 0.5000 | 9.3000 | 0.5000 | 0 | 0 |

| | | | | | | | | |
|---|---|---|---|---|---|---|---|---|
| 28.0000 | 1.1032 | 9.2087 | 4.6000 | 2.3000 | 4.6000 | 2.3000 | 0 | 0 |
| 29.0000 | 1.0896 | 8.6627 | 17.0000 | 2.6000 | 17.0000 | 2.6000 | 0 | 0 |
| 30.0000 | 1.2520 | 14.6520 | 3.6000 | 1.8000 | 3.6000 | 1.8000 | 0 | 0 |
| 31.0000 | 1.2736 | 15.0383 | 5.8000 | 2.9000 | 5.8000 | 2.9000 | 0 | 0 |
| 32.0000 | 1.2666 | 14.5732 | 1.6000 | 0.8000 | 1.6000 | 0.8000 | 0 | 0 |
| 33.0000 | 1.2683 | 14.5954 | 3.8000 | 1.9000 | 3.8000 | 1.9000 | 0 | 0 |
| 34.0000 | 1.2163 | 12.1091 | -0.0000 | 0 | -0.0000 | 0 | 0 | 0 |
| 35.0000 | 1.2116 | 11.9452 | 6.0000 | 3.0000 | 6.0000 | 3.0000 | 0 | 0 |
| 36.0000 | 1.2044 | 11.7686 | 0 | 0.0000 | 0 | 0.0000 | 0 | 0 |
| 37.0000 | 1.2005 | 11.5585 | 0 | -0.0000 | 0 | -0.0000 | 0 | 0 |
| 38.0000 | 1.1907 | 10.8433 | 14.0000 | 7.0000 | 14.0000 | 7.0000 | 0 | 0 |
| 39.0000 | 1.2008 | 11.6063 | 0.0000 | 0.0000 | 0.0000 | 0.0000 | 0 | 0 |
| 40.0000 | 1.2029 | 11.8678 | -0.0000 | -0.0000 | -0.0000 | -0.0000 | 0 | 0 |
| 41.0000 | 1.1489 | 12.3211 | 6.3000 | 3.0000 | 6.3000 | 3.0000 | 0 | 0 |
| 42.0000 | 1.1905 | 12.8993 | 7.1000 | 4.4000 | 7.1000 | 4.4000 | 0 | 0 |
| 43.0000 | 1.1159 | 10.0297 | 2.0000 | 1.0000 | 2.0000 | 1.0000 | 0 | 0 |
| 44.0000 | 1.1720 | 10.3286 | 12.0000 | 1.8000 | 12.0000 | 1.8000 | 0 | 0 |
| 45.0000 | 1.1239 | 8.5923 | 0 | 0.0000 | 0 | 0.0000 | 0 | 0 |
| 46.0000 | 1.1837 | 9.3932 | -0.0000 | -0.0000 | -0.0000 | -0.0000 | 0 | 0 |
| 47.0000 | 1.1927 | 10.4307 | 29.7000 | 11.6000 | 29.7000 | 11.6000 | 0 | 0 |
| 48.0000 | 1.1924 | 10.5784 | -0.0000 | -0.0000 | -0.0000 | -0.0000 | 0 | 0 |
| 49.0000 | 1.1933 | 10.6397 | 18.0000 | 8.5000 | 18.0000 | 8.5000 | 0 | 0 |
| 50.0000 | 1.1974 | 11.1493 | 21.0000 | 10.5000 | 21.0000 | 10.5000 | 0 | 0 |
| 51.0000 | 1.1611 | 10.7458 | 18.0000 | 5.3000 | 18.0000 | 5.3000 | 0 | 0 |
| 52.0000 | 1.1284 | 9.8370 | 4.9000 | 2.2000 | 4.9000 | 2.2000 | 0 | 0 |
| 53.0000 | 1.1439 | 10.2848 | 20.0000 | 10.0000 | 20.0000 | 10.0000 | 0 | 0 |
| 54.0000 | 1.1284 | 10.0918 | 4.1000 | 1.4000 | 4.1000 | 1.4000 | 0 | 0 |
| 55.0000 | 1.1046 | 9.5643 | 6.8000 | 3.4000 | 6.8000 | 3.4000 | 0 | 0 |
| 56.0000 | 1.2070 | 12.8084 | 7.6000 | 2.2000 | 7.6000 | 2.2000 | 0 | 0 |
| 57.0000 | 1.2182 | 13.0325 | 6.7000 | 2.0000 | 6.7000 | 2.0000 | 0 | 0 |
| 0 | 0 | 0 | 22.7030 | -28.7641 | 822.7030 | 163.0359 | 800.0000 | 191.8000 |

Line FLow and Losses

| From Bus | To Bus | P MW | Q MVar | From Bus | To Bus | P MW | Q MVar | Line Loss MW | Line Loss MVar |
|---|---|---|---|---|---|---|---|---|---|

LF_Result =

| | | | | | | | | | |
|---|---|---|---|---|---|---|---|---|---|
| 1.0000 | 2.0000 | -86.8546 | 26.9104 | 2.0000 | 1.0000 | 87.4891 | -24.7700 | 0.6345 | 2.1404 |
| 2.0000 | 3.0000 | -84.4891 | 39.5642 | 3.0000 | 2.0000 | 86.8871 | -32.7242 | 2.3980 | 6.8400 |
| 3.0000 | 4.0000 | -53.2405 | 2.6995 | 4.0000 | 3.0000 | 53.5377 | -1.7285 | 0.2971 | 0.9710 |
| 4.0000 | 5.0000 | -10.9341 | 6.6358 | 5.0000 | 4.0000 | 11.0286 | -6.4362 | 0.0945 | 0.1997 |
| 4.0000 | 6.0000 | -11.1344 | 10.3879 | 6.0000 | 4.0000 | 11.2266 | -10.0706 | 0.0922 | 0.3173 |
| 6.0000 | 7.0000 | 20.5002 | -17.8827 | 7.0000 | 6.0000 | -20.3606 | 18.5942 | 0.1395 | 0.7115 |
| 6.0000 | 8.0000 | 45.1999 | -10.0263 | 8.0000 | 6.0000 | -44.5149 | 13.5218 | 0.6850 | 3.4955 |
| 8.0000 | 9.0000 | -174.7672 | 52.6384 | 9.0000 | 8.0000 | 177.8460 | -36.9333 | 3.0788 | 15.7052 |
| 9.0000 | 10.0000 | -17.8261 | -20.6547 | 10.0000 | 9.0000 | 18.0851 | 21.8327 | 0.2589 | 1.1781 |
| 9.0000 | 11.0000 | -15.6005 | -27.3326 | 11.0000 | 9.0000 | 15.8413 | 28.1243 | 0.2409 | 0.7917 |
| 9.0000 | 12.0000 | -3.2463 | -11.5066 | 12.0000 | 9.0000 | 3.3336 | 11.9040 | 0.0873 | 0.3975 |
| 9.0000 | 13.0000 | -4.5943 | -19.4325 | 13.0000 | 9.0000 | 4.7751 | 20.0263 | 0.1808 | 0.5938 |
| 13.0000 | 14.0000 | 12.2824 | -8.7619 | 14.0000 | 13.0000 | -12.2558 | 8.8495 | 0.0266 | 0.0876 |
| 13.0000 | 15.0000 | 44.5610 | -4.2127 | 15.0000 | 13.0000 | -44.0831 | 5.7565 | 0.4779 | 1.5438 |
| 1.0000 | 15.0000 | -133.6913 | 17.0681 | 15.0000 | 1.0000 | 136.6806 | -1.7853 | 2.9894 | 15.2828 |
| 1.0000 | 16.0000 | -69.1604 | 7.6301 | 16.0000 | 1.0000 | 71.1926 | 1.5907 | 2.0322 | 9.2208 |
| 1.0000 | 17.0000 | -83.3907 | 2.7270 | 17.0000 | 1.0000 | 84.9226 | 4.2241 | 1.5318 | 6.9512 |
| 3.0000 | 15.0000 | -32.6466 | -28.5174 | 15.0000 | 3.0000 | 32.9307 | 29.4470 | 0.2842 | 0.9297 |
| 4.0000 | 18.0000 | -31.4692 | -21.9620 | 18.0000 | 4.0000 | 31.4692 | 25.1768 | 0 | 3.2148 |
| 4.0000 | 18.0000 | -31.4692 | -21.9620 | 18.0000 | 4.0000 | 31.4692 | 25.1768 | 0 | 3.2148 |
| 5.0000 | 6.0000 | 1.9714 | 12.4952 | 6.0000 | 5.0000 | -1.9266 | -12.4001 | 0.0448 | 0.0951 |
| 7.0000 | 8.0000 | 81.5664 | -0.5293 | 8.0000 | 7.0000 | -80.7179 | 4.8756 | 0.8485 | 4.3463 |
| 10.0000 | 12.0000 | 16.7407 | 0.9501 | 12.0000 | 10.0000 | -16.6727 | -0.6403 | 0.0680 | 0.3098 |
| 11.0000 | 13.0000 | 8.4270 | -10.5024 | 13.0000 | 11.0000 | -8.3908 | 10.6213 | 0.0362 | 0.1189 |
| 12.0000 | 13.0000 | 8.4184 | 3.0193 | 13.0000 | 12.0000 | -8.4058 | -2.9784 | 0.0126 | 0.0409 |
| 12.0000 | 16.0000 | 28.3241 | -5.1317 | 16.0000 | 12.0000 | -28.1926 | 5.7256 | 0.1315 | 0.5939 |
| 12.0000 | 17.0000 | 43.5967 | -5.0163 | 17.0000 | 12.0000 | -42.9226 | 8.0556 | 0.6741 | 3.0393 |
| 14.0000 | 15.0000 | 61.1629 | -0.2250 | 15.0000 | 14.0000 | -60.5979 | 2.0324 | 0.5650 | 1.8074 |
| 18.0000 | 19.0000 | -4.2692 | -2.4892 | 19.0000 | 18.0000 | 4.3636 | 2.6294 | 0.0944 | 0.1402 |
| 19.0000 | 20.0000 | -1.0636 | -2.0294 | 20.0000 | 19.0000 | 1.0753 | 2.0474 | 0.0117 | 0.0180 |
| 21.0000 | 20.0000 | -1.2247 | 8.3036 | 20.0000 | 21.0000 | 1.2247 | -7.9025 | 0.0000 | 0.4011 |
| 21.0000 | 22.0000 | 1.2247 | -1.0630 | 22.0000 | 21.0000 | -1.2233 | 1.0652 | 0.0014 | 0.0022 |
| 22.0000 | 23.0000 | -8.4858 | -4.2212 | 23.0000 | 22.0000 | 8.4920 | 4.2307 | 0.0062 | 0.0096 |
| 23.0000 | 24.0000 | -2.1920 | -1.5317 | 24.0000 | 23.0000 | 2.2003 | 1.5445 | 0.0083 | 0.0128 |
| 24.0000 | 25.0000 | -13.8395 | -6.7203 | 25.0000 | 24.0000 | 13.8395 | 7.7100 | -0.0000 | 0.9897 |
| 24.0000 | 25.0000 | -13.8395 | -6.7203 | 25.0000 | 24.0000 | 13.8395 | 7.7100 | -0.0000 | 0.9897 |
| 24.0000 | 26.0000 | 11.6392 | 126.2501 | 26.0000 | 24.0000 | -11.6392 | -120.7490 | -0.0000 | 5.5011 |
| 26.0000 | 27.0000 | 11.6392 | 5.7210 | 27.0000 | 26.0000 | -11.4289 | -5.3973 | 0.2103 | 0.3237 |
| 27.0000 | 28.0000 | 20.7289 | 5.8973 | 28.0000 | 27.0000 | -20.4999 | -5.5437 | 0.2290 | 0.3535 |
| 28.0000 | 29.0000 | 25.0999 | 7.8437 | 29.0000 | 28.0000 | -24.8623 | -7.5102 | 0.2375 | 0.3335 |

| | | | | | | | | | |
|---|---|---|---|---|---|---|---|---|---|
| 7.0000 | 29.0000 | -61.2058 | -74.8625 | 29.0000 | 7.0000 | 61.2058 | 80.2383 | 0 | 5.3757 |
| 25.0000 | 30.0000 | -7.5395 | -4.5100 | 30.0000 | 25.0000 | 7.6077 | 4.6120 | 0.0682 | 0.1020 |
| 30.0000 | 31.0000 | -4.0077 | -2.8120 | 31.0000 | 30.0000 | 4.0575 | 2.8880 | 0.0499 | 0.0760 |
| 31.0000 | 32.0000 | 1.7425 | 0.0120 | 32.0000 | 31.0000 | -1.7330 | 0.0021 | 0.0095 | 0.0141 |
| 32.0000 | 33.0000 | -3.7956 | -1.8960 | 33.0000 | 32.0000 | 3.8000 | 1.9000 | 0.0044 | 0.0040 |
| 34.0000 | 32.0000 | -7.1286 | -6.4315 | 32.0000 | 34.0000 | 7.1286 | 7.0104 | -0.0000 | 0.5789 |
| 34.0000 | 35.0000 | 7.1286 | 2.5856 | 35.0000 | 34.0000 | -7.1084 | -2.5553 | 0.0202 | 0.0303 |
| 35.0000 | 36.0000 | 13.1084 | 5.9076 | 36.0000 | 35.0000 | -13.0478 | -5.8320 | 0.0606 | 0.0756 |
| 36.0000 | 37.0000 | 15.1232 | 0.8064 | 37.0000 | 36.0000 | -15.0773 | -0.7485 | 0.0459 | 0.0579 |
| 37.0000 | 38.0000 | 17.8178 | 0.2093 | 38.0000 | 37.0000 | -17.6744 | 0.0130 | 0.1434 | 0.2223 |
| 37.0000 | 39.0000 | -2.7405 | 0.6834 | 39.0000 | 37.0000 | 2.7418 | -0.6813 | 0.0013 | 0.0021 |
| 36.0000 | 40.0000 | -2.0753 | 5.1417 | 40.0000 | 36.0000 | 2.0817 | -5.1318 | 0.0064 | 0.0099 |
| 22.0000 | 38.0000 | 9.7091 | 3.1560 | 38.0000 | 22.0000 | -9.6950 | -3.1344 | 0.0141 | 0.0216 |
| 11.0000 | 41.0000 | -9.8274 | -13.3763 | 41.0000 | 11.0000 | 9.8274 | 15.1421 | 0 | 1.7658 |
| 41.0000 | 42.0000 | -8.8351 | -8.3555 | 42.0000 | 41.0000 | 9.0670 | 8.7499 | 0.2319 | 0.3943 |
| 41.0000 | 43.0000 | 12.4409 | 9.4668 | 43.0000 | 41.0000 | -12.4409 | -8.7040 | 0.0000 | 0.7628 |
| 38.0000 | 44.0000 | 32.3827 | 22.1722 | 44.0000 | 38.0000 | -32.0688 | -21.5367 | 0.3139 | 0.6355 |
| 15.0000 | 45.0000 | -42.9303 | -72.5080 | 45.0000 | 15.0000 | 42.9303 | 78.8588 | 0.0000 | 6.3508 |
| 14.0000 | 46.0000 | -38.4072 | -192.0305 | 46.0000 | 14.0000 | 38.4072 | 214.4382 | -0.0000 | 22.4077 |
| 46.0000 | 47.0000 | -38.4072 | -2.4174 | 47.0000 | 46.0000 | 38.6503 | 3.1362 | 0.2431 | 0.7188 |
| 47.0000 | 48.0000 | -8.9503 | 8.6914 | 48.0000 | 47.0000 | 8.9702 | -8.6659 | 0.0199 | 0.0255 |
| 48.0000 | 49.0000 | -1.2304 | -0.0766 | 49.0000 | 48.0000 | 1.2313 | 0.0780 | 0.0009 | 0.0014 |
| 49.0000 | 50.0000 | -8.8439 | 1.7315 | 50.0000 | 49.0000 | 8.8896 | -1.6585 | 0.0457 | 0.0730 |
| 50.0000 | 51.0000 | 12.1104 | 12.1585 | 51.0000 | 50.0000 | -11.8258 | -11.7067 | 0.2847 | 0.4518 |
| 10.0000 | 51.0000 | -29.8258 | -146.5936 | 51.0000 | 10.0000 | 29.8258 | 159.5301 | 0 | 12.9365 |
| 13.0000 | 49.0000 | -26.8219 | -81.1190 | 49.0000 | 13.0000 | 26.8219 | 92.1839 | 0.0000 | 11.0649 |
| 29.0000 | 52.0000 | -19.3434 | -7.6096 | 52.0000 | 29.0000 | 19.8682 | 8.2903 | 0.5248 | 0.6806 |
| 52.0000 | 53.0000 | -14.9682 | -6.0903 | 53.0000 | 52.0000 | 15.1245 | 6.2920 | 0.1563 | 0.2018 |
| 53.0000 | 54.0000 | 4.8755 | 3.7080 | 54.0000 | 53.0000 | -4.8216 | -3.6414 | 0.0538 | 0.0665 |
| 54.0000 | 55.0000 | 8.9216 | 5.0414 | 55.0000 | 54.0000 | -8.7788 | -4.8546 | 0.1428 | 0.1868 |
| 11.0000 | 43.0000 | -14.4409 | -42.7136 | 43.0000 | 11.0000 | 14.4409 | 45.3836 | 0 | 2.6700 |
| 44.0000 | 45.0000 | 44.0688 | 23.7488 | 45.0000 | 44.0000 | -42.9303 | -21.4830 | 1.1384 | 2.2659 |
| 40.0000 | 56.0000 | -2.0817 | -0.4094 | 56.0000 | 40.0000 | 2.0817 | 0.4450 | 0 | 0.0356 |
| 56.0000 | 41.0000 | 7.4490 | 5.2624 | 41.0000 | 56.0000 | -7.1332 | -4.9489 | 0.3158 | 0.3135 |
| 56.0000 | 42.0000 | 2.0012 | 4.4068 | 42.0000 | 56.0000 | -1.9670 | -4.3499 | 0.0342 | 0.0569 |
| 39.0000 | 57.0000 | -2.7418 | -1.5348 | 57.0000 | 39.0000 | 2.7418 | 1.6258 | 0.0000 | 0.0909 |
| 57.0000 | 56.0000 | 3.9582 | 2.6092 | 56.0000 | 57.0000 | -3.9318 | -2.5698 | 0.0264 | 0.0394 |
| 38.0000 | 49.0000 | 1.2156 | -2.5192 | 49.0000 | 38.0000 | -1.2093 | 2.5289 | 0.0063 | 0.0098 |
| 38.0000 | 48.0000 | 7.7711 | -9.0355 | 48.0000 | 38.0000 | -7.7398 | 9.0837 | 0.0313 | 0.0483 |
| 9.0000 | 55.0000 | -15.5788 | -67.7314 | 55.0000 | 9.0000 | 15.5788 | 72.8885 | -0.0000 | 5.1571 |

0 0 0 0 ` +

```
0         0         0         0   22.7030  169.1962
```